UMTRI-2005-24 SEPTEMBER 2005

CRITICAL PROFILER ACCURACY REQUIREMENTS

STEVEN M. KARAMIHAS

Technical Report Documentation Page

1. Report No.	2. Government Accession No.	3. Recipient's Catalog No.
UMTRI-2005-24		

4. Title and Subtitle	5. Report Date
Critical Profiler Accuracy Requirements	September 2005
	6. Performing Organization Code
	8. Performing Organization Report No.
7. Author(s)	
S. M. Karamihas	

9. Performing Organization Name and Address	10. Work Unit No. (TRAIS)
The University of Michigan Transportation Research Institute 2901 Baxter Road Ann Arbor, Michigan 48109	11. Contract or Grant No.
	13. Type of Report and Period Covered Draft Final Report Jan. 2004 - Aug. 2005
12. Sponsoring Agency Name and Address	14. Sponsoring Agency Code

15. Supplementary Notes

16. Abstract

This report defines critical accuracy requirements for a reference profiling device. The work was performed under a Federal Highway Administration (FHWA) pooled fund study TPF-5(063) "Improving the Quality of Pavement Profiler Performance." The requirements include the waveband of interest, the required accuracy, the sampling and footprint requirements, the method of profile comparison. A tentative testing program is defined for benchmarking the accuracy and repeatability of profiles from candidate reference devices, and their longitudinal distance measurement accuracy. A method is also recommended for comparison of profiles from production profilers to the output of reference profiling devices.

17. Key Words	18. Distribution Statement
road roughness, longitudinal profile, profile measurement, reference profile measurement, International Roughness Index (IRI)	Unlimited

19. Security Classif. (of this report)	20. Security Classif. (of this page)	21. No. of Pages	22. Price
Unclassified	Unclassified	115	

TABLE OF CONTENTS

Chapter **Page**

CHAPTER 1. INTRODUCTION 1

CHAPTER 2. GOAL OF THE REFERENCE DEVICE 5

CHAPTER 3. WAVEBAND OF INTEREST 7
- Response to Vertical Vibration 8
  - Passenger Car Vertical Dynamics 8
  - Truck Vertical Vibration 10
  - Human Sensitivity to Vertical Vibration 10
- Roughness Indices 11
  - International Roughness Index 12
  - Ride Number 14
  - Michigan Ride Quality Index 15
  - Truck Response Indices 16
  - Simulated California Profilograph Index 19
- Wavelength Range Analysis 21
  - Linear Response Theory 21
  - Input Spectra 24
  - Analysis Results 26

CHAPTER 4. ACCURACY REQUIREMENTS 29
- Elevation Resolution 30
- Elevation Accuracy 31
  - Precision 32
  - Bias 35
- Slope Accuracy 36
- Profiler Gain Limits 36
  - Review 38
  - Further Development 40
- Phase and Coherence 44
- Longitudinal Distance Measurement 45
- Lateral Tracking 46

CHAPTER 5. PROFILE COMPARISON METHOD 47
- Introduction 48
- Theoretical Development 48
- Synchronization 50
- Rating of Agreement 51
- Processing Steps 52

Synchronization 52
Rating of Agreement 55
Threshold Development 56
Waveband Analysis 59

CHAPTER 6. SAMPLING AND FOOTPRINT REQUIREMENTS 61
Longitudinal Sampling 63
Background 63
Theoretical Study of IRI 66
Filtering for Simulated Profilograph Index 72
Tire Envelopment 73
Vehicle Dynamics Models 74
Profile Envelopment Filters 77
Tire Bridging 81
Footprint Width 84

CHAPTER 7. BENCHMARK TESTS 85
Test Sections 87
Repeatability 89
Accuracy 89
Detailed Measurements 90
Rod and Level Measurements 93
Longitudinal Distance 94
Alternative Methods for Accuracy Testing 95

CHAPTER 8. REVIEW OF EXISTING DEVICES 97
Inclinometer-Based Devices 97
Support Spacing 97
Recording Interval 99
Support Footprint 100
Rod and Level 100
Other Devices 101

CHAPTER 9. RECOMMENDATIONS 103
Critical Requirements 103
Benchmark Testing 104
Comparison to the Reference Device 105
Future Research 106

CHAPTER 10. REFERENCES 107

LIST OF FIGURES

Figure **Page**

Figure 1. Passenger car suspension isolation. 9
Figure 2. Weighting curve for human response to vertical vibration. 11
Figure 3. Quarter-car model. 13
Figure 4. IRI gain for profile slope. 14
Figure 5. RN gain for profile slope. 15
Figure 6. RQI gain for profile slope. 16
Figure 7. NRCC test vehicle transfer function. 18
Figure 8. Prem model of truck response to road roughness. 19
Figure 9. TRI gain for profile slope. 20
Figure 10. Simulated California profilograph, gain for profile slope. 20
Figure 11. Relationship between input and output slope PSD functions. 22
Figure 12. Linear response with linear scaling. 24
Figure 13. Index error estimate for Road 1. 26
Figure 14. IRI gain for profile elevation. 33
Figure 15. Sample white noise slope profile. 34
Figure 16. Sample profile smoothed with a 2.25-m (7.38-ft) moving average. 34
Figure 17. Standard deviation of elevation error, smoothed profiles. 35
Figure 18. Profile comparison using transfer functions. 37
Figure 19. IRI gain limit on white noise slope. 42
Figure 20. Composite IRI gain limit on four sample roads. 43
Figure 21. Composite gain limit for 11 indices on 4 sample roads. 44
Figure 22. Cross correlogram of two profiles. 51
Figure 23. Three highly correlated repeat measurements. 53
Figure 24. Three moderately correlated repeat measurements. 53
Figure 25. IRI agreement versus cross correlation level. 58
Figure 26. IRI agreement associated with cross correlation level. 58
Figure 27. Simple example of aliasing. 64
Figure 28. Use of filtering to reduce the influence of aliasing. 66
Figure 29. IRI error versus recording interval, Road 01. 70
Figure 30. IRI error versus recording interval, Road 04. 70

Figure 31. Third-order Butterworth low-pass response at various intervals. 73
Figure 32. Tire models for response to road roughness.....74
Figure 33. Tire response to a cleat.....75
Figure 34. Force at the axle in response to an impulse.....78
Figure 35. Road to spindle transmissibility over an impulse at low speed.....78
Figure 36. Road to spindle transmissibility over an impulse at higher speed. 79
Figure 37. Comparison of tire envelopment weighting functions. 80
Figure 38. Penetration of macrotexture into a tire.....81
Figure 39. Filter comparison.....84
Figure 40. The TRRL Beam at the IRRE. 91
Figure 41. Rod and level with a large foot pad.....93
Figure 42. DipStick response to sinusoids.....98
Figure 43. DipStick gain, small recording interval.....99

LIST OF TABLES

Table **Page**

Table 1. Wavelength threshold for slope gain reduction to 1 percent of the peak. 12

Table 2. Model coefficients for four sample roads. 25

Table 3. Long wavelength thresholds. 28

Table 4. Short wavelength thresholds. 28

Table 5. Resolution requirements. 31

Table 6. Effective moving-average baselength. 68

LIST OF ACRONYMS

AASHTO – American Association of State Highway and Transportation Officials

ARRB – Australian Road Research Board

ASTM – American Society of Testing and Materials

DOT – Department of Transportation

DLC – Dynamic Load Coefficient

DLI – Dynamic Load Index

FHWA – Federal Highway Administration

GC – Golden Car

IRI – International Roughness Index

IRRE – International Road Roughness Experiment

NCHRP – National Cooperative Highway Research Program

NRCC – National Research Coucil of Canada

PI – Profilograph Index

PSD – Power Spectral Density

PTRN – Pre-Transform Ride Number

RIDE – Roughness Index for Driving Expenditure

RN – Ride Number

RPUG – Road Profiler User's Group

RQI – Ride Quality Index

SMA – Stone Matrix Asphalt

TRI – Truck Ride Index

TRN – Truck Ride Number

TRRL – Transport and Road Research Laboratory

CHAPTER 1. INTRODUCTION

In early efforts by the highway community to measure pavement condition, one of the most important quantities was found to be the roughness of the surface.(1) Many techniques have evolved for measuring roughness, and virtually all of them focus on measuring the vertical deviations of the road surface along a longitudinal line of travel in a wheel path, known as the *profile*.(2) Equipment for making these measurements also evolved, starting with straight edge devices in the early 1900s, to vehicles that can measure a profile while traveling at normal traffic speed. The first design for obtaining measurements at traffic speed was called a *profilometer*.(3) Today, the comparable systems are called *inertial profilers*. These produce *longitudinal profiles*, which provide vertical elevation as a function of longitudinal distance along a prescribed path.

Valid measurement of a profile is a matter of determining the vertical and longitudinal dimensions with accuracy appropriate to the objectives of the measurement. Although this is simple in concept, absolute measurement of the vertical dimension is difficult to accomplish. Road surface elevation covers many orders of magnitude from very small deviations caused by texture to very large deviations on hills and other large grade changes. However, the objectives of profile measurements are usually limited to capturing those aspects of the longitudinal profile that affect vibration of motor vehicles. Thus, vertical dimensions do not have to be accurate on an absolute scale, but only accurate relative to the surrounding road surface.

Today, a great variety of devices that produce longitudinal profile exist.(4,5,6) Most applications of these devices require that they provide measurements of roughness on a stable, consistent scale. As a result, verification of the accuracy of these devices has become a significant concern of State highway agencies. The first step in this process is to establish a *reference profiling device*, which provides a measurement of longitudinal profile as a standard for verifying the measurements of other devices.

This report defines critical accuracy requirements for a reference profiling device. The work was performed under a Federal Highway Administration (FHWA) pooled fund study TPF-5(063) "Improving the Quality of Pavement Profiler Performance." The pooled fund participants chose the definition and development of a reference profiling device as their two highest priorities. This report defines the requirements, and provides the information needed to continue with the development or procurement of a device.

The success of a profiler certification program depends on accurate and relevant reference profile measurements. Numerous types of equipment and procedures for obtaining a reference profile measurement are in use today, but they all suffer one or more of the following deficiencies:

- They are labor intensive.
- They do not record profile at a short enough interval to properly measure the needed short wavelength content.

- They do not apply sufficient anti-aliasing measures to ensure that the output roughness values are relevant to vehicle response.
- Often, the accuracy, precision, or resolution of these devices are not significantly better or even as good as the devices undergoing validation.
- They have not been properly verified themselves.

The objective of this project is to provide a definition of the performance requirements for a reference profiling device. The report provides the objective criteria, such as the accuracy, repeatability, and sampling procedures required of a reference device. The report also defines a testing methodology needed to qualify candidate profilers for use as reference devices. These criteria will provide a basis for specification and procurement of a device.

The testing methodology described in this report seeks to qualify *candidate reference profiling devices* for use in profiler certification programs. Part of the testing methodology includes the comparison of candidate reference profiling devices to very accurate *benchmark profile measurements*. Should a candidate reference device agree sufficiently well with the benchmark measurements, it will "qualify" as acceptable. In turn, the qualified reference device(s) will provide the benchmark measurements for certification of *production profiling devices* for construction quality control and pavement network monitoring.

Five important themes guided the work. First, critical accuracy requirements must ensure that overall roughness values and the spatial distribution of roughness are correct. Second, whenever possible, requirements must take the form of specifications on performance rather than specification of a method. Third, the project must emphasize qualification of a reference device that could certify profilers for construction quality control. Such a device would also meet the less stringent requirements for certification of devices for network-level roughness measurement. Fourth, accuracy requirements must target measurement of index values that are computed from profile to within 1 percent. This will permit the establishment of absolute thresholds for key performance qualities. This way, multiple devices may qualify, so long as they all adhere to the minimum requirements. Note that pooled fund participants are free to purchase any candidate reference device they wish, but they are encouraged to link their procurement requirements to the recommendations in this report. Finally, the project will use the best available information. While the project included no testing, significant analysis was performed. Further, data from the 2004 FHWA profiler round-up provided valuable insight for many of the technical decisions made in this project.(6)

The structure of this report follows the steps that were taken to complete the research. Chapter 2 describes the goal of the reference device. All the technical work that follows derives from this description. Chapter 3 defines the relevant waveband of interest. Long and short wavelength boundaries summarize the waveband that is needed to measure current and anticipated roughness indices. Chapter 4 defines accuracy requirements over the relevant waveband. The accuracy requirements depend on the availability of extremely accurate benchmark profile measurements.

Chapter 5 reviews a profile comparison method. This method is recommended for use when comparing production profiler output to reference measurements. It is also recommended as a supplement to the accuracy requirements, inasmuch as it will be used to make sure candidate reference profiler output agrees sufficiently with the benchmark measurements.

Chapter 6 establishes sampling and footprint requirements for the reference device. Chapter 7 presents options for making the benchmark profile measurements. Note that the sampling and footprint requirements in chapter 6 will be observed when making the benchmark profile measurements recommended in chapter 7. Chapter 7 also outlines the rest of the requirements for accuracy and repeatability of candidate reference devices. These requirements include a proposed set of qualification tests.

Chapter 8 reviews currently used reference devices in light of the recommendations for waveband, accuracy, sampling practices, and footprint size provided in chapters 3, 4, and 6.

Chapters 3 through 8 provide a tremendous amount of technical background, but the technical approach, important findings and key recommendations consistently appear in the first few pages of these chapters, before the first major heading. Chapter 9 summarizes all the recommendations from this project. The chapter lists all the critical requirements that are recommended for a reference profiling device, and describes further work that is needed to verify or improve the recommendations.

Most of the findings and recommendations presented in this report are based on very good background research, and are likely to stand the test of time. An exception is the sampling and footprint requirements. While these requirements are based on the best available information, it is expected that future research will improve the state of the art beyond the information in this report. Another exception is the testing methodology for benchmarking candidate reference profilers. The method recommended in this report was selected in response to the pooled fund participants' desire to proceed with the testing as soon as possible after the release of this report. Other testing methodologies are possible, as described in chapter 7, but they would require more lengthy development.

CHAPTER 2. GOAL OF THE REFERENCE DEVICE

The goal of the reference device is to measure an accurate longitudinal road profile as a benchmark for validation of the performance of production profilers. The device must provide a profile, and resulting index values, that may serve as a standard for comparison by production profilers. The profile it provides must include all the road features that excite major vehicle system vibration modes. Of primary interest are those vehicle vibrations that degrade ride quality, exercise the vehicle suspension, and affect tire vertical loads. In so doing, the device shall also be able to produce reference values of common pavement roughness indices, specifically the International Roughness Index (IRI) and Ride Number (RN), as well as anticipated roughness indices that are likely to be proposed in the future.

In past profiler verification activities, the reference device has often been considered a source of the correct index value, rather than a method of determining the correct profile. A more meaningful profiler verification testing program requires that profiles are measured correctly, and that the production profiler is only considered valid when it provides a profile that agrees with the reference measurement. Correct index values are also required, but this should be a secondary requirement that derives from the primary profile reference. This is important for three reasons:

1. Agreement in the overall roughness index value is not sufficient to verify a profiler. This is because summary index values may agree as a result of compensating error, without a reasonable level of agreement between profiles. In this instance, a large number of test sections are needed to detect problems using summary index values alone, whereas study of the profiles themselves often uncover measurement problems with only a small number of tests.
2. Comparing profiles provides diagnostic information when they do not agree. In particular, comparison of profiles may help isolate measurement errors to a specific waveband, or help to determine which components of a profiling device may be functioning incorrectly.
3. Agreement in profile requires agreement in the location and severity of concentrated roughness. If profilers are to be verified for use in construction quality control and quality assurance, it will be necessary to know the severity of localized roughness, both as a basis for assessing penalties to the contractor and to help make decisions about the best remedy. In addition, accurate profiles will help motivated contractors to learn what rough features penalized their smoothness score the most, and how to avoid them in the future.

Of course, “agreement of profile” must be defined very carefully. First, perfect agreement is not possible. Some tolerances must be placed on the level of precision, while systematic bias of any kind must be discouraged. Second, the relevant aspects of the profile signal must be emphasized, and the irrelevant aspects must be ignored. This is usually expressed in terms of a waveband of interest. In practical terms, it means that

aspects of profile that cause vehicle vibrations, usually defined as the "roughness," will be included in the judgment of agreement, and those that do not, such as the grade and texture, will be excluded.

Agreement in profile must emphasize those aspects of the road surface that affect the IRI, since measurement of the IRI is the most common use for a profiler. Further, acceptable agreement with a reference device must provide confidence that IRI values will be measured accurately in the field by the production device. In addition to the IRI, a reference profiler must be able to verify accurate measurement of other roughness indices. This includes the RN, and other indices that are likely to be of interest in the near future; for example, roughness indices that are customized to predict the severity of truck dynamic loading. The reference profiler must also be able to measure content that affects vehicles over a broad range of common travel speeds. Lastly, for the purposes of comparison to old methods, a reference profile should include content that is sufficient to compute the response of straightedge-based roughness measurement devices, such as California profilographs and common rolling straightedges.

Other aspects of vehicle response of interest may include durability, cargo vibration, road loading, and general prediction of ride quality. Inasmuch as these performance qualities can be defined in terms of major vehicle vibration modes that are common to the general highway vehicle fleet, the relevant aspects of profile should be included. However, many aspects of road response that do not affect vehicle occupants or cargo through direct contact will not be included, such as those profile features that cause noise.

The reference profiler should only be expected to cover a finite range of roughness. It must be accurate on very smooth pavements, because it may be used to verify profilers for use on new construction. However, it will not be required to include precise detail about severely rough features that cause loss of contact between the tire and the road.

Pavement evaluators measure road profile for three common purposes: (1) monitoring of the overall health of a road network, (2) evaluation of the smoothness of a specific pavement project, often newly constructed or newly resurfaced roads, and (3) research. The reference device must serve as a benchmark for profilers in all three applications, with the exception that only responses of the vehicle are of interest. As such, it is anticipated that the engineering requirements for the reference device will ensure enough accuracy to verify a profiler for network monitoring, project monitoring, and research applications that encompass vehicle response. However, the recommended set of test conditions, and the required level of agreement between a production profiler's output and the reference measurement will be customized to the application.

Lastly, the reference device must provide the foundation for a profiler certification program within any interested agency. As such, the cost of a single unit must be within reach of an interested agency, and the labor cost associated with the measurement process should be kept to a minimum. Further, the device must be portable, so that a reference measurement site may be established at any location. While a reference device that may operate without traffic control would be a great advantage, the device must provide the profile of a pre-defined longitudinal path within a tight tolerance. Thus, the device is likely to operate only under traffic control.

CHAPTER 3. WAVEBAND OF INTEREST

This chapter defines the waveband of interest for a reference profiler. American Association of State Highway and Transportation Officials (AASHTO) Specification MP-11 currently specifies that inertial profiling systems "accommodate" wavelengths from about 0.15 m to 91.4 m (6 in to 300 ft).[7] This range of wavelengths represents a trade-off between the intended uses of a profiler and common practice. The recommendations here, combined with the accuracy requirements established in chapter 4 and the profile comparison method described in chapter 5, provide a systematic performance specification for the waveband of a reference device.

Requirement: *A general purpose reference device for road roughness measurement must capture wavelengths from 0.15 m to 67 m (6 in to 220 ft).*

This range includes the waveband required by most of the roughness indices established in the literature. The limits of the range were established though detailed analysis of the wavelength sensitivity of each roughness index, combined with knowledge of the spectral content of common road profiles. The profiling community has expressed interest in versions of the IRI at speeds other than the standard value of 80 km/h (49.7 mi/h). As such, the range includes the wavelengths that would be needed if the Golden Car simulation speed varied from 40 km/h to 120 km/h (25 mi/h to 75 mi/h).

The range is also consistent with the need to capture vehicle vibration responses relevant to passenger vibrations (particularly in the vertical direction), tire dynamic loading, roughness induced vehicle wear, and cargo vibration in both cars and trucks. The major vibrations that affect these performance qualities typically occur in the frequency range from 0.5 to 80 Hz. As such, a reference device that measures wavelengths from 0.4 m to 67 m (1.4 ft to 220 ft) will be valid for these motions at a speed of 120 km/h (75 mi/h). Further, the range is likely to be valid for future roughness indices, and most anticipated uses of profiles for the purpose of estimating or simulating road vehicle response.

Although the wavelength range above is required for a general purpose reference device, accurate measurement of the IRI is the highest priority. A reference device with the exclusive purpose of verifying the measurement of profile for calculation of the IRI must be valid for wavelengths from 0.9 m to 35 m (2.95 ft to 115 ft).

The wavelength sensitivity is an important aspect of the device, but it does not completely define all of the performance qualities that a reference device must possess. For example, the long wavelength boundary of the range is not the same as the long wavelength cutoff of a high-pass filter that is native to many profilers. In fact, the reference device should provide accurate profile out to the long wavelength limit with a gain near unity and very little phase shift. These requirements are established in chapter 4. Further, the short wavelength boundary of the range will interact strongly with the sampling scheme and footprint of the device. Desirable performance depends on the ability of the device to capture the essential short wavelength aspects of the road surface with direct relevance to the way a tire would react to it. This is covered in chapter 6.

The rest of this chapter provides the detailed background and analysis needed to establish the wavelength range recommended here. First, human response to vibration and major modes of vibration that are common to many vehicles are briefly reviewed. Next, this chapter reviews the wavelength sensitivity of well-known roughness indices. The chapter concludes with systematic analyses of many of the indices. These analyses provide the basis for the wavelength limits.

RESPONSE TO VERTICAL VIBRATION

This section briefly reviews the basics of passenger car vertical vibrations, truck vertical vibrations, and human response to vertical vibration. This section shows that the frequency range of interest for these phenomena is 0.5 to 80 Hz.

Passenger Car Vertical Dynamics

Since the outset of the automotive industry, vehicle design has converged on an architecture in which the vehicle body (sprung mass) is separated from the wheels (unsprung masses) by a suspension system. This design was necessary to isolate the vehicle occupants from the severe vibration that would arise from imperfections in the road surface in the absence of a suspension system.

Road roughness is normally depicted in terms of deviations in vertical elevation. However, because the "ride" vibrations on a motor vehicle are experienced as accelerations on the body it is helpful to think of road roughness as an acceleration input at the tires. Expressing roughness as acceleration rather than displacement yields an input that increases with frequency as shown to the left of figure 1. Figure 1 shows an example of a rough asphalt road with significant distress. However, the increase in content with frequency is common to profiles of most all in-service pavements.

To minimize ride vibrations a suspension is interposed, which has the gain properties shown in the middle of figure 1. For frequencies very close to zero, the suspension simply transmits the input from the road directly into the sprung mass. This is the case in which the vehicle is simply following the road up and down very long undulations (i.e., hills and valleys) with no dynamic response. Near 1 Hz the vehicle amplifies the accelerations. However, at higher frequencies it dramatically reduces the accelerations transmitted to the vehicle body. As evident in the right hand graph the ride accelerations tend to be concentrated in the range of 1 to 10 Hz.

This response is very similar to that associated with the IRI. The peak value of response for the IRI at 15.78 m (51.8 ft) corresponds to a frequency of 1.41 Hz at the travel speed of 80 km/h (49.7 mi/h). This is the "body bounce" resonance frequency, which is an aspect of vertical vibration behavior that is common to nearly every road vehicle.

Passenger car body vibrations in the vertical direction are typically about 1 Hz, which at highway speed is excited by wavelengths in the road on the order of 30 m (100 ft). To achieve the best possible ride these frequencies need be as low as possible; yet, the practical constraints of suspension design currently limit them to about 1 Hz, with little possibility to reduce them further. For example, the lower frequency of body vibration

may help reduce the vibrations felt by vehicle occupants, but it would increase suspension stroke. This would violate a design requirement of most vehicles, which places limits on "rattle space" associated with suspension packaging. The design of most vehicle suspensions involves a trade-off between suspension stroke, tire dynamic loading, and body acceleration that limits the range of body bounce frequencies in common practice.[8] On some vehicles, such as sports cars, in which ride is not the top priority the frequencies may be slightly higher (e.g., on the order of 1.5 to 2 Hz).

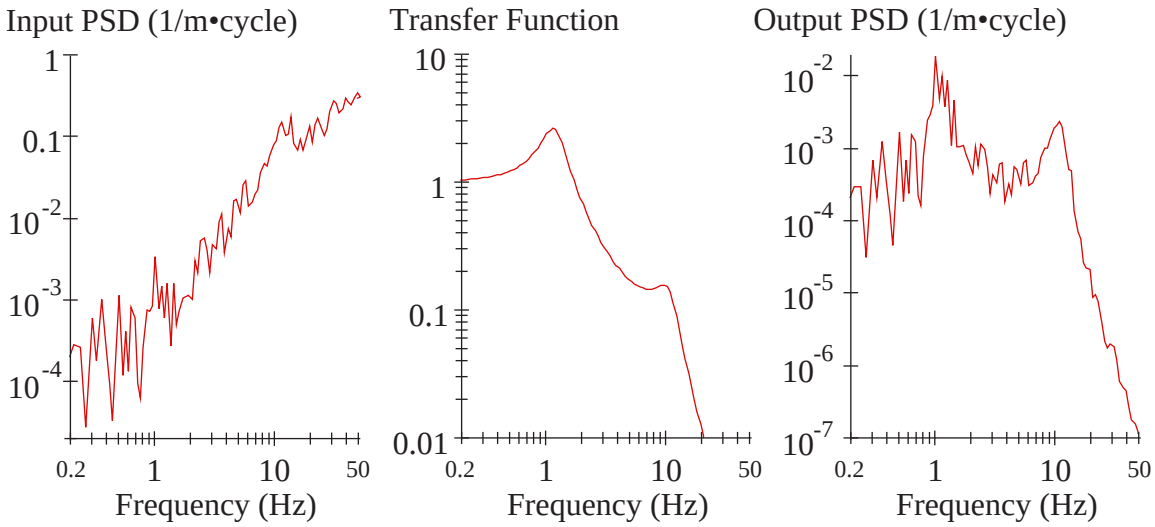


Figure 1. Passenger car suspension isolation.

A second peak in the response occurs near 10 Hz in figure 1. This resonance frequency corresponds to a mode of vibration in which the axle vertical motion is exaggerated compared to the road input. Although the suspension helps isolate the vehicle body from much of this, significant vibration is still transmitted to the sprung mass. This mode of vibration is called *axle hop*. Axle hop corresponds to the peak in IRI response at 2.30 m (7.6 ft). At a speed of 80 km/h (49.7 mi/h), this is an axle hop resonance frequency of 9.7 Hz.

The axle hop resonant frequency varies primarily with the tire stiffness and wheel and axle mass properties, but generally falls in the range of 10 to 13 Hz. Consequently, at normal highway speeds it is most sensitive to roughness features in the wavelength range from 2 to 3 m (6.6 to 9.8 ft). However, because the axle hop responds to excitation not just at its resonant frequency, but to adjacent frequencies as well, it is sensitive to wavelengths shorter than 2 m (6.6 ft) also. Future trends in automotive design, particularly with electric and hybrid cars, may lead to stiffer tires and lighter wheels pushing the wheel hop frequencies upward, such that axle hop frequencies of 15 Hz may be common.

Other important motions also exist within common passenger cars. For example, body motion in cars occurs in two modes: heave and pitch. In the heave mode, the front and rear of the vehicle move together. In the pitch mode, the front and rear vibrate out of phase. Further, a solid axle will exhibit a vertical mode, and a mode called *tramp*, in which the left and right wheels vibrate out of phase. However, these frequencies typically

occur in the ranges listed above. The vehicle body will also exhibit a roll mode, in which the body rotates about the longitudinal axis. This causes side-to-side "toss" of the occupant, particularly in taller vehicles such as sport utility vehicles. Typical design guidelines for automobiles require that the roll resonant frequency is similar to that of body bounce.[9] Some modes of tire vibration may also affect the ride quality of passenger cars. For example, a vibration mode exists within the tire in which the tread and outer belt move longitudinally with respect to the rim. This mode typically occurs in the range from 30 to 50 Hz.[10] Vertical motion of the "tread resonance" occurs at frequencies of up to 90 Hz. These motions may affect vibrations in the vehicle body in extreme cases, but the suspension isolates the body from most of their influence.

Truck Vertical Vibration

Gillespie provided a detailed listing of the vibration modes observed on a tractor van-trailer. These included: (1) body motion of both units in six degrees of freedom, (2) axle vibrations, (3) motions associated with body structural compliance, (4) suspended cab vibrations, and (5) vibrations of specialized mounted hardware, such as the battery box, fuel tank, exhaust stack, etc.[11] With the exception of body roll, these motions were associated with resonance frequencies from 1.45 to 20.4 Hz.

As in automobiles, major modes of vertical vibration include body pitch and bounce and axle vertical (hop) and roll (tramp) motion. While truck dynamic behavior is more diverse than in cars, similar design constraints exist. As such, most heavy vehicles will exhibit rigid body vibration modes in the range of 1.2 to 5 Hz. Prem confirmed this in an analytical study of suspension and mass properties found in the literature.[12] Fu reported estimates of truck body motion natural frequencies from 1.2 to 2.3 Hz using suspension test data, and assuming that each suspension was loaded to its rated value.[13] Loading a truck below its capacity increases the resonant frequency. Additionally, when trucks experience smooth pavement they appear stiffer because of suspension friction. This also raises the natural frequency of the system.[14] This explains extension of the range to 5 Hz. Axle hop typically occurs in the frequency range from 9 to 20 Hz.[11] Overall, the frequency range for heavy truck ride is about 0.5 to 25 Hz.

The lowest resonant frequencies for heavy truck vibration usually occur for body roll motion. This is because design requirements for handling, rather than ride, take precedence. As a result, a typical resonant frequency for truck body roll motion is 0.5 Hz, and values above 1 Hz are rare. Fortunately, roads are very consistent side to side for long wavelengths.[15,16] As a result, the roll mode gets very little excitation from the road.

The critical body and axle modes of vibration that affect truck ride and cargo vibration also affect dynamic loading of the roadway. Cebon quotes 1.5 to 4.0 Hz for body motion as "broadly representative" of single axle truck suspensions in use.[17] In a review of truck-generated road damage, Cebon also quotes 8 to 15 Hz for axle hop and axle tramp.[18]

Human Sensitivity to Vertical Vibration

Sensitivity to vibration of the human body in a sitting position has been quantified by numerous studies. Many of these are summarized by Griffin.[19] It is generally recognized

that the human body has minimum tolerance to vertical vibration at about 5 Hz due to a resonance of the organs in the abdominal cavity. Thus, cars are designed to minimize transmission of road inputs at this frequency.

Human sensitivity to vibration has become a mature topic, such that the research findings have gone into practice in the form of standards for evaluation of human vibration environments.[20,21] In these standards, a frequency weighting is often given for vertical vibration of a seated subject. This weighting is applied to the measured acceleration under the human-vehicle interface. Figure 2 shows the weighting curve for British Standard 6841. Note that the weighting is most sensitive to vibration near 5 Hz, and covers a range from 0.5 to 80 Hz. This suggests that a relevant road profiler should expect to measure wavelengths which correspond to this range at speed. At 120 km/h (75 mi/h), the range corresponds to about 0.4 to 67 m (1.4 to 220 ft). At 40 km/h (25 mi/h), it corresponds to about 0.2 to 22 m (0.66 to 73 ft).

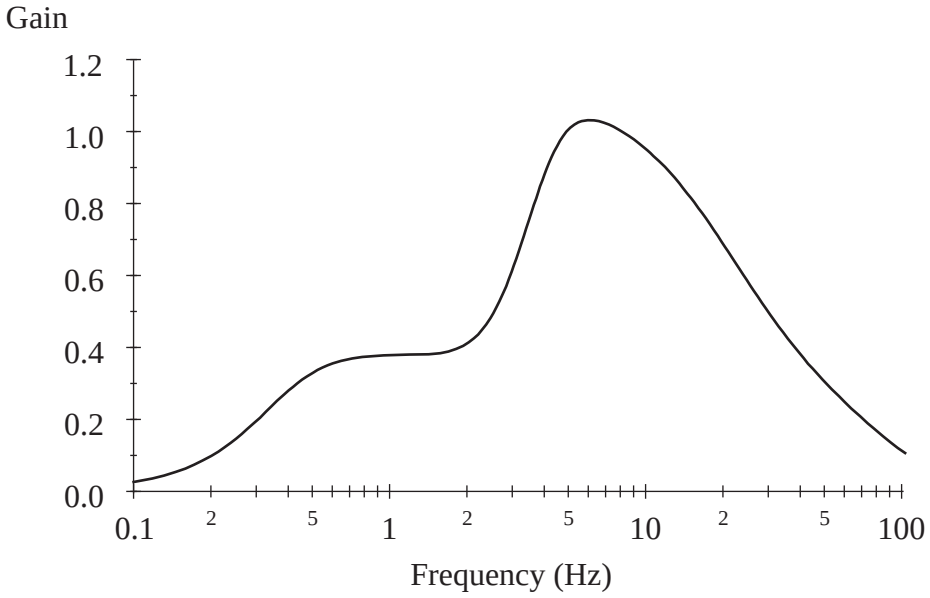


Figure 2. Weighting curve for human response to vertical vibration.

ROUGHNESS INDICES

This section reviews the wavelength sensitivity of existing roughness indices. The most common applications of road profilers have typically prompted the development of a roughness index. Thus, the wavelength range needed for measurement of these indices is considered essential for a useful reference profile measurement. This range is also likely to cover the waveband needed by future indices that are developed to estimate vehicle response. Whenever possible, the discussion emphasizes gain characteristics of an index in response to profile slope, rather than elevation. This is because the content of slope profiles is typically much more consistent over the spectrum than elevation profiles. Thus, the gain for profile slope provides a much more proportional view of the importance of each waveband to the final index value.

Table 1 summarizes the review. The table lists several of the indices covered here, and the wavelength thresholds at which the gain of each index, or index component, falls below 1 percent of the peak value. Abbreviations in the table are defined in the explanations that follow. The table suggests that wavelengths from 0.22 to 180.0 m (0.72 to 591 ft) may be required for a reference profiler with broad application. However, this method of characterizing each index does not represent the contribution the roughness at the threshold wavelength may make to the overall index value. The results of a more systematic treatment are provided in tables 3 and 4.

Table 1. Wavelength threshold for slope gain reduction to 1 percent of the peak.

Index	Purpose	Long (m)	Short (m)
IRI	general	137.8	0.39
RN	automobile user comfort	61.2	0.26
RQI, long band	automobile user comfort	180.0	2.64
RQI, medium band	automobile user comfort	89.3	0.67
RQI, short band	automobile user comfort	17.9	0.22
TRN	truck occupant comfort	21.9	4.34
RIDE	truck operating cost	—	0.44
TRI	truck occupant comfort	41.1	3.66
DLI	truck dynamic loading	429.2	0.46

International Roughness Index

The IRI is the most commonly used roughness index in the U.S. It serves as the primary indicator of road surface roughness within most State departments of transportation, and is reported by most States to the FHWA Highway Performance Monitoring System.[22,23,24] The IRI is calculated in four steps.[25]

Step 1: Convert the profile to slope.

Step 2: Apply a 250-mm (9.84-in) moving average.

Step 3: Simulate the response of the "Golden Car" model.

Step 4: Accumulate the average rectified value of the result.

Figure 3 illustrates the Golden Car model.[26] The model represents one corner of a vehicle, inasmuch as it predicts the response of one tire and suspension system to a road profile, with the weight supported by the suspension resting over it. This is called a *quarter-car model*. The Golden Car model predicts the spatial derivative of suspension stroke in response to the profile using a quarter-car model with standard settings for speed and the vehicle properties depicted in figure 3. The values are:

V = 80 km/h (49.7 mi/h)

$m_u/m_s = 0.15$

$k_t/m_s = 653$ 1/sec^2

$k_s/m_s = 63.3$ 1/sec^2

$c_s/m_s = 6$ 1/sec

Note that the moving average baselength (B) of 250 mm (9.84 in) is also a standard aspect of the IRI calculation. This is applied before the Golden Car simulation to represent tire envelopment.

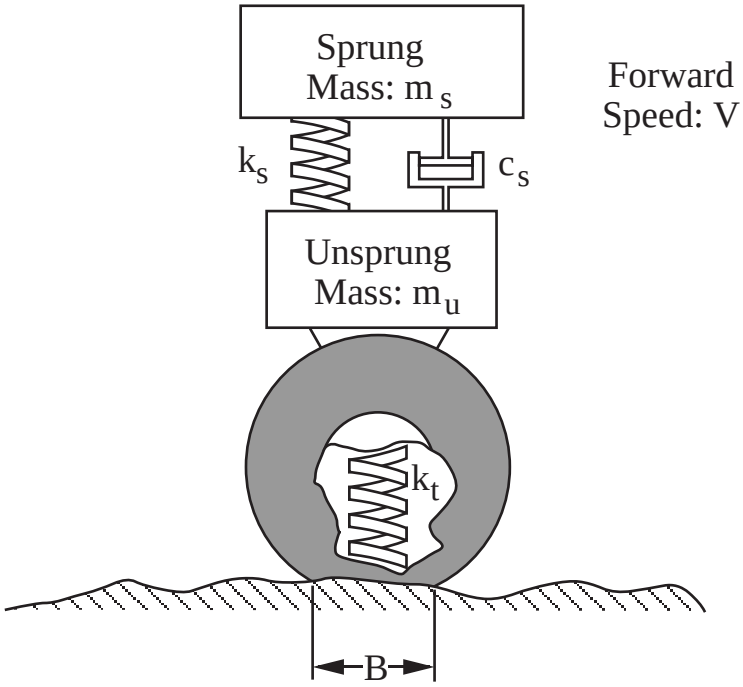


Figure 3. Quarter-car model.[27]

The wavelength response of the IRI is often characterized by the plot in figure 4. This plot provides the gain for profile slope. The gain for profile slope is commonly used instead of gain for elevation, because roads typically have slope spectra with much more uniform content than elevation spectra. The IRI is most sensitive to wavelengths from 1.3 to 30 m (4.27 to 98.4 ft), with peak values of sensitivity at 2.30 m (7.55 ft) and 15.78 m (51.8 ft).[25,28] The IRI covers a very broad range of wavelengths. For example, the gain does not fall beneath 1 percent of the peak value until the wavelength is shorter than 0.39 m (1.3 ft) or longer than 137.8 m (452 ft). Although the IRI is sensitive to a broad range of wavelengths, not all parts of the range will necessarily have a strong effect on the final index. Some studies have examined the effect of high-pass filtering on the IRI, and noted that a filter cutoff value at a much shorter wavelength than 137.8 m (452 ft) is needed to reduce the IRI, even slightly.

A recent study of profile measurement procedures reported that a second order Butterworth filter did not reduce the IRI of an artificial white noise slope profile more than 0.1 percent until the cutoff value fell below 45.3 m (149 ft).[28] Note that the content above the cutoff wavelength is not completely eliminated, so longer wavelength content contributed to the IRI. (The cutoff wavelength defines the wavelength at which the content is reduced to about 70.7 percent.) The same type of analysis for this study verified the 45.3 m (149 ft) cutoff, and showed that a 1 percent reduction occurred when the cutoff wavelength was about 22.5 m (74 ft). Another study showed that the IRI of a segment of road was reduced by about 3.3 percent when a cotangent filter was applied

with a cutoff of 30.5 m (100 ft).[29] These results do not provide sufficient basis for establishing filter cutoff values, since the relationship between reduction in IRI and filter cutoff depends strongly on the spectral characteristics of the road. They simply help to characterize the broad range of interest.

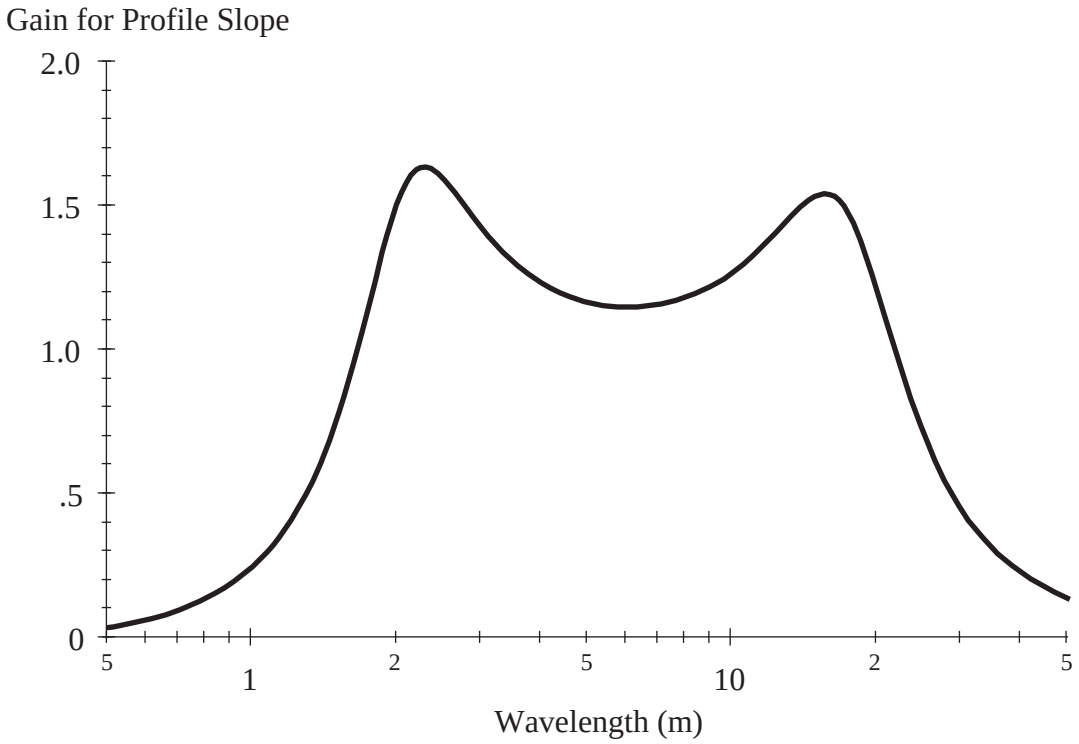


Figure 4. IRI gain for profile slope.

Ride Number

The RN estimates user perception of of ride comfort. It was developed in the 1980s by the National Cooperative Highway Research Program (NCHRP), and standardized in the 1990s by the FHWA.[26,30,31] The index provides a prediction of mean panel rating from profile.

The RN calculation algorithm is very similar to that of the IRI. The profile is converted to slope, and subjected to a 250-mm (9.84-in) moving average. However, instead of passing through a Golden Car model, the smoothed slope profile passes through a band pass filter. Although the filter uses the same algorithm as the quarter-car model, the parameters are set to provide the best prediction of mean panel rating from two studies of road user opinion.[32] The index value is calculated from the filtered profile in two steps. First, the root mean square is calculated. The resultant value is the pre-transform Ride Number (PTRN). Second, the index is cast onto a 0-to-5 scale using an exponential transform:

$$RN = 5 \bullet e^{-160 \bullet PTRN} \quad (1)$$

The transform requires PTRN in unitless slope (e.g., m/m). Note that, in practice, the RN should be calculated from a pre-transform value that represents the mean square of PTRN for the left and right side.[32] For the purposes of this discussion, the profile from only one side is considered.

The wavelength response of the RN is often characterized by the plot in figure 5. This plot provides the gain for profile slope. The wavelength response of the RN reaches a peak value at 5.95 m (19.5 ft), but it is primarily sensitive to wavelengths from 0.38 m (1.25 ft) to 11.4 m (37.4 ft).[28] However, the gain does not fall beneath 1 percent of the peak value until the wavelength is shorter than 0.26 m (0.85 ft) or longer than 61.2 m (201 ft).

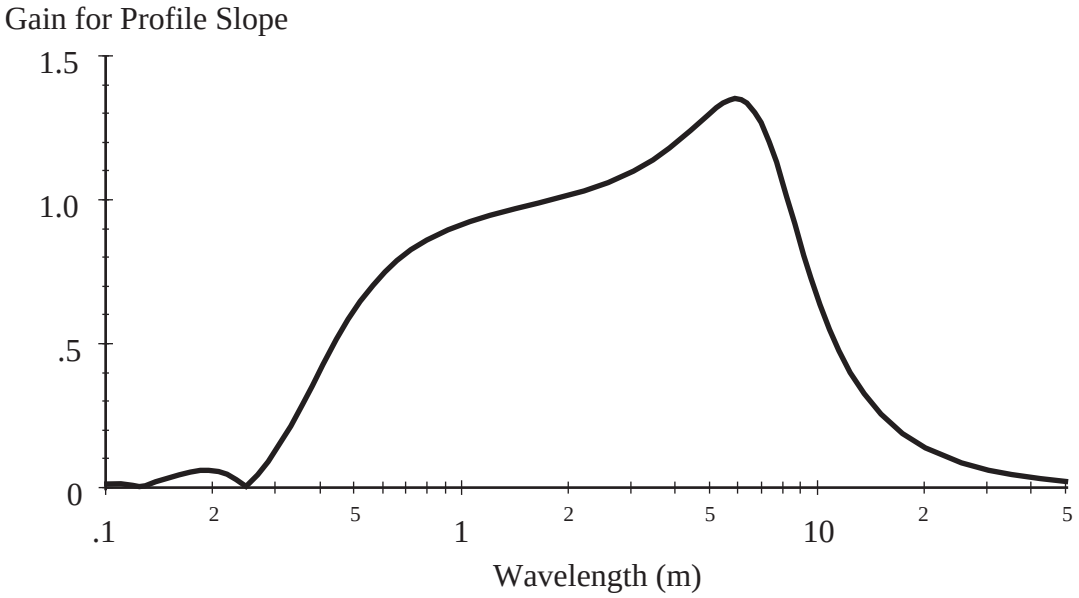


Figure 5. RN gain for profile slope.

A recent study of profile measurement procedures reported that a second order Butterworth high-pass filter did not reduce the RN of an artificial white noise slope profile more than 0.1 percent until the cutoff value fell below 17.4 m (57.1 ft).[28] The same type of analysis for this study verified the 17.4 m (57.1 ft) cutoff, and showed that a 1 percent reduction occurred when the cutoff wavelength was about 8.6 m (28.2 ft).

Michigan Ride Quality Index

In the late 1960s, the Michigan Department of State Highways sought to develop a roughness index to predict user opinion from profile. A research study linked user opinion to wavelengths in profile power spectral density (PSD) functions.[33] Based on this work, the Department developed a set of electronic filters to produce a profile-based statistic called Ride Quality Index (RQI).[34] The RQI is composed of profile response in three wavebands. Each waveband is isolated using third-order Butterworth filters (both low-pass and high-pass) with cutoff values of 0.61 to 1.52 m (2 to 5 ft) for the "short" waveband, 1.52 to 7.62 m (5 to 25 ft) for the "medium" waveband, and 7.62 to 15.24 m

(25 to 50 ft) for the "long" waveband. The variance in each waveband is calculated after filtering, and the overall index is:

$$RQI = 3.077 \bullet ln(VAR_1 \bullet 10^8) + 6.154 \bullet ln(VAR_2 \bullet 10^8) + 9.231 \bullet ln(VAR_3 \bullet 10^8) + 141.85 \quad (2)$$

where VAR_1 is the variance in the longer waveband, VAR_2 is the variance on the middle waveband, and VAR_3 is the variance in the short waveband.

Figure 6 shows the sensitivity of each waveband to profile slope after applying the weighting coefficients in equation 2. (Strictly speaking, the plot does not represent the relative influence of each waveband on the overall index. This is because the coefficients are applied after the variance values are passed through a logarithm. This step will tend to moderate the influence of each waveband compared to the others.) Note that when the gain characteristics are cast in terms of slope, the short waveband appears to be less important to the overall index than equation 2 may imply. Table 1 lists the thresholds at which the gain for each waveband passes below 1 percent of the peak value. For the long waveband, the long wavelength threshold is 180.0 m (591 ft). For the short waveband, the short wavelength threshold is 0.22 m (0.72 ft).

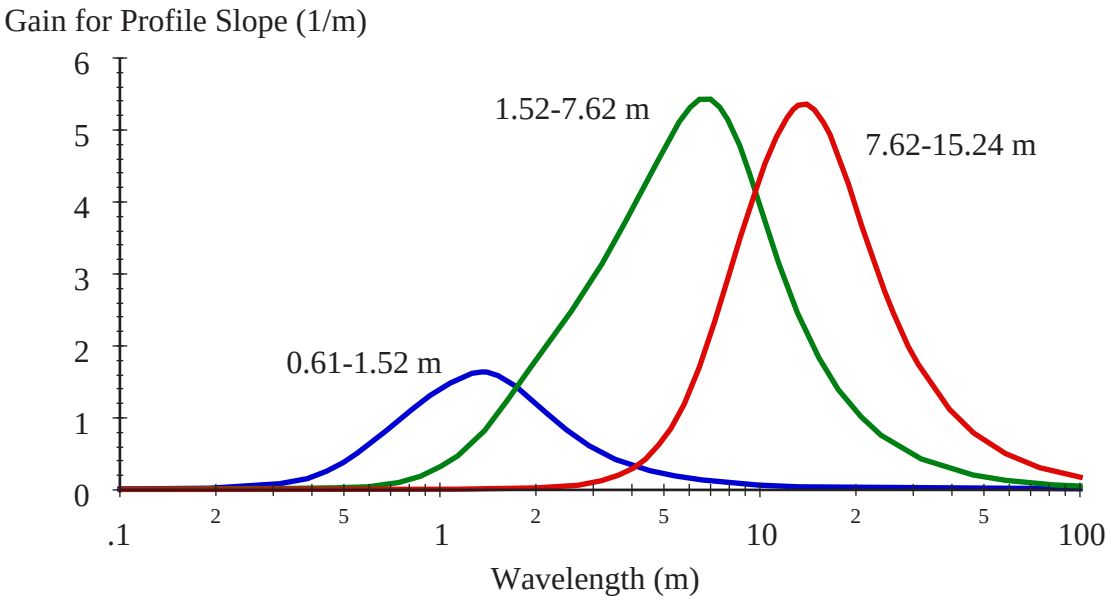


Figure 6. RQI gain for profile slope.

Truck Response Indices

Multiple indices have been proposed for estimating the effect of roads on the dynamic response of trucks. De Pont measured the dynamic wheel forces imposed by a heavy truck on 68 road segments, and characterized the level of dynamic loading using the dynamic load coefficient (DLC).[35] The dynamic load coefficient is the standard deviation of the truck axle load, normalized by its mean value.[36] The study examined several alternatives to the IRI, using the linear quarter-car model with various sets of

suspension, tire, and mass properties that have appeared in the literature. The study also examined a non-linear version of the IRI, which included a typical level of truck suspension friction. None of the alternatives predicted DLC better than the IRI. The results of this study suggest that the wavelength of interest for the IRI may capture most of the information that is needed to predict dynamic tire loads.

Truck Ride Number

Hassan created a roughness index for prediction of truck driver opinion of ride quality from measured profile.[37] This study optimized a roughness index for correlation to the opinion of 30 truck drivers in 28 trucks over 29 roads in Victoria, Australia. The index was calculated from profile slope PSD in third octave bands. The optimal index included a range of roughness from a center frequency of 0.0513 cycles/m (0.0156 cycles/ft) to a center frequency 0.2051 cycles/m (0.0625 cycles/ft). This corresponds to wavelengths from 4.9 m (16 ft) through 19.5 m (64 ft). The root mean square profile slope over the seven bands are calculated to form a "PI" value, which is used to compute the Truck Ride Number (TRN) on a 0-to-5 scale:

$$TRN = 5 \bullet e^{-159 \bullet PI^{0.865}} \tag{3}$$

Note that the total range extends beyond the wavelengths at the center frequencies. The actual range is 4.34 m (14.3 ft) through 21.9 m (71.8 ft).

Roughness Index for Driving Expenditure

Papagiannakis proposed a predictive roughness index for driving expenditure (RIDE).[38] The intent of the index was to estimate truck operating costs from road profile. The index applies a measured transfer function of truck acceleration response to the PSD of profile slope. The resultant spectral density of predicted acceleration (above the trailer suspension) is then integrated to obtain the mean square acceleration. The transfer function, shown in figure 7, was measured on a reference vehicle owned by the National Research Council of Canada (NRCC) traveling at 80 km/h (50 mi/h). The index covers a range of frequencies from "0 to 50 Hz." At 80 km/h (50 mi/h), this is a range of wavelengths from infinity down to about 0.44 m (1.46 ft). (Of course, the response of the index does diminish as the frequency approaches zero, but the details of this are not clear within the literature.)

The response of the index is most concentrated in the range from 2.5 to 4.5 Hz, which corresponds to wavelengths from 4.9 to 8.9 m (16.2 to 29.2 ft) at 80 km/h (50 mi/h). This critical frequency range was determined by the stiffness of the test vehicle suspension and the amount of weight supported by it. Although the test trailer is treated in the index development as a reference vehicle, it is mounted with a rather uncommon rubber block suspension. Tests at a suspension measurement facility found that this suspension is stiffer than typical highway trailer suspension, which explains the emphasis on a relatively high natural frequency for body motion.[40,41]

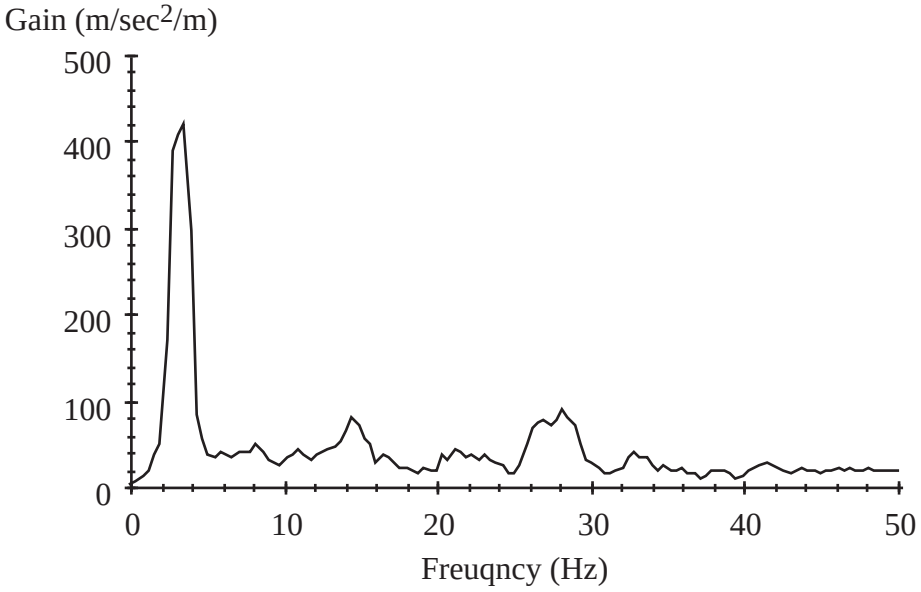


Figure 7. NRCC test vehicle transfer function.(39)

Truck Ride Index

Prem proposed a suite of roughness indices to cover a range of truck responses relevant to pavement asset management.(42) The indices are based on a three degree of freedom model of vertical truck vibration, encompassing the quarter-truck model for vehicle behavior and a driver and seat model for occupant comfort. The Truck Ride Index (TRI) is calculated in the following steps:

Step 1: Apply a quarter-car model to the profile with a standard set of parameters that were selected to represent a standard truck. Versions were proposed for speeds of 60 km/h (37.3 mi/h) and 100 km/h (62.1 mi/h).

Step 2: Apply a driver and seat model to the result, using the motion of the sprung mass as input.

Step 3: Apply the frequency weighting curve for human tolerance to vertical vibration from British Standard BS 6841.

Step 4: Calculate the root mean square weighted acceleration.

Figure 8 shows the quarter-car model, with a driver and seat model added above the vehicle body mass. This illustrates the process in concept, but the quarter-car model and driver/seat model are not coupled in the actual calculation.

Figure 9 shows the sensitivity to profile slope of the TRI at 100 km/h (62.1 mi/h). This transfer function includes the influence of four filters: (1) a moving average with a baselength of 300 mm (11.8 in), (2) a quarter-car model, (3) a one degree of freedom seat and driver model, and (4) a frequency weighting for human discomfort. The discomfort weighting must be applied using the same simulated travel speed as the quarter-car model. Together, these four items define the wavelength sensitivity of the TRI.

The TRI at 100 km/h (62.1 mi/h) is most sensitive to wavelengths from 7.1 to 17.3 m (23.3 to 56.8 ft), with a peak value of sensitivity at 10.8 m (35.5 ft). The IRI covers a very broad range of wavelengths. Relative to the IRI, the TRI at 100 km/h (62.1 mi/h) emphasizes long wavelength content, including significant values of gain for wavelengths above 50 m (164 ft). For example, the gain does not fall beneath 1 percent of the peak value until the wavelength is shorter than 3.7 m (12 ft) or longer than 41.1 m (135 ft).

Prem proposed other indices that apply the same model and use the same mechanical properties, but summarize other responses on the vehicle. For example, the Dynamic Loading Index (DLI) is based on the root mean square of predicted dynamic wheel force. (This response is proportional to $z_r - z_u$.)

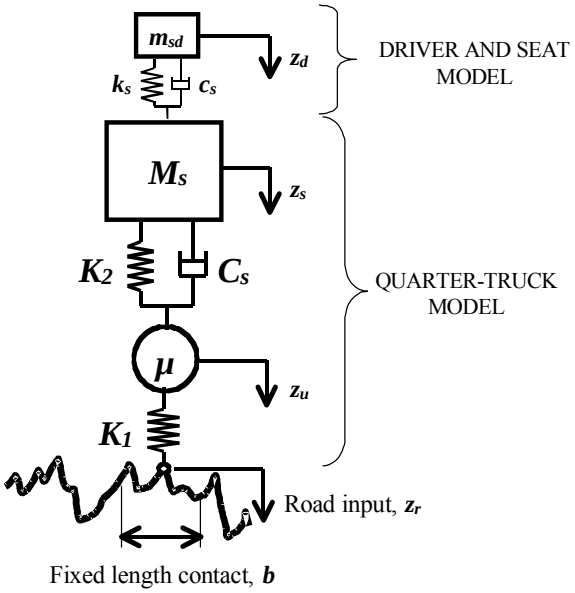


Figure 8. Prem model of truck response to road roughness.[12]

Simulated California Profilograph Index

A common use of lightweight profilers is to simulate the response of a California profilograph for construction quality control and assurance. Figure 10 shows the response of a simulated California profilograph to profile slope. The response covers a very broad range of wavelengths. The gain does not reduce to less than 1 percent of the peak value until a wavelength of over 1000 m (3281 ft) on the long end of the range and a wavelength of lower than 0.1 m (0.33 ft) on the short end.

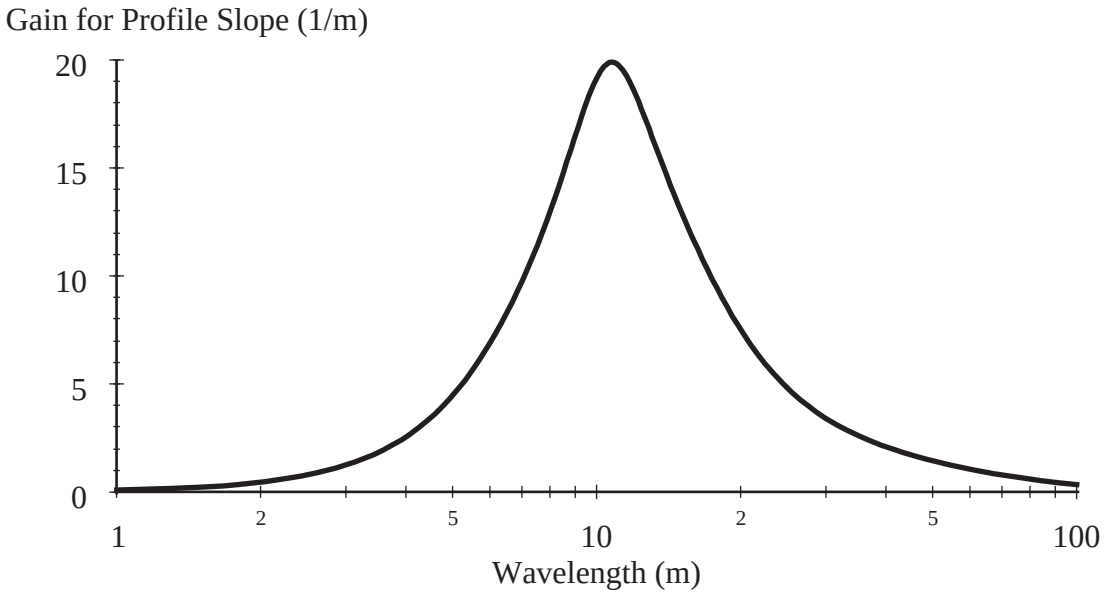


Figure 9. TRI gain for profile slope.[1]

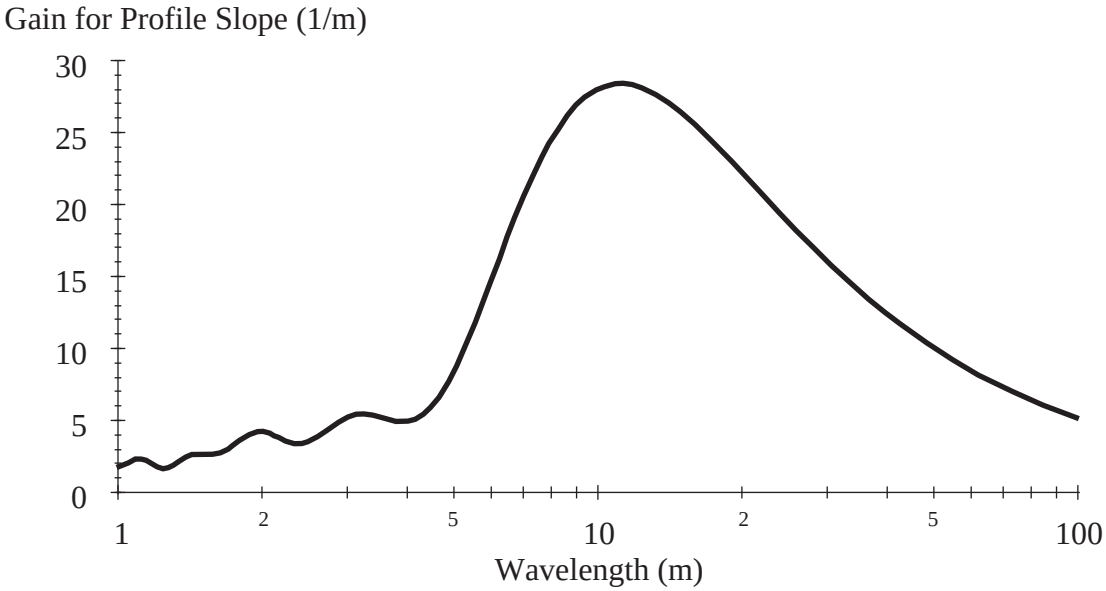


Figure 10. Simulated California profilograph, gain for profile slope.

Automated profilograph trace reduction procedures have evolved into very systematic and objective algorithms.(43) However, the non-linear aspects of the algorithm, such as the use of a blanking band and the practice of accumulating the index as the sum of scallops, makes the precise influence of each portion of the waveband on the final index

[1] This plot does not look like the one provided by Prem.(12,42) Prem shows the transfer function for profile slope to occupant spatial vertical velocity. Since the index is calculated from acceleration, figure 9 shows the transfer function from profile slope to spatial acceleration. This provides a more relevant comparison to the other transfer functions in this chapter.

value hard to predict. Figure 10 shows that content from about 7 to 30 m (23 to 98 ft) is likely to dominate the location and number of scallops, but content over the rest of the range affects the size of those scallops. This is particularly true when a null blanking band is used. Indeed, the point of the null band is to include short wavelength, low amplitude, "chatter" in the measurement.(44)

The response of a profilograph to long wavelength content is very high. However, most profilograph reduction algorithms include some provision for trend removal.(45) Often, profilograph trace reduction algorithms rely on the native high-pass filter that is applied by the profiler to provide drift removal. These procedures ensure that the trace follows the datum line faithfully, so that inflections within the profile that affect vehicles generate a scallop by crossing that line. When trend removal is applied as a component of simulated trace reduction, the California profilograph index does not challenge the long wavelength range of interest for a reference device. In fact, index calculations that are made from profile should include a standardized high-pass filter or drift removal procedure, to prevent long-wavelength content from carrying potential shorter, and more relevant, scallops away from the zero datum line.

The gain for slope at short wavelengths is small, but the content there is significant under a null blanking band. However, most profiler generated profilograph traces pass through a smoothing filter before they are reduced. Typically, the filter is a third-order Butterworth low-pass filter with a cutoff wavelength of 0.6 m (2 ft). This procedure, rather than the content of the original trace, determine the short wavelength sensitivity of the profilograph index (PI). Nevertheless, quality estimates of profilograph response from profilers require careful selection of sampling procedures and sensor footprint, particularly under a null blanking band.(46)

WAVELENGTH RANGE ANALYSIS

The wavelength response plot provides a very useful snapshot of the sensitivity of a profile index. However, an objective definition of the range requires more detailed analysis. For example, the IRI is often thought of as an analysis procedure that takes a profile as input and produces an index value as output. The IRI algorithm is actually a linear filter that takes a profile, in units of elevation, as input and produces a modified signal, in units of slope, as output. The final IRI is the average rectified value of the output signal.

Linear Response Theory

Well-established methods exist for studying the contribution of a given frequency range to the overall statistical properties of random signals.(47) They are typically developed for the temporal frequency domain, but have been adapted for the spatial frequency, or *wave number*, domain.(48,49) The key mathematical equations from the literature are repeated here for the spatial frequency domain. Afterward, they are used to calculate the wavelength range of interest for several roughness indices. For a simple vehicle simulation model, such as the quarter-car model used within the IRI calculation,

the conversion from temporal frequency to spatial frequency is done by relating wave number (ν) to frequency (f) using the traveling speed (V):

$$\nu = f / \mathrm{V} \tag{4}$$

Note that wave number has units of cycles per length, and is the inverse of wavelength (λ):

$$\nu = 1/\lambda \tag{5}$$

If a stationary random signal passes through a linear process, the output signal will also be stationary and random. Further, the spectral density of the output profile is related to the spectral density of the input signal by:

$$G_{out}(\nu) = \left|H(\nu)\right|^2 \bullet G_{in}(\nu) \tag{6}$$

Where G_{in} is the spectral density of the input signal, expressed as a function of wave number, H is the linear response gain, and G_{out} is the spectral density of the output signal.

Using equation 6, the spectral density of the output signal may be calculated if the spectral density of the input signal and the response gain are known. Figure 11 illustrates the calculation. The road profile slope PSD serves as the input, G_{in}. The transfer function, H, of the IRI algorithm is applied to it. The transfer function in figure 11 does not have the same appearance as the one shown in figure 4, because it has been squared. The result, G_{out}, is the PSD shown at the right of the figure. Note that the output transfer function exhibits features of both the input profile spectrum and the IRI transfer function, such as a bias toward low wave numbers (long wavelengths) and two local peak values, respectively.

Equation 6 and figure 11 demonstrate routine methods of linear response theory. This type of analysis appears in the classical literature for a two degree of freedom system similar to the quarter-car model.[50,51]

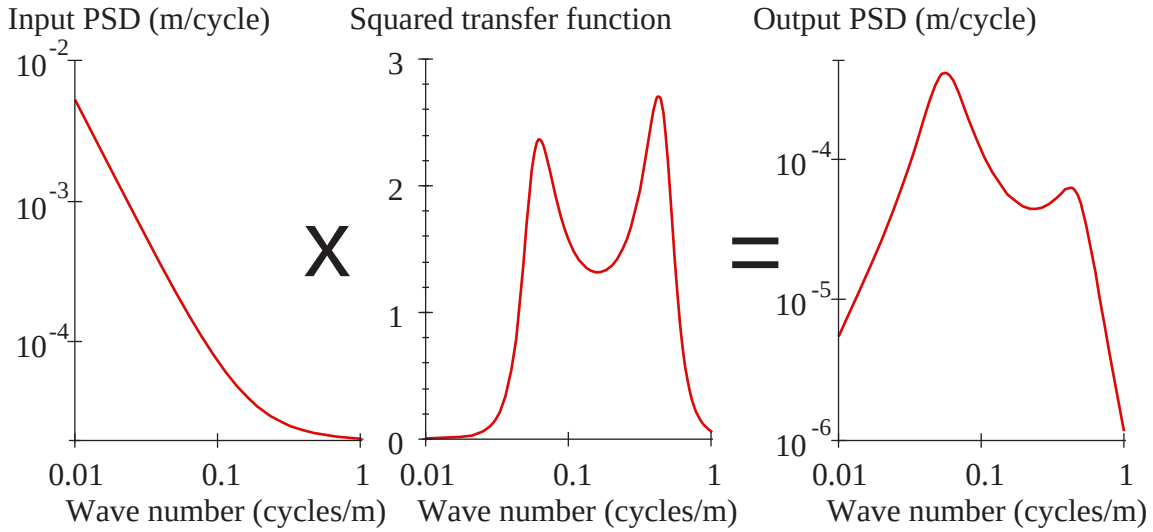


Figure 11. Relationship between input and output slope PSD functions.

Spectral densities are scaled so that they function as the partial derivative of mean square with respect to wave number. Thus, the integral of a spectral density function is the mean square of the overall signal. Further, the mean square is equal to the variance when the mean of the signal is zero. For a one-sided spectral density function[2], the variance is calculated as follows:

$$\sigma^2 = \int_0^\infty G_{out}(\nu) \bullet d\nu \tag{7}$$

Or:

$$\sigma^2 = \int_0^\infty |H(\nu)|^2 \bullet G_{in}(\nu) \bullet d\nu \tag{8}$$

If the input signal is Gaussian[3], the output signal will be Gaussian as well. In this case, the average rectified value is proportional to the root mean square.(48)

$$ARV = \sqrt{\frac{2}{\pi}} \bullet \sigma \tag{9}$$

Thus, the expected value of IRI for a road profile may be estimated using equations 8 and 9 if the profile is Gaussian and its spectral density is known. Further, the contribution to the IRI of a given range of wavelengths from λ_2 to λ_1 (wave numbers from ν_1 to ν_2) can be estimated:

$$\sigma_{2-1}{}^2 = \int_{\nu_1}^{\nu_2} |H(\nu)|^2 \bullet G_{in}(\nu) \bullet d\nu \tag{10}$$

Equations 8 and 10 are very useful when interpreting PSD functions. Equation 8 means that the area under a PSD is equal to its overall mean square value. Equation 10 means that the area under the curve over some range of wave numbers equals the contribution to mean square of that range. With this in mind, the relative contribution of a given range of wavelengths to a roughness index may be estimated at a glance. However, figure 11 provides a skewed visual representation of this because of the log scaling. In figure 11, the low wave number (long wavelength) range erroneously appears to be the most significant to the mean square of the output. Figure 12, which shows the same data with linear scaling, provides a more appropriate view. In figure 12, the relative contribution of each range of wave numbers is displayed in correct proportion, and the high wave number (short wavelength) range appears more significant.

The ratio of $\sigma_{2\text{-}1}$ to σ defines the fraction of a mean square roughness index that resulted from content in the wavelength range from λ_1 to λ_2. This relationship also holds for the IRI, as long as the original profile was Gaussian. (Few road profiles truly are

---

[2] See reference 47 for a definition of "one-sided spectral denisty function."

[3] See reference 47 for a definition of "Gaussian."

Gaussian. Nevertheless, the methods described here provide an objective method of estimating the wavelength range of interest for a roughness index.) This method will be used to calculate how much of the wavelength range may be excluded at either end without causing significant errors in the final roughness value.

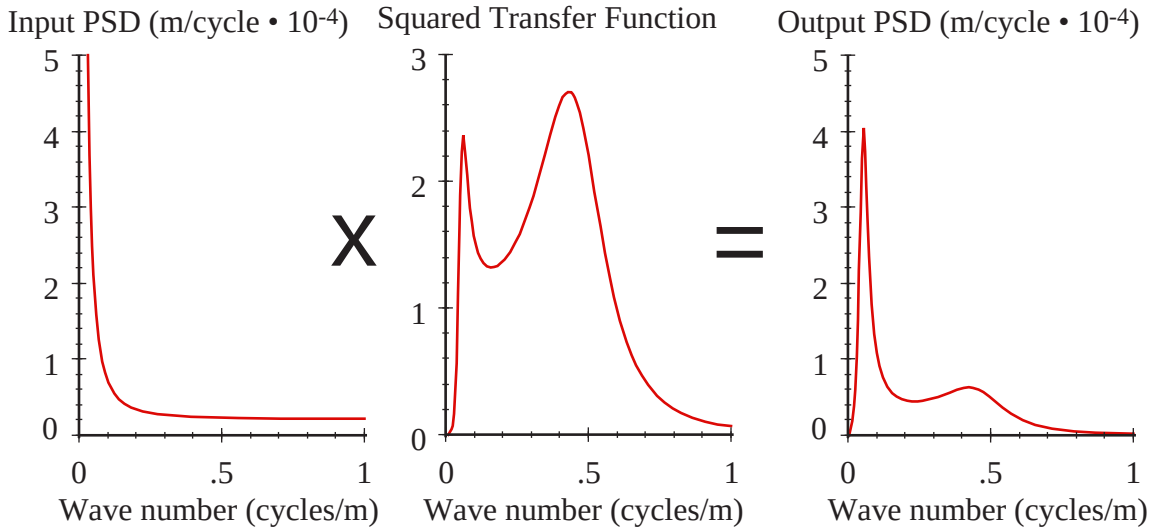


Figure 12. Linear response with linear scaling.

Input Spectra

Several spectral models of single-track road profiles have been proposed in the literature.[15,52,53,54,55,56] These models fit measured road spectral density functions to an assumed standard shape. La Barre proposed a spectral model for European roads in which PSD of profile slope was constant for high wave numbers (short wavelengths), but the PSD of elevation was constant for low wave numbers (long wavelengths).[54] Equation 11 shows the model for PSD of slope:

$$G'(\nu) = G_0 \bullet \left[1 + \left(\frac{\nu_0}{\nu}\right)^2\right] \tag{11}$$

Note that G_0 and ν_0 are constants within the model. The first term in the brackets corresponds to a slope PSD with uniform content over all wave numbers. A stationary random signal of this kind is called *white noise slope*. The second term corresponds to an elevation PSD with uniform content over all wave numbers (i.e., *white noise elevation*). The break point between white noise slope and white noise elevation is determined by the value of ν_0. A study of European roads found that the break point to be about 15.2 m (50 ft) for "rigid constructions" and 6.1 m (20 ft) for "flexible constructions."

Robson suggested an alternative model for PSD of elevation:[56]

$$G(\nu) = G_0 \bullet \nu^{-2.5} \tag{12}$$

This model provides an appealing summary of the overall roughness of the road, because it includes a single fitting parameter (G_0) that increases in proportion to the mean square

of roughness. However, it is restricted to a prescribed balance between long and short wavelength content that is often not appropriate. For this study, the LaBarre and Robson models do not provide enough flexibility to study the waveband of interest for a roughness index over diverse road types. In particular, a desirable spectral model must provide a mathematical representation of "wavy" roads with significant long wavelength content, as well as "choppy" roads with significant short wavelength content.

Sayers proposed a model that combines white noise elevation, white noise slope, and white noise (spatial) acceleration. For PSD of elevation, the model is:

$$G(\nu) = G_e + \frac{G_s}{(2\pi\nu)^2} + \frac{G_a}{(2\pi\nu)^4} \tag{13}$$

Where G_e, G_s and G_a are constants that must be fitted to a measured PSD. For slope, the model is:

$$G'(\nu) = \frac{G_e}{(2\pi\nu)^{-2}} + G_s + \frac{G_a}{(2\pi\nu)^2} \tag{14}$$

This model is much more general.[57] It provides a way to study the response of roughness indices to a variety of roads. Sayers provided coefficients for four example roads that cover a diverse range of spectral shape: (1) a "normal" road of moderate roughness, (2) a road with long wavelengths, (3) a rough road with some short wavelength content, and (4) a "limit roughness" case.[49] Table 2 provides the coefficients.

Table 2. Model coefficients for four sample roads.[49]

Name	Description	G_a 1/(m•cycle) x 10^{-6}	G_s m/cycle x 10^{-6}	G_e m^3/cycle x 10^{-6}
Road 1	Normal	0	20	0
Road 2	Long Waves	7	20	0
Road 3	Short Waves	0	100	1
Road 4	Limit Roughness	0	300	8

Note that equation 14 may be directly linked to equation 11. For a ν_0 value that corresponds to a wavelength of about 6.1 m (20 ft), cited as an appropriate value for "flexible constructions," the ratio G_a/G_S is 1.06. For a ν_0 value that corresponds to a wavelength of about 15.2 m (50 ft), cited as an appropriate value for "rigid constructions", the ratio G_a/G_S is 0.17.

These four roads provide a very diverse set of examples. The "normal" road is white noise slope, which crudely approximates many in-service pavements on moderate roughness. The "long waves" road includes a balance between white noise slope and white noise elevation that is typical of many fresh asphalt overlays. This is because the paving operation removes short wavelength content, but the lack of grade control often leaves the long wavelength content unmodified. Long wavelength content, which is represented by white noise elevation, therefore dominates the roughness of the finished product. The "short waves" road has a balance between white noise acceleration and white noise slope that is common among many new or un-distressed concrete pavements.

This is because concrete pavements are often built with careful grade control, which helps eliminate long wavelength roughness. The "limit roughness" road represents the skew toward short wavelength roughness (white noise acceleration) that exists on pavements with significant surface distress. Note that the overall roughness level of these examples will not affect the analyses discussed below. Rather, the relative importance of each part of the waveband will determine the results.

Analysis Results

This section systematically examines the wavelength range of interest for the IRI, PTRN, RQI, TRN, TRI, and DLI. The wavelength range for the IRI is also analyzed at two alternate simulation speeds: 40 km/h (25 mi/h) and 120 km/h (75 mi/h). These options are given the name "Golden Car 40" (GC_{40}) and "Golden Car 120" (GC_{120}). The DLI and TRI were analyzed at their simulation speed of 100 km/h (62.1 mi/h), and the TRI was analyzed again at a simulation speed of 60 km/h (37.3 mi/h). The three wavebands for the RQI were treated separately, because the nonlinear aspects of combining them would complicate the analysis.

This study derived the PSD for the response of each index to the four profile PSDs listed in table 2. The output PSD was then decimated from the long wavelength side until the predicted roughness reduced by 1 percent. Figure 13 shows the outcome for the IRI and the PTRN. The figure shows the error level that occurs when all content above a given wavelength is omitted from the input profile PSD. A negative value of error indicates that the index would be underestimated. An absolute error of 1 percent is considered unacceptable, as shown. For the "normal" road, the IRI reaches the threshold when the content above wavelengths of 18 m (59.1 ft) is removed. The PTRN reaches the threshold at a wavelength of 7.6 m (24.9 ft).

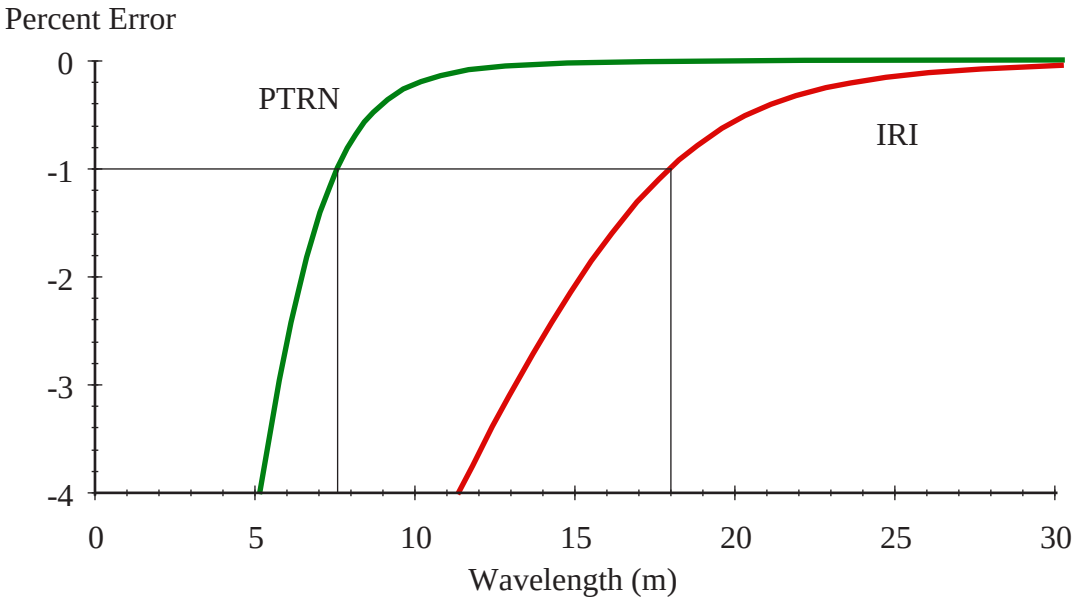


Figure 13. Index error estimate for Road 1.

Table 3 lists long wavelength thresholds. The threshold for each index was at a maximum on Road 2, which had the most significant long wavelength content. The DLI_{100} had the longest threshold, at 107.1 m (353.6 ft). However, the sensitivity to such long wavelengths may be a simple artifact of the index's linear calculation method. (The Golden Car model used for the calculation of IRI would produce a similarly long threshold if it was used to calculate an index based on tire load, rather than suspension stroke.) Very long wavelength features on the road typically cause low acceleration levels in trucks. For low input levels, truck suspension friction increases their effective stiffness, and drives up the natural frequency of response. As a result, the roll-off in response toward long wavelengths is probably more aggressive than a quarter-car filter would predict. No other index emphasizes wavelengths that are so long. The next longest threshold occurred for the GC_{120} on Road 2. In this case, the threshold was 52.6 m (172.4 ft). Since this index is likely to go into practice over the next decade, the waveband of interest for a reference profiler must extend to a value greater than or equal to 52.6 m (172.4 ft).

Interpret the long wavelength boundary with care. This should not be recommended as a high-pass filter cutoff value. A filter cutoff value typically describes the wavelength at which the gain is reduced to about 70.7 percent. A high-pass filter with a cutoff value of 52.6 m (172.4 ft) would remove content from the profile that is significant to many of the indices listed in table 3. Instead, most filters should apply a cutoff that is much longer than 52.6 m (172.4 ft). For example, the third-order Butterworth filter with a cutoff wavelength of 60.9 m (200 ft) has a gain value of about 0.84 at a wavelength of 52.6 m (172.4 ft). Alternatively, the gain is about 0.98 when the cutoff value is 91.44 m (300 ft).

Table 4 shows the short wavelength thresholds. As expected, the PTRN and the short waveband of the RQI require the shortest wavelengths. The shortest threshold occurs on Road 4, where short wavelength content is the most significant. The shortest threshold value, 0.17 m (0.56 ft), is actually shorter than the baselength used by the IRI and RN to help represent tire envelopment. With this in mind, it is very important that a profiler provide data that properly represents the enveloping properties of common tires. This may be done in two ways. One type of valid profiler may measure the road surface in great detail, so that the shape of the road profile is reproduced down to wavelength values smaller than 0.17 m (0.56 ft). (Chapter 6 will explain that this requires a sampling interval much smaller than 0.17 m (0.56 ft).) A low-pass filter with bridging and enveloping properties similar to that of a tire would then be used to provide the proper low-pass filtering. A second type of valid profiler may sense the pavement in a manner that is analogous to a common tire.

Table 3. Long wavelength thresholds.

	wavelength at 1 percent error (m)			
Index	Road 1	Road 2	Road 3	Road 4
IRI	18.0	33.7	17.7	17.3
GC_{40}	9.2	14.9	8.8	8.2
GC_{120}	26.9	**52.6**	26.7	26.4
PTRN	7.6	12.1	6.8	6.0
RQI_{LONG}	19.7	26.9	19.7	19.7
RQI_{MEDIUM}	7.8	11.0	7.7	7.5
RQI_{SHORT}	1.9	1.9	1.7	1.6
TRN	20.3	21.5	20.2	20.2
TRI_{100}	20.6	38.6	20.6	20.5
TRI_{60}	12.4	22.1	12.3	12.3
DLI_{100}	19.3	**107.8**	19.2	19.0

Table 4. Short wavelength thresholds.

	wavelength at 1 percent error (m)			
Index	Road 1	Road 2	Road 3	Road 4
IRI	1.13	1.51	1.02	0.90
GC_{40}	0.64	0.71	0.56	0.51
GC_{120}	1.63	2.48	1.53	1.39
PTRN	0.37	0.39	0.19	**0.17**
RQI_{LONG}	4.25	5.61	4.22	4.18
RQI_{MEDIUM}	0.93	1.06	0.83	0.73
RQI_{SHORT}	0.35	0.36	0.24	0.21
TRN	4.42	4.59	4.41	4.41
TRI_{100}	4.30	6.00	4.26	4.21
TRI_{60}	2.61	3.39	2.55	2.47
DLI_{100}	1.34	4.12	1.00	0.71

CHAPTER 4. ACCURACY REQUIREMENTS

This chapter explores accuracy requirements for a reference profiling device over the wavelength range from 0.15 to 67 m (6 in to 220 ft). The concept of placing limits on resolution, precision and bias of profile elevation readings is rejected. This is because the amplitude of an elevation profile is typically dominated by the longest wavelengths that are included. As a result, precision and bias requirements place an unwarranted premium on the measurement of long wavelength content. Worse yet, a profiler may satisfy precision and bias criteria, even if it does a poor job of measuring short wavelength content.

The recommended accuracy requirements are based on the profiler "gain." Within this concept, the true profile is considered an input, and the measured profile is considered the output. For a gain of 1 across the entire spectrum and no phase distortion, the true profile is reproduced perfectly. The gain requirement recommended here extends a method by Prem to include all of the indices listed in tables 3 and 4. The gain requirement guarantees that all of the indices are measured with an error of no more than 1.00 percent.

Requirement: *A reference profiler must have a gain error no greater than 1.00 percent for wavelengths from 0.15 to 0.35 m (6 in to 1.16 ft), no greater than 0.25 percent for wavelengths from 0.35 to 35.9 m (1.16 to 118 ft), and no greater than 1.00 percent for wavelengths from 35.9 to 67 m (118 to 220 ft).*

The gain error will be calculated though comparison to extremely accurate benchmark profile measurements, as described in chapter 7. As described in chapter 6, the gain for the short wavelength portion of the range may be much less than one, so long as the roll-off is sufficiently similar to that of a vehicle tire. The candidate reference profiler gain will be the average of the gain characteristics for at least five test sections, calculated over one-third octave bands. Each test section shall be at least 160.9 m (528 ft) long. The gain shall be calculated from the PSD of profile slope. One section shall cover twice the length for special evaluation of long wavelength content.

Requirement: *A reference profiler must exhibit no inherent phase distortion over the wavelength range from 0.15 to 67 m (6 in to 220 ft).*

Phase distortion is not permitted over the wavelength range of interest, because the reference device must serve as a benchmark for production profiler performance, which includes limits on phase distortion.

Reference profiling devices do not serve as the verification standard for longitudinal distance measurement. Nevertheless, profile accuracy, and accuracy in profile index values, depend on accurate longitudinal distance measurement.

Requirement: *A reference profiler must measure longitudinal distance correctly to within 0.1 percent.*

This is a common standard for inertial profilers as well.

Measurement of reference-quality profiles requires very accurate placement of the device along the lateral position of interest. Nevertheless, no explicit requirement is recommended for lateral tracking accuracy. Instead, the impact of lateral tracking errors is incorporated into the accuracy requirements implicitly, inasmuch as poor tracking performance will penalize the accuracy ratings defined in this chapter, and the repeatability ratings defined in chapter 7.

Recommendation: *No explicit requirement is needed for lateral tracking accuracy. Advise designers and operators of candidate profiling devices that poor lateral tracking is likely to critically degrade their accuracy and repeatability.*

This chapter provides the basis for these recommendations. A review of profiler precision and bias criteria is provided. The gain method recommended by Prem is reviewed in detail. This method was originally developed to verify a profiler's ability to measure the waveband of interest for the IRI. This method is extended to the waveband of interest for multiple applications, and improved to include a more systematic treatment of the relevant wavelength range. Finally, longitudinal distance measurement and lateral tracking are discussed.

ELEVATION RESOLUTION

Profile elevation resolution is a traditional method of placing engineering tolerances on profiler performance. Sayers proposed a classification system for devices that measure road roughness in the 1980s, when response-type systems were common.[25] The system included two classes for road profilers. Class 1 profilers provided "a series of accurate elevation points closely spaced along the traveled wheel path." Class 1 devices were reference profilers, with the ability to reproduce the true profile accurately. Class 2 devices provided profiles with sufficient accuracy for road surveys of IRI, but without the reproducibility needed for Class 1 applications. Class 2 devices were expected to include high-speed profilers with no provisions for reducing lateral wander from the intended wheel path. The report observed that wander affected the IRI by up to 5 percent on road segments that were 320 m (1056 ft) long.

The classification system quoted requirements for precision of individual elevation measures as follows:

$$\text{Class 1 precision (mm)} \leq 0.25 \bullet \text{IRI (m/km)} \quad (15)$$

$$\text{Class 2 precision (mm)} \leq 0.50 \bullet \text{IRI (m/km)} \quad (16)$$

Experiments determined that the needed precision was a function of roughness. For example, Class 1 status for a smooth road of 1 m/km (63.36 in/mi) required a precision level of 0.25 mm (10 mils). On a very smooth road of 0.5 m/km (31.68 in/mi), precision of 0.125 mm (5 mils) was required.

Specification of vertical resolution is a common practice. American Society for Testing and Materials (ASTM) Standard E 1364-95 requires vertical resolution values that depend on roughness, and are somewhat more stringent than equations 15 and 16.[58] The requirements are listed in table 5. ASTM E 950-98, which pertains to inertial profilers, requires 0.1 mm (4 mils) resolution for Class 1, 0.1–0.2 mm (4-8 mils)

resolution for Class 2, 0.2–0.5 m (8-20 mils) resolution for Class 3 and resolution greater than 0.5 mm (20 mils) for Class 4.[59] (Profiler manufacturers rarely quote anything but Class 1.) Expectations for accuracy in measurement of the PI are provided in ASTM E 1274-88.[60] It specifies recording resolution for digital systems of 0.25 mm (10 mils) and a calibrated accuracy of 0.5 mm (20 mils).

Table 5. Resolution requirements.[59]

IRI Range (m/km)	Resolution (mm)	
	Class 1	Class 2
0.0–0.5	0.125	0.25
0.5–1.0	0.25	0.5
1.0–3.0	0.5	1.0
3.0–5.0	1.0	2.0
5.0–7.0	1.5	3.0
≥ 7.0	2.0	4.0

Profiler manufacturers often quote the elevation resolution of their devices. Fernando listed the resolution value of 0.005 mm (0.2 mils) for an Australian Road Research Board (ARRB) Walking Profiler that participated in a profiler equipment evaluation experiment.[61] Currently, ARRB lists 0.01 mm (0.4 mils) per 250 mm (9.84 in) distance step in their advertisements for the Walking Profiler. Inertial profiler manufacturers typically list values of resolution for their devices of about 0.025 mm (1 mil), which is the maximum value allowed for compliance with AASHTO MP 11-03.[7] "Dynamic resolution," or the resolution that may be expected when an inertial profiler is operating at speed, may be much larger. Values of 0.06–0.282 mm (2.4-11.1 mils) have appeared in the literature.[28,62]

In this report, no specifications are recommended for elevation resolution. Resolution and precision of elevation measurements are typically much finer than their accuracy. A profiling device with the needed resolution may suffer from systematic errors in elevation that compromise its ability to provide the overall profile accurately. In one of the first major profiler comparison studies, Sayers lists a quoted resolution of 0.1 mm (4 mils) for rod and level elevation accuracy, but estimates a "more realistic accuracy figure" of 0.5 mm (20 mils).[63] The gap between these two values is attributed to difficulties in setting the rod precisely in the required location. ASTM E 950-98 specifies precision and bias values on profile elevation for a Class 1 of 0.38 mm (15 mils) and 1.25 mm (50 mils), respectively. These values are several times greater than the limits on resolution.

Instead of resolution requirements on individual elevation values, this chapter places performance requirements on the accuracy of the entire profile signal. The manufacturer of a profiling device is then free to choose the needed resolution as an aspect of the measurement method.

ELEVATION ACCURACY

ASTM E 950-98 is currently the most widely used method for rating the repeatability and accuracy of profilers.[59] It includes a classification system for profilers that is based

on a composite level of precision among repeat elevation measurements and a composite level of bias in elevation compared to a reference measurement. The values are based on a minimum of 10 profile measurements. The individual elevation measurements are compared over a distance of 320 m (1056 ft) at 0.3-m (1-ft) intervals. Class 1 performance requires a composite precision level of 0.38 mm (15 mils) or less, and a composite bias of 1.25 mm (50 mils) or less. AASHTO PP 49-03 and Texas Specification TEX-1001-S use the same method, but require a precision of no greater than 0.51 mm (20 mils) and a bias of no greater than 1.52 mm (60 mils).[64,65] These specifications also include some improvements in the statistical treatment of profile elevation values.

The main weakness of the "elevation precision and bias" approach is the emphasis on long wavelength content. In most road profiles, the amplitude of elevation content is roughly proportional to wavelength.[15,56] Thus, short wavelength features often appear as relatively small deviations in elevation. Comparison of elevation values prevents the detection of short wavelength measurement problems. The emphasis on long wavelength content also places a premium on the specific characteristics of the high-pass filter used in the profile computation. This is unfortunate, because the very long wavelength content is not of interest in most road applications. (See chapter 3.)

Precision

The precision of elevation at a given point is quantified by the standard deviation of all elevation measurements at that location. The composite precision level over the entire profile is the average of all standard deviation values. A major weakness of this approach is the placement of a tolerance on elevation that is the same over the entire wavelength range. Performing analyses on profile elevation over a broad range of wavelengths biases the results by assigning disproportionate weight to the long wavelength content.[26] Short wavelength content in a profile may be significant to important road qualities, even at a low amplitude. This is because the reversals between upward and downward slopes occur more quickly at shorter wavelengths, so a lower amplitude is needed to cause the same peak acceleration in a vehicle. The consequence of placing precision limits on elevation values over a broad waveband, therefore, is that short wavelength content may exhibit an unacceptable level of error with little penalty to the precision level.

Consider the influence profile elevation errors may have on the IRI. The wavelength response of the IRI is often characterized by the plot in figure 4. This plot provides the gain for profile *slope*. The response of the IRI is of the same order of magnitude for wavelengths ranging from about 1.3 to 30 m (4.27 to 98.4 ft). Errors in profile with roughly equal slope amplitudes are expected to have a similar impact on the IRI in this range.

The gain for profile *elevation* is shown in figure 14. This plot demonstrates that the IRI responds most heavily to elevation for wavelengths from 1.5 to 3 m (4.9 to 9.8 ft). Precision limits on elevation over a broad waveband are unnecessarily restrictive for wavelength content below 1.5 m (4.9 ft) and above 3 m (9.8 ft) to ensure the needed precision in the band from 1.5 to 3 m (4.9 to 9.8 ft). Worse yet, the threshold values may have to be insufficient in the 1.5 to 3 m (4.9 to 9.8 ft) range so that equipment can pass in the long wavelength range. (This is the case in current standards.)

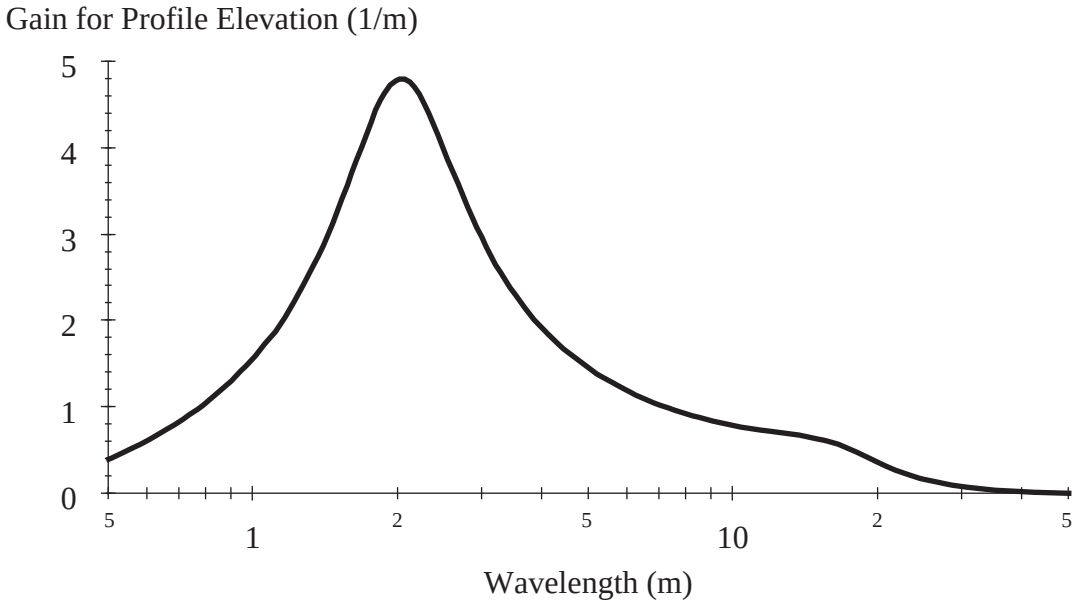


Figure 14. IRI gain for profile elevation.

Consider the profile shown in figure 15. This profile is pseudo-random white noise slope, which is a rough approximation of the spectral characteristics of common profiles. It was artificially generated using random numbers.(66) The level of white noise gives this profile an IRI value of about 1.82 m/km (115 in/mi). For this example, it will be treated as a reference measurement. If a profiler reproduced the reference profile measurement perfectly but applied a moving average to smooth it before the precision calculation, some of the short wavelength content would be missing.(67) Short wavelength features have low elevation amplitudes. They appear in the elevation trace as chatter but do not contribute to the larger fluctuations. Thus, applying the moving average may cause only a small standard deviation in elevation measurement error.

When the profile is smoothed using a 2.25-m (7.38-ft) moving average the trace in figure 16 is produced. The standard deviation of elevation error of this smoothed profile, when compared to the original, is 0.38 mm (15 mils). This is the Class 1 precision limit in ASTM E 950-98. This implies that wavelengths under 2.25 m (7.38 ft) need not even be included in the measurement to pass the precision criteria. Note that the smoothing reduced the overall IRI to 0.83 m/km (52.3 in/mi), which is less than half of the correct value.

Figure 17 shows the results when this example is repeated over a range of moving average baselength values. Figure 17 shows the variation in standard deviation of elevation measurement error that occurs as the baselength of the moving average is increased. The baselength must be increased to over 4.0 m (13.1 ft) before the AASHTO PP 49-03 precision limit is violated. When this filter is applied, the IRI is reduced to 0.58 m/km (36.7 in/mi). With a baselength of 4.0 m (13.1 ft), a significant portion of the wavelength range of interest for the IRI is removed, and much of the range of interest for the RN and RQI is removed.(32,68)

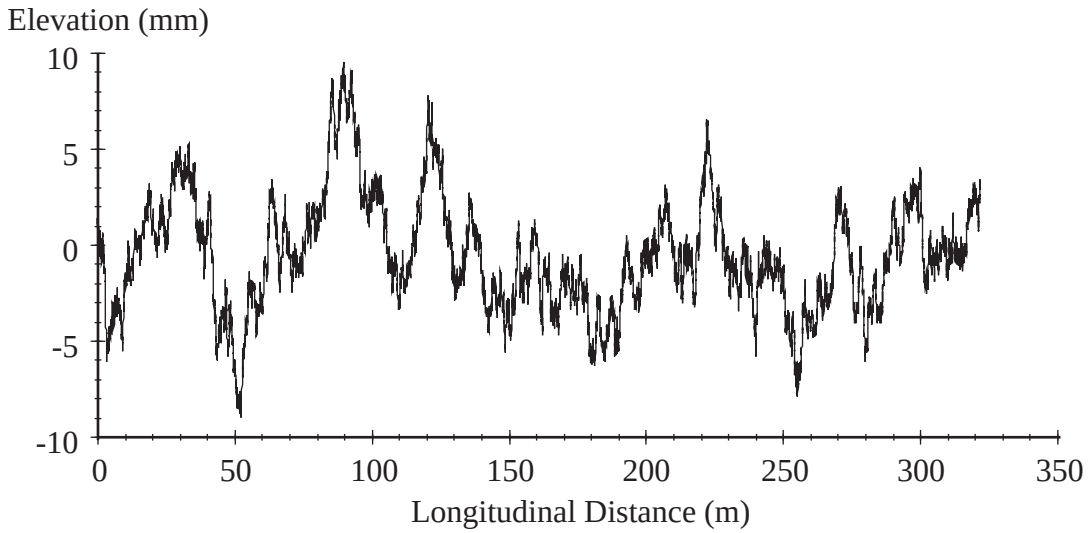


Figure 15. Sample white noise slope profile.

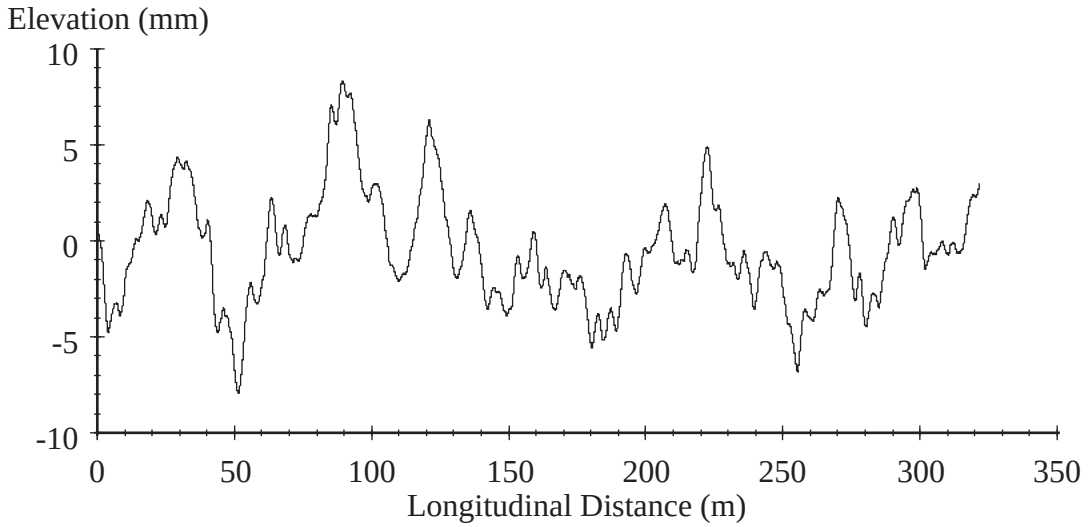


Figure 16. Sample profile smoothed with a 2.25-m (7.38-ft) moving average.

The example above demonstrates the indifference of the elevation precision criteria to omissions in short wavelength content. Additionally, a high level of spurious short wavelength content may exist within a profile measurement without causing a failure in precision requirements. Karamihas reported that when a sinusoidal error is added to a profile with a wavelength of 2.32 m (7.61 ft), it can add up to 1.52 m/km (96.3 in/mi) to the roughness of a profile without violating the ASTM E 950-98 Class 1 precision limit.[69]

Of course, the precise amount of the wavelength range ignored by the precision criterion depends on the specific wavelength content of the reference profile and the level of genuine error that exists in the test measurements. Further, this example made the assumption of Gaussian random roughness. Few profiles follow this assumption in practice because of the presence of localized rough features. Nevertheless, some

significant portion of the short wavelength range of interest is not sufficiently captured by placing limits on elevation precision.

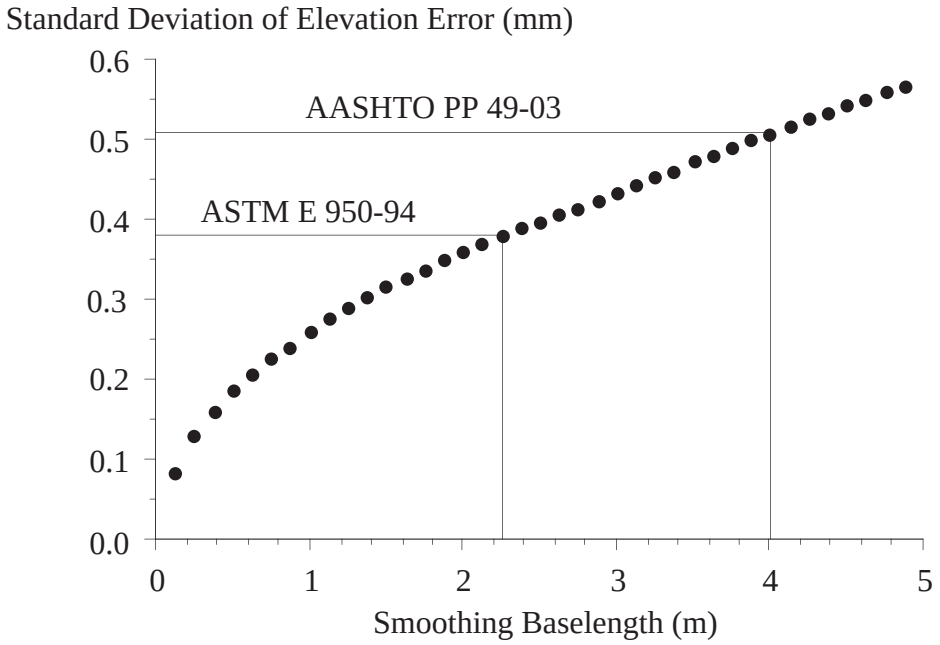


Figure 17. Standard deviation of elevation error, smoothed profiles.

Bias

Bias in elevation measurement at a given point is rated by comparing the elevation value at that point to the elevation value of a reference profile. The difference between the two is the bias level. Typically, the bias at an individual location is the average of 10 absolute bias measurements. The composite bias level over the entire profile is the average of all bias values. ASTM E 950-98 specifies an average bias limit of 1.25 mm (50 mils) for Class 1 equipment and 2.50 mm (100 mils) for Class 2 equipment.[59] AASHTO PP 49-03 and Texas Specification TEX-1001-S specify a maximum value of 1.52 mm (60 mils).[64,65]

Several theoretical cases can be imagined in which limiting the bias as defined above fails to emphasize the proper aspects of agreement between profile measurements. For example, ASTM E 950-98 does not specify a method of eliminating vertical offset between profiles, yet only rare applications of profile measurement are concerned with absolute elevation. A simple vertical offset between otherwise equivalent profiles will appear as a bias. In addition, many profiles that have been high-pass filtered to exclude wavelengths over 91.4 m (300 ft), as specified in the Standard, have an average elevation value under 1.25 mm (50 mils). It is therefore possible to qualify as a Class 1 instrument on a very smooth pavement by reporting a profile of all zeros. A thorough discussion of these and other statistical weaknesses of ASTM E 950-98 is provided by Li.[70]

Like the precision criteria discussed above, the bias criterion places too much emphasis on long wavelength content and may ignore critical levels of error in the measurement of short wavelength features. In particular, the practice of applying the

same high-pass filter to the reference measurement as the profiler under comparison governs the critical waveband. Most profilers apply a high-pass filter with a cutoff wavelength of about 91.4 m (300 ft) that is designed to avoid modifying wavelength content below 60 m (197 ft). Not all of this range is needed in most applications.[15] Since profile elevation in a given waveband is roughly proportional to wavelength, the longest part of the included waveband will have the greatest influence on the results, even though the wavelength range over about 35 m (115 ft) affects the IRI very little.

Li suggested some important improvements to the statistical methods used in ASTM E 950-98.[70] Although many of the suggested practices are used with AASHTO PP 49-03 and Tex-1001-S, they do not improve the relevance of specifying limits on precision and bias of profile elevation. Li found that, even with the modified statistical methods, "IRI bias...does not have any useful correlation with either the profile bias defined in ASTM E950 or the modified profile bias..." He concluded: "...a profiler that is accurate by the standard of profile bias may not guarantee an accurate measurement of IRI." The paper shows that no statistical relationship exists between bias in IRI measurement and composite bias in profile elevation measurement.

SLOPE ACCURACY

A profile accuracy specification may place tolerances on slope measurements in lieu of elevation. An accuracy specification may require all slope measurements to be accurate to within 1 percent. This would guarantee accurate index values to within 1 percent. For example, an IRI of 0.3 m/km (19 in/mi) is considered extremely smooth. A slope specification may simply require that all points within the slope value are accurate to within $3x10^{-6}$, which is 1 percent of 0.3 m/km (19 in/mi).

A raw requirement on slope accuracy would not succeed, because it presumes that all portions of the spatial frequency range have equal importance. On common road profiles, slope values become more and more extreme as the distance interval between readings decreases.[71] A slope accuracy threshold is only meaningful if careful specifications are set of profile recording interval and low-pass filtering. While this approach is an improvement over current practice, an even better approach treats a profile, and a reference profile measurement, as a signal. The method described below and the method proposed in chapter 5 perform comparisons on the entire profile as a signal, rather than individual readings.

PROFILER GAIN LIMITS

One of the earliest formal evaluations of a profiler characterized its performance using the gain.[34] Prem developed a method of validating pavement profile measurements using the transfer function between a reference profile and profiles collected by a (production) device under evaluation.[72] In this method, the reference profile measurement is treated as the input, and each repeat profile measurement by the candidate device is treated as the output with a linear relationship to the reference profile. For each repeat measurement, a transfer function is calculated. The transfer function gain

values at each wavelength (or wave number) are then averaged across the set of repeats. Limits are placed on the composite transfer function that represents expected error limits in IRI. Figure 18 provides an example.

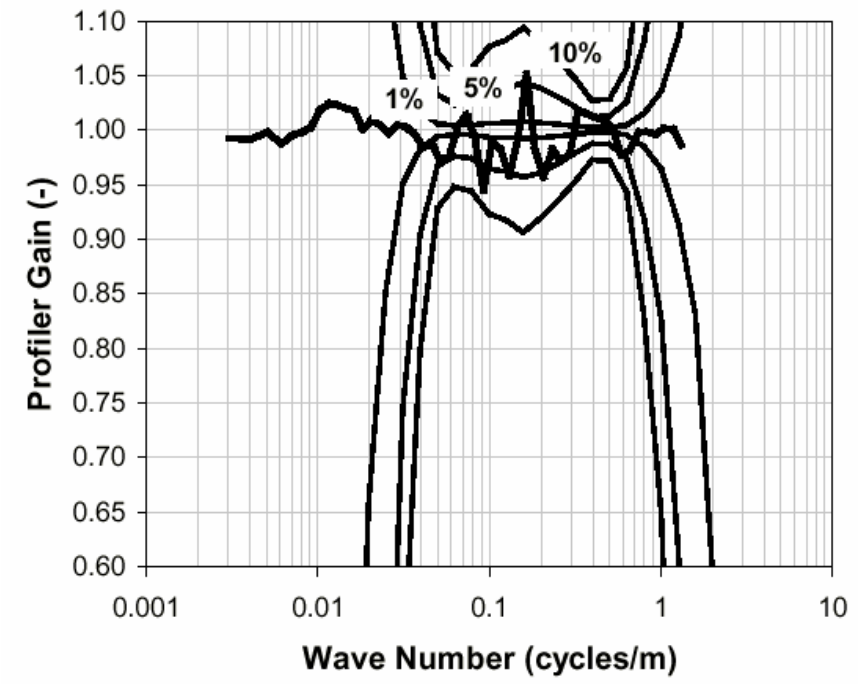


Figure 18. Profile comparison using transfer functions.(72)

This approach has several advantages:

- The error limits can be customized for any index of interest, so only the relevant waveband is emphasized.
- This method may succeed with fewer measurement sites than simple comparison of summary index values. This is because profilers that may produce the same index value because of compensating error in the overall index value are not likely to produce acceptable transfer functions.
- The gain plot may provide diagnostic information about the source of error, particularly if the measurement error is confined to a narrow band or one end of the range of interest.

These advantages make the specification of profiler gain limits a useful tool for validation of profilers for pavement network evaluation, or any other application where a profiler must produce accurate index values on a lot by lot basis. A disadvantage of this method is complexity. Thresholds are set on values of accuracy across the entire spectrum, rather than a single figure of merit. As such, cross correlation is proposed as a supplemental tool for rating profiler accuracy and repeatability, as described in chapter 5.

The reference profiling device sought by this report must provide accurate profiles for indices other than the IRI. To this end, the "gain method" recommended by Prem for IRI

measurement is reviewed here, and expanded to include many of the indices covered in chapter 3.

Review

Prem derives transfer function gain limits for various errors in IRI (in percent) on a range of measured road profiles.[72] A range of profiles were needed, because the appropriate gain limits were somewhat sensitive to the spectral content of the profile under study. The method is developed theoretically here, rather than numerically, to help study the sensitivities of the process. (Either approach depends on the assumption of random, stationary and Gaussian profile signals.)

When the gain of the profiler itself is a function of wave number, the measured profile spectral density ($G_{measured}$) is related to the true profile spectral density (G_{in}) by:

$$G_{measured}(\nu) = \left|H_{profiler}(\nu)\right|^2 \bullet G_{in}(\nu) \tag{17}$$

where $H_{profiler}$ is the gain function for the profiler. Thus, the spectral density of the signal after the IRI algorithm has been applied is:

$$G_{out}(\nu) = \left|H_{profiler}(\nu)\right|^2 \bullet \left|H_{IRI}(\nu)\right|^2 \bullet G_{in}(\nu) \tag{18}$$

and the measured IRI may be estimated as follows:

$$IRI = \sqrt{\frac{2}{\pi}} \bullet \sigma_{(measured)} \tag{19}$$

where $\sigma_{measured}$ is the root mean square, and the mean square is:

$$\sigma^2_{(measured)} = \int_0^\infty \left|H_{profiler}(\nu)\right|^2 \bullet \left|H_{IRI}(\nu)\right|^2 \bullet G_{in}(\nu) \bullet d\nu \tag{20}$$

The true IRI is the value that would be measured if the profiling device reproduced the profile with a gain of unity for all wavelengths:

$$IRI = \sqrt{\frac{2}{\pi}} \bullet \sigma \tag{21}$$

where σ is the root mean square, and the mean square is:

$$\sigma^2 = \int_0^\infty \left|H_{IRI}(\nu)\right|^2 \bullet G_{in}(\nu) \bullet d\nu \tag{22}$$

The method by Prem sought to derive limits on profiler gain with four specific mathematical properties:

1. The resultant composite level of error in IRI is fixed. For this discussion, the percent error in IRI is represented by $100 \bullet \varepsilon$.

2. The limit on profiler gain is derived for 41 one-third octave wave-number bands ranging from "band -30," with a center wave number of 2^{-10} cycles/m ($6.096 \bullet 10^{-11}$ cycles/ft), to "band 10," with a center wave number of $2^{(10/3)}$ cycles/m (3.072 cycles/ft). For this discussion, the lower and upper band numbers are denoted as N1 and N2, respectively.
3. The gain limits are adjusted for each one-third octave band so that each band contributes to error in IRI equally.
4. The profiler gain is assumed to be constant over each one-third octave band.

Since the analysis is confined to a finite number of wavebands, the mean square, which is used to estimate the IRI, may be expressed as a sum:

$$\sigma^2 = \sum_{i=N1}^{N2} \sigma_i^2 \tag{23}$$

where σ_i is the root mean square within a given one-third octave band, N1 is -30 and N2 is 10. Each term in the sum is the contribution to mean square of each band:

$$\sigma_i^2 = \int_{\nu_a}^{\nu_b} \left|H_{IRI}(\nu)\right|^2 \bullet G_{in}(\nu) \bullet d\nu \,,\ \nu_b = 2^{(i+1/2)/3} \,,\ \nu_a = 2^{(i-1/2)/3} \tag{24}$$

The profiler gain is assumed to be constant within each one-third octave band, with a value of H_i. Thus, the measured mean square value is:

$$\sigma_{(measured)}{}^2 = \sum_{i=N1}^{N2} H_i^2 \bullet \sigma_i^2 \tag{25}$$

If the measured IRI exceeds the true value by $100 \bullet \varepsilon$ percent, the measured mean square will differ from the true value by $(1+\varepsilon)^2$. If the contribution to IRI error must be the same in each band, the gain error for each band is inversely proportional to its share of the mean square:

$$H_i^2 = 1 + C \bullet \sigma^2 / \sigma_i^2 \tag{26}$$

The first term in the expression is the desired gain of unity. The second term in the expression is the "error" portion of the squared gain. The ratio of mean square values in the second term guarantees adherence to "property 3" above. The constant C constrains the overall error, ε, to the desired value. Thus,

$$\sigma^2 \bullet (1+\varepsilon)^2 = \sum_{i=N1}^{N2} \left[1 + C \bullet \frac{\sigma^2}{\sigma_i^2}\right] \bullet \sigma_i^2 \tag{27}$$

Equation 27 expands to:

$$\sigma^2 \bullet (1+\varepsilon)^2 = \sum_{i=N1}^{N2} \sigma_i^2 + C \bullet \sigma^2 \bullet (N2 - N1 + 1) \tag{28}$$

The first term on the right side of equation 27 reduces to σ^2, and cancels with the same value on the left side. The constant C is:

$$C = \frac{2\varepsilon + \varepsilon^2}{N2 - N1 + 1} \tag{29}$$

Recall that the constant C serves as a dial to adjust the overall error level (ε) in IRI. For small levels of error, C is roughly proportional to ε. For the wavelength range specified in "property 2" above, and an error in IRI of 1 percent:

$$C \approx \frac{1}{2050} \tag{30}$$

When this value of C and the resultant σ_i values for a white noise slope profile are inserted into equation 26, the gain limits listed by Prem are reproduced very closely.(72) The theoretical development here shows that the profiler gain limits are dependent on the overall IRI error level, but they are equally dependent on the number of one-third octave wavebands included in the analysis:

$$H_i^2 = 1 + \frac{2\varepsilon + \varepsilon^2}{N2 - N1 + 1} \bullet \sigma^2 / \sigma_i^2 \tag{31}$$

Thus, doubling the wave-number range for the analysis roughly cuts the required gain error in half within the most of the range, with no change in the expected IRI error level. Expanding the wave-number range simply spreads the error out over more bands. As the limits of the range gets farther away from the most relevant portion, the extremely low sensitivity of the IRI algorithm is balanced by progressively outrageous values of gain error.

The relative gain error thresholds reported by Prem are a very useful tool for studying sources of IRI error. However, the recommended absolute gain error levels depend on an arbitrary choice of the waveband covered by the analysis.

Further Development

This section further develops the use of gain limits to specify profiler performance. These analyses seek to improve the relationship between gain limits in each waveband and the expected error level in IRI. The gain limits are then extended to include all of the roughness indices covered in chapter 3 on the four examples of road spectra described in chapter 3.

This section repeats the development of the gain method, above, with two exceptions. First, the theory is modified to examine the case of negative gain error. That is, the case in which the profiler underestimates the roughness. Second, an infinite range of wave numbers, and hence an infinite range of wavelengths, is covered. These two changes will allow the spectral content of the profile, rather than the analyst, decide what range of wavelengths contributes to error in the final IRI. This is because the gain can not pass below a value of zero, so wavebands that did not contribute significantly to the IRI can not contribute significantly to error in IRI.

When an infinite number of one-third octave bands is included, equation 25 changes to:

$$\sigma_{(\text{measured})}{}^2 = \sum_{-\infty}^{\infty} H_i^2 \bullet \sigma_i^2 \tag{32}$$

The term H_i again represents the profile gain for "band i," but it reduces the gain value:

$$H_i^2 = \max(1 - C \bullet \sigma^2 / \sigma_i^2, 0) \tag{33}$$

The value of the "max" function is the larger of the two values inside the parentheses. The max function is needed because the gain for a given one-third octave band may not have a value lower than zero. For convenience, equation 33 reduces to:

$$H_i^2 = 1 - \min(C \bullet \sigma^2 / \sigma_i^2, 1) \tag{34}$$

where the "min" function returns the lower of the two values in parentheses. The first term in the "min" function is designed to make sure that each one-third octave band reduces the IRI by the same amount. The second term takes precedence when the band of interest contributes less to the IRI than the error in the relevant bands. The contributions from these bands are removed altogether.

For an overall error in IRI of ε:

$$\sigma^2 \bullet (1-\varepsilon)^2 = \sum_{-\infty}^{\infty} \left[1 - \min(C \bullet \frac{\sigma^2}{\sigma_i^2}, 1) \right] \bullet \sigma_i^2 \tag{35}$$

Equation 35 expands to:

$$\sigma^2 \bullet (1-\varepsilon)^2 = \sum_{-\infty}^{\infty} \sigma_i^2 - \sum_{-\infty}^{\infty} \min(C \bullet \sigma^2, \sigma_i^2) \tag{36}$$

The first term on the right side of equation 35 reduces to σ^2, and cancels with the same value on the left side. Equation 36 further reduces to:

$$2 \bullet \varepsilon - \varepsilon^2 = \sum_{-\infty}^{\infty} \left[\min(C, \frac{\sigma_i^2}{\sigma^2}) \right] \tag{37}$$

For small values of ε:

$$\varepsilon \approx \frac{1}{2} \sum_{-\infty}^{\infty} \left[\min(C, \frac{\sigma_i^2}{\sigma^2}) \right] \tag{38}$$

Since the constant C appears in a non-linear term, a closed-form solution is much harder to obtain. This can be done using an analytical expression for the transfer function of the IRI and the input spectrum, but a numerical solution is more convenient.

Equations 34 and 38 were used to derive the gain function that corresponds to an overall error in IRI of 1 percent. Figure 19 shows the result on a road of white noise

slope. For clarity, the figure shows the gain as a function of wavelength, rather than wave number. The most critical wavelength range is centered at 2 m (6.56 ft). The permitted gain error for this band is -0.25 percent. Note that the wavelength range of interest listed in tables 3 and 4 for this case is 1.13 to 18.0 m (3.70 to 59.1 ft). No part of this wavelength range is allowed to have an absolute error level greater than 4 percent.

Figure 20 shows the gain error permitted for four sample roads. These are the four roads used to develop the wavelength range of interest in chapter 3. The figure shows a composite gain criterion. First, the gain error for each waveband is the lowest error found for the four sample roads. Second, the permitted error is reflected about a value of 1, such that the same limits on downward-biased gain error is applied for upward-bias gain error.

This method was expanded to include all of the indices that served as a basis for the wavelength range of interest: IRI, Golden Car suspension stroke at a simulation speed of 40 km/h (25 mi/h), Golden Car suspension stroke at a simulation speed of 120 km/h (75 mi/h), PTRN, the three components of RQI, TRN, TRI at two speeds, and DLI. Figure 21 shows the result. The figure shows the smallest gain error allowed for any combination of the four sample roads and 11 index options covered in tables 3 and 4. This provides a criterion for the spatial frequency response of a reference profiling device, which will ensure accurate measurement of existing and likely future indices that estimate vehicle response.

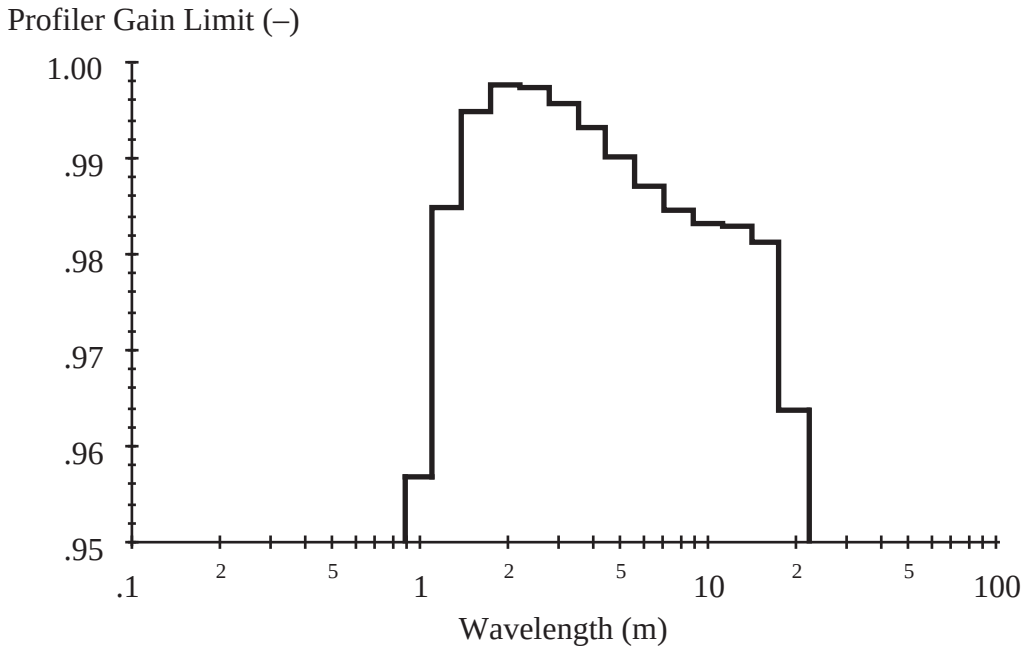


Figure 19. IRI gain limit on white noise slope.

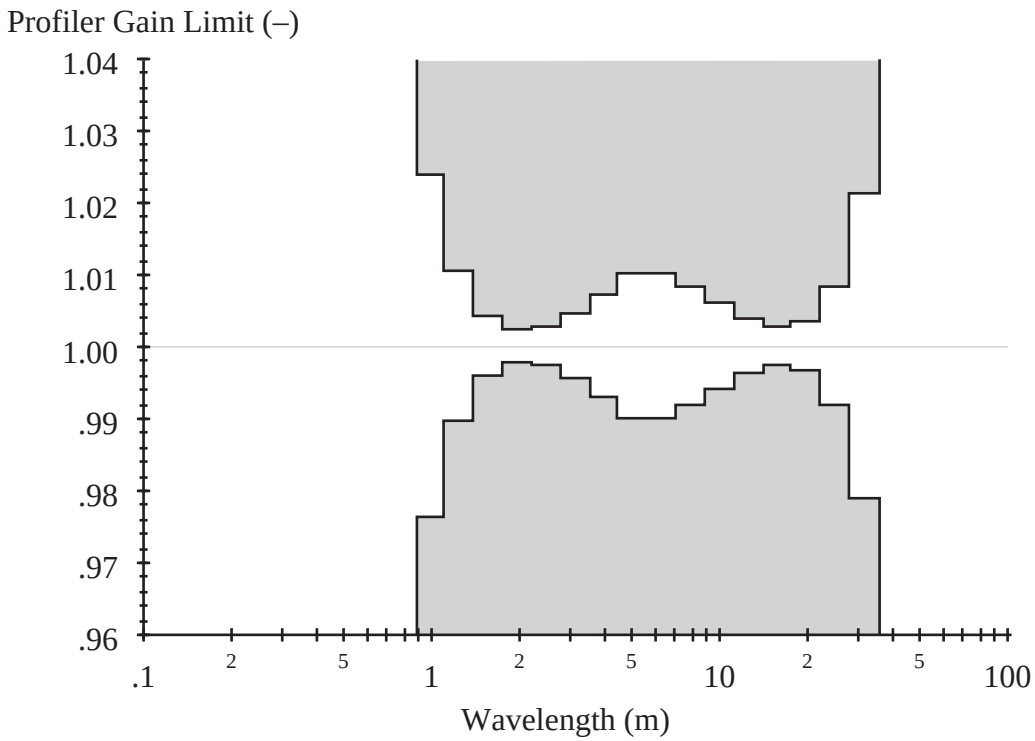


Figure 20. Composite IRI gain limit on four sample roads.

In figure 21, the most restrictive gain limit occurs at the band with a center wavelength near 10 m (32.8 ft). Here, the limit on gain error is about 0.1 percent. In the range from 0.35 to 35.9 m (1.16 to 118 ft) the permitted gain error never exceeds 0.4 percent. Over these 20 one-third octave bands, the average gain error that is allowed is very close to 0.25 percent. To make the process less complicated, the recommended accuracy requirement for a reference profiler will be a gain error of no greater than 1.00 percent for wavelengths from 0.15 to 0.35 m (6 in to 1.16 ft), no greater than 0.25 percent for wavelengths from 0.35 to 35.9 m (1.16 to 118 ft), and no greater than 1.00 percent for wavelengths from 35.9 to 67 m (118 to 220 ft). (The established range of interest is 0.15 to 67 m (6 in to 220 ft).)

Application of this technique requires the measurement of a very accurate benchmark profile to which the candidate reference profiling device's output may be compared. Potential methods for making this measurement are recommended in chapter 7.

Note that fluctuations in the calculated gain function are very sensitive to the measurement and calculation process. Unless this method is applied carefully, a quality reference device may be disqualified because of poor processing techniques. First, increasing the density of the wavebands will cause the gain values to cover a greater range without any change in the original profiles under comparison. For example, a profile may pass when one-third octave bands are used, but fail under one-sixth octave bands. One-third octave bands are recommended.

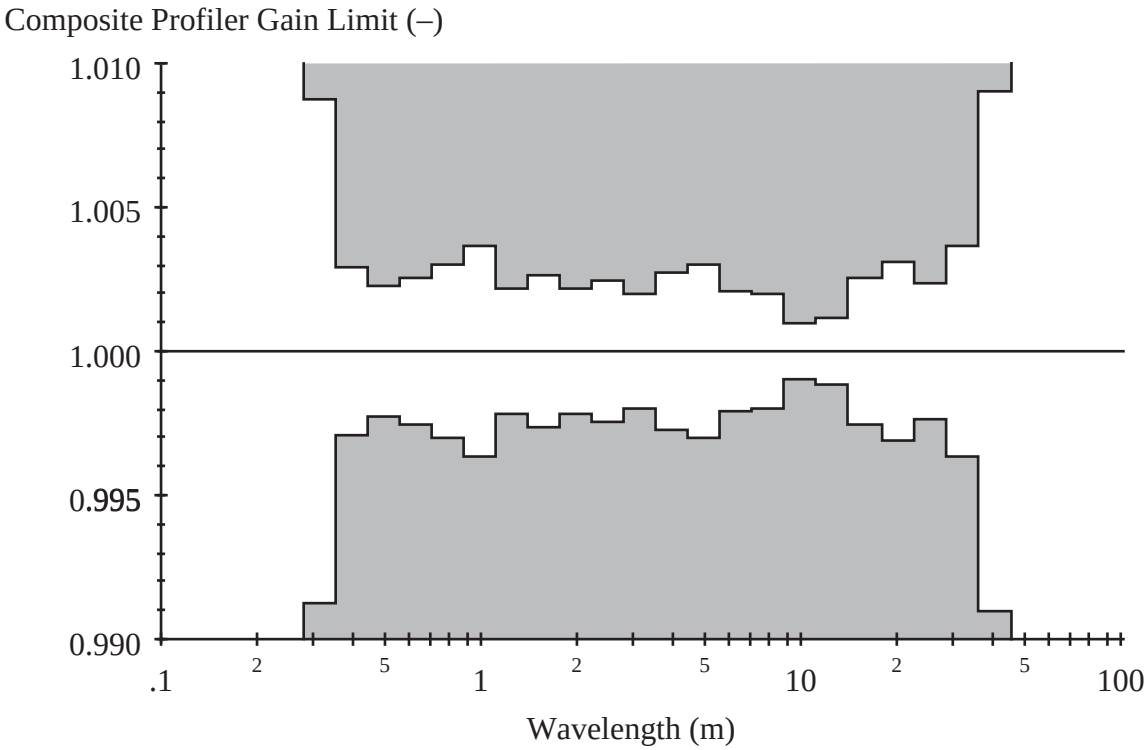


Figure 21. Composite gain limit for 11 indices on 4 sample roads.

Second, spectral estimates improve significantly for longer samples (e.g., longer test sections). On the other hand, verification measurements for the reference profile are likely to be expensive and time consuming. A section length of 160.9 m (528 ft) is recommended, but verification of longer wavelength content may require much longer measurements. If this is the case, the benchmark measurement will proceed using the sampling requirements recommended in chapter 6 over 160.9 m (528 ft). Supplemental measurements with a longer sample interval may be required on longer sections of pavement, with the express purpose of verifying measurement of the long wavelength range.

Third, Prem demonstrated the process by averaging the gain function of a profiler over five pavement sections.(72) The profiler under study exhibited gain characteristics on individual sites that fluctuated between 0.75 and 1.25 over the critical wavelength range. On the other hand, the average of the five gain functions was beneath an error level of 5 percent over the same range. The same method is recommended here, where the five or more sections should contain as much diversity in roughness, grade, and texture as possible.

PHASE AND COHERENCE

Expanding the technique to include the phase relationship and coherence would provide tremendous diagnostic information for all profile comparisons. The phase relationship would help validate the spatial distribution of roughness, which is critical if the profiling device must produce reference measurements.

For the reference device, spatial distortion is not permitted over the wavelength range from 0.15 to 67 m (6 in to 220 ft). In practical terms, this means that the device should have no inherent sources of spatial distortion in this range, such as a high-pass filter with a non-linear phase response. The level of permitted spatial distortion may be specified using either a direct specification on phase lag, or a specification on group delay. (For road profiles, group delay is expressed in units of length, rather than time.) However, neither method has ever been implemented in a practical setting. This is due in part to the fact that the calculated phase relationship between profiles often produces a very noisy plot, with a high level of variation. For long wavelength content, this is because the profiles under comparison are typically too short to get a proper estimate of the phase relationship. For short wavelength content, poor estimates of phase shift are caused by incompatibility between longitudinal distance measurements.

An appealing possibility is to specify group delay of less than 0.6 m (2 ft) over the wavelength range of interest. This is a roughly the level of shift of localized rough features that would cause problems in the field. However, a robust data set would be required to standardize the test methods, the needed segment length, the proper sampling procedures, and calculation methods for proper estimation of group delay.

The coherence function provides an assessment of the relationship between two signals at each wavelength. The coherence function is penalized if any content exists in a profile measurement from a source other than the true profile. A minimum level of coherence at a given wave number between the candidate reference device and the benchmark measurements would ensure a systematic linear relationship between them. No specifications are recommended on coherence, but the coherence plots should be scanned for problems.

LONGITUDINAL DISTANCE MEASUREMENT

Accurate measurement of longitudinal distance is important for several reasons. In construction quality control, profiles often provide a way to find localized areas of the pavement that need corrective action. Finding these areas on the pavement depends on accurate longitudinal distance measurement. For all applications, accuracy in measured roughness depends directly on longitudinal distance measurement accuracy. A given percentage in longitudinal distance measurement error causes roughly the same percentage error in IRI, and up to half that level of error in RN.[28] Finally, the profile comparison methods recommended in this report are only valid when longitudinal distance measurement is compatible between profiles.

Inertial profilers are typically expected to measure longitudinal distance correctly to within 0.1 percent. ASTM E 950-98 and AASHTO PP 49-03 require verification that inertial profilers measure longitudinal distance measurement accurately within 0.1 percent.[59,64] This is a reasonable standard for accuracy of reference profiling devices as well. Note that a reference profiling device need not be much more accurate than the production profilers that are compared to it. This is because they will not serve as the reference for longitudinal distance measurement. Instead, longitudinal distance will be verified using a steel tape.[73]

LATERAL TRACKING

The lateral position of a profile within a lane affects the measured roughness significantly on most pavements.[28] In the Ann Arbor Road Profilometer Experiment, Sayers reported that a 25 cm (9.84 in) variation in lateral positioning of the high-speed test vehicles was common, even when the target wheel track was marked.[63] However, existing reference devices operate at very low speed, and wander very little so long as the profile position of interest is clearly marked.

While it is highly recommended that candidate reference profilers follow the proper path accurately, it is not mandated. This way, the critical accuracy requirements do not exclude innovative non-contacting devices or devices with a high production rate, simply because their lateral tracking behavior is hard to measure. On the other hand, the performance requirements that are placed on accuracy and repeatability in this chapter and in chapter 7 will require accurate lateral tracking inasmuch as that is needed to make reference quality profile measurements.

CHAPTER 5. PROFILE COMPARISON METHOD

This chapter describes the use of cross correlation for rating the agreement between profiles. The rating of agreement represents repeatability when it is applied to two measurements of the same profile by the same device. It represents reproducibility when it is applied to two measurements of the same profile by different devices, and it represents accuracy when a measurement from one of those devices is deemed to be correct.

Cross correlation is recommended as a measure of accuracy to supplement to the gain method described in chapter 4. When candidate reference devices are compared to benchmark profile measurements, the gain criteria and cross correlation results will be considered side by side. Cross correlation is also proposed as a method of rating the repeatability of candidate reference devices.

Requirement: *Profile measurements from a reference device must cross correlate to benchmark profiles over a range of pavement surface types as follows:*

Correlation in IRI filter output to at least 0.98.

Correlation within the long waveband to at least 0.98.

Correlation within the medium waveband to at least 0.98.

Correlation within the short waveband to at least 0.94.

Repeat measurements from a reference device must also exhibit composite cross correlation above the same thresholds.

Chapter 7 recommends a testing program for correlation, including the number of runs and range of test pavements. The three wavebands listed above are defined in this chapter. Together, these wavebands cover the entire wavelength range of interest for a reference device. This chapter recommends isolation of these wavebands using third-order Butterworth filters. The filters shall be applied once in the forward direction, and again in the reverse direction. This cancels the phase shift associated with the filter, and doubles the order. Correlation of IRI filter output is also included, because that part of the wavelength range of interest is so important in current practice. Further, correlation in IRI filter output is directly related to expected accuracy in IRI measurement.

Note that the criteria above require lesser correlation in the short waveband than the others. This is allowed because correlation in the short waveband depends heavily on the sampling practices and the footprint of a given device. This report recommends sampling and footprint requirements that are based on the best available information. However, it is anticipated that the state of knowledge in this area will improve in the near future. When the most relevant sampling practices are known, they may alter the benchmark. At present, perfect correlation to the current benchmark may prompt unproductive effort.

Cross correlation is also recommended as a method of comparing conventional measurements of profile to the output of a reference device within profiler certification programs:

Recommendation: *Cross correlation should replace precision and bias in elevation measurement as a standard for profile accuracy and repeatability. Profile certification for construction quality control should require:*

Correlation in IRI filter output to at least 0.94.

Correlation within in the long waveband to at least 0.94.

Correlation within in the medium waveband to at least 0.94.

Correlation within in the short waveband to at least 0.88.

The long, medium, and short wavebands should collectively cover the wavelength range of interest defined in this report.

The rest of the chapter provides details about the adaptation of the cross correlation method to road profile comparison and the establishment of thresholds for profile agreement. Most of the content of this chapter appears in a recent paper.(74)

INTRODUCTION

The method described in this chapter is intended for rating repeatability, reproducibility, or accuracy of profiles. It is based on the cross correlation function described by Bendat and Piersol for measurement of time delays between signals, rating the general dependence of one signal on another, or recovery of a given signal within noise.(47) In this application, it is meant to rate the relationship between two profile measurements, often when one of them is deemed to be correct. The method is adapted to detect a longitudinal distance offset between profiles and rate the agreement between them when the offset is removed.

The output of the cross correlation method yields much of the diagnostic information that is provided by the coherence and gain plots, but can be summarized in a single value for a given index of interest, or one value per waveband. When the method is customized for a given index, a high rating requires that the overall roughness level of two profiles is equivalent and that both of them distribute roughness equally within a profile. For example, when the method is applied to the IRI, a high rating requires that features which contribute to the IRI appear in the same locations with the same shape. This qualifies the method as a good candidate for certifying profilers for construction quality control, where the ability of a profiler to locate and prioritize isolated rough spots is important.

THEORETICAL DEVELOPMENT

Cross correlation values are obtained by performing an integral of the product of two profiles with a given longitudinal offset. A cross correlation function is a collection of correlation values expressed versus longitudinal offset. If profiles were truly random functions, the correlation values would be zero at all values of offset except zero. Profiles

are not random functions, and repeat measurements are never completely synchronized. Therefore, correlation functions between profiles of the same site fluctuate with offset distance, but are expected to reach a peak level at the offset needed to synchronize them.

For two measures of road profile, the cross-correlation function is defined as:

$$R_{pq}(\delta) = \lim_{L\to\infty} \frac{1}{L} \int_0^L P(x)Q(x+\delta)dx \tag{39}$$

where P and Q are each measurements of road profile as a function of distance x. The cross correlation function, R, exists as a continuous function of the offset distance δ between the profiles. Actual measures of road profile are finite in length. For a given length, L, the cross correlation function can be estimated by:

$$R_{pq}(\delta) \approx \frac{1}{L} \int_0^L P(x)Q(x+\delta)dx \tag{40}$$

Since the profile is sampled at discrete intervals, the integral must be replaced by a summation:

$$R_{pq}(\delta) \approx \frac{1}{N} \sum_{i=1}^{N} P_i Q_{i+\delta/\Delta} \tag{41}$$

where the subscripts indicate discrete sample numbers, recorded at an interval of Δ. The number of samples, N, is the value needed to cover the overall length of interest. (The value of N will be the highest integer value that does not exceed L/Δ.) Using equation 41 requires that the offset value δ is an integer multiple of the sample interval.

Equation 41 has two weaknesses when applied to road profiles. First, it yields a cross correlation function in units of elevation squared. A more desirable rating system would be normalized to produce a value of 1 for perfect correlation:

$$\rho_{pq}(\delta) = \frac{1}{\sigma_P \sigma_Q} \sum_{i=1}^{N} \hat{P}_i \hat{Q}_{i+\delta/\Delta} \tag{42}$$

where the hats over the letters "P" and "Q" indicate that the profiles are offset vertically to have a mean value of zero. The values σ_P and σ_Q represent the standard deviation of profiles P and Q, respectively. Equation 42 produces a -1 to 1 rating of the correlation, and will only produce a value of 1 when the shape of both profiles are exactly the same and they are synchronized. This is because the estimated cross correlation function is normalized by the product of the standard deviation of each profile.

A second weakness is that differences in overall roughness are not penalized by the standard cross correlation function. Two profiles that have the exact same shape but very different amplitudes would be rewarded with a perfect rating by equation 42. To compensate for this, the following factor is applied to the normalized cross correlation function:

$$f = \frac{\min(\sigma_P, \sigma_Q)}{\max(\sigma_P, \sigma_Q)} \tag{43}$$

This adjustment factor diminishes the value of correlation when the standard deviation of the profiles are not equal.

The recommended procedure for applying this method requires the profiles to be filtered, so their mean values are expected to be small. Nevertheless, the procedure also includes removal of the mean value. The computation is most efficient when each profile is shifted vertically to have a mean of zero and normalized by its standard deviation before the cross correlation function is calculated. Unfortunately, this may lead to errors when the roughness in the longer profile, "Q," is not evenly distributed along its length. Instead, the profile must be shortened, or "cropped," to include only the N samples needed each time the summation is performed. This is much less efficient, because the removal of the mean, calculation of the standard deviation, and filtering must be repeated for each value of offset. (In equation 42, the range of profile "P" never changes so it only needs to be conditioned once, but "Q" must be conditioned every time.)

It is essential that the same filters be applied to both profiles before using this analysis. If the profiles are not filtered similarly the results will be clouded by the differences in waveband. It is also helpful to convert the profiles to slope before computing the correlation coefficient. If elevation is used, the agreement for the longest wavelength range included in the analysis has a disproportionate influence on the results. Whatever filter is used, the best practice is to filter the profile "Q" each time the summation is performed. This is required to ensure that the effect of the filter initialization is the same in both profiles. The drawback is the filter must be applied every time a point in the cross correlation function is generated. This can be avoided if the filter initialization is not considered important by measuring a significant amount of profile ahead of the segment of interest. When that is done, both profiles may be filtered just once, as long as no part of either profile that is affected by the initialization falls within the range of samples called for by equation 42.

SYNCHRONIZATION

For research studies and profiler certification tests that involve several measurements of the same road section by a single device or a collection of devices, it is often desirable to *synchronize* the profiles by adjusting their longitudinal offset to make sure they all cover exactly the same stretch of road. A common way to synchronize a set of profile measurements is to simply plot them and read a distance offset from the plots. Since cross correlation provides a rating of agreement between profiles as a function of offset, it can be used to automate this process. The procedure is based on matching two measurements of a section of road and finding the offset associated with the highest level of correlation. If the profile measurements are filtered and normalized as described above, the output of the algorithm is a number between -1 and 1 that describes the agreement of the two measurements at each offset.

Figure 22 shows a *cross correlogram*, which displays the cross correlation between a measurement by a lightweight inertial profiler and a slow-speed reference measurement as a function of offset. Both were converted to slope profile and band-pass filtered to include only content in the wavelength range from about 1.5 to 7.6 m (5 to 25 ft). Because this road profile is very similar to a random signal, the level of correlation is very poor except where the measurements are synchronized. The function has a value less than 0.2 everywhere except when the longitudinal distance offset is near 0.3 m (1 ft). The peak value of 0.898 occurs at the correct offset of 0.35 m (1.15 ft).

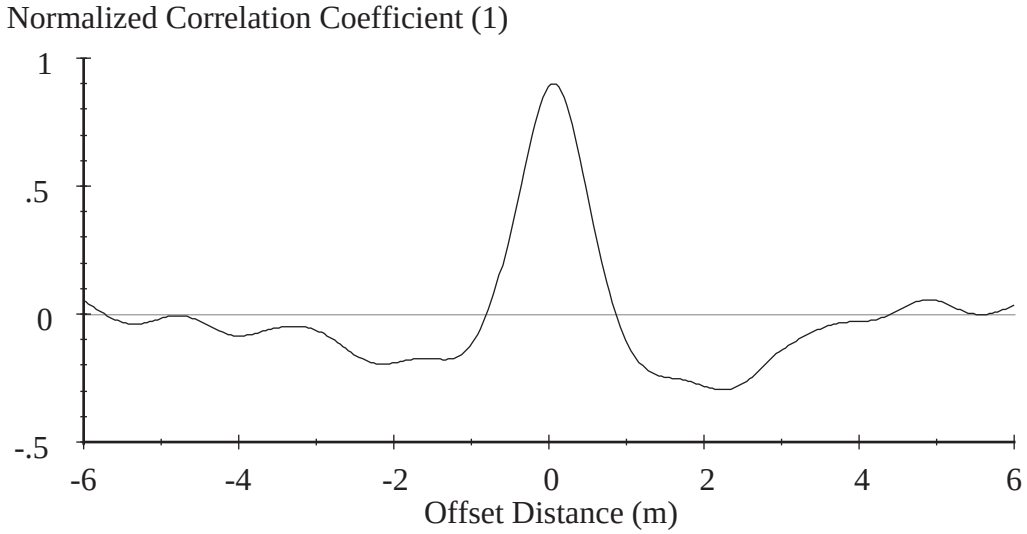


Figure 22. Cross correlogram of two profiles.

RATING OF AGREEMENT

If the measurements compared in figure 22 agreed perfectly, the maximum correlation coefficient would be unity. However, differences between the measurements, even when they are lined up properly, still exist. This lowers the maximum correlation level. Once two measurements are synchronized, the peak correlation value used to establish their longitudinal offset provides a quantitative rating of the agreement between them. This can be used to rate the agreement between two measurements from the same instrument, measurements from unlike instruments, or agreement of a measurement to a reference profile. Regardless of the type of comparison, cross correlation yields a rating of agreement in the waveband of interest when the profiles have been filtered identically.

Using cross correlation to evaluate agreement between profile measurements is much more rigorous than comparison of summary roughness indices. Two profilers might produce the same index value even though the profiles are not the same. In contrast, cross correlation of filtered profiles requires the same level of roughness and that rough features appear in the same location and have the same shape in each. Thus, it does not reward compensating error. This reduces the number of repeat measurements needed to reveal profile measurement problems. This method also offers the ability to diagnose measurement errors by considering a variety of wavebands. For example, bad agreement

for short wavelengths but good agreement for long wavelengths suggests a problem with the height sensors and the opposite often suggests a problem with the accelerometer.

A powerful adaptation of this method is to pass two profiles through the IRI algorithm, then cross-correlate the filtered output. This has the advantage of comparing only those aspects of the profile that are important to the IRI and applying appropriate weighting to them. (Of course, if another index is of interest, filter the profile using its algorithm.) High correlation using this procedure requires not only that the overall IRI values match, but that the roughness is spatially distributed the same way in both measurements. This may be important if the profiles are intended for location of isolated rough spots, or if they are to be used in construction quality control.

Figure 23 provides an example of profiles with very high correlation. The figure shows three repeat measurements by a device after they have passed through the filters in the IRI algorithm. Note that the filtered profile includes positive and negative values. (When the IRI of this section is calculated, all of these values are rectified.) The signals in figure 23 compare to each other with an average correlation higher then 0.995. The traces overlay so well that they are barely distinguishable from each other. Figure 24 provides an example of moderate correlation. It shows three repeat measurements from the same device on a different pavement section after they have passed through the filters in the IRI algorithm. These compare with an average correlation of about 0.84. The traces do not overlay nearly as well, and do not agree on the severity of roughness in locations of elevated IRI. At few locations, such as 74 and 76 m (242.7 and 249.3 ft), concentrated roughness appears in only one or two of the measurements.

PROCESSING STEPS

Synchronization

Synchronization of profiles using cross correlation is performed with the following steps:

Step 1: Identify a fixed profile (Q) that is already consistent with the desired longitudinal reference. It will be considered the location reference. The profile will have a sample interval Δ, a total length L_Q, and a total number of samples N_Q ($=L_Q/\Delta$).

Step 2: Cut a segment out of the correlated, or shifted, profile (P) of shorter length than the reference profile, L_p. Preprocess it as follows.

Step 2a: Filter it.

Step 2b: Interpolate the filtered profile to the sample interval of the reference profile. The result is the profile p, which is a portion of the original profile P. It will have N_p samples ($=L_p/\Delta$).

Step 2c: Offset the profile vertically so that the mean is zero.

The cropped, filtered, interpolated, and shifted version of profile P is given the symbol $\hat{p}$, and will include N_p samples.

Step 2d: Calculate the variance of profile $\hat{p}$. The result is σ_p.

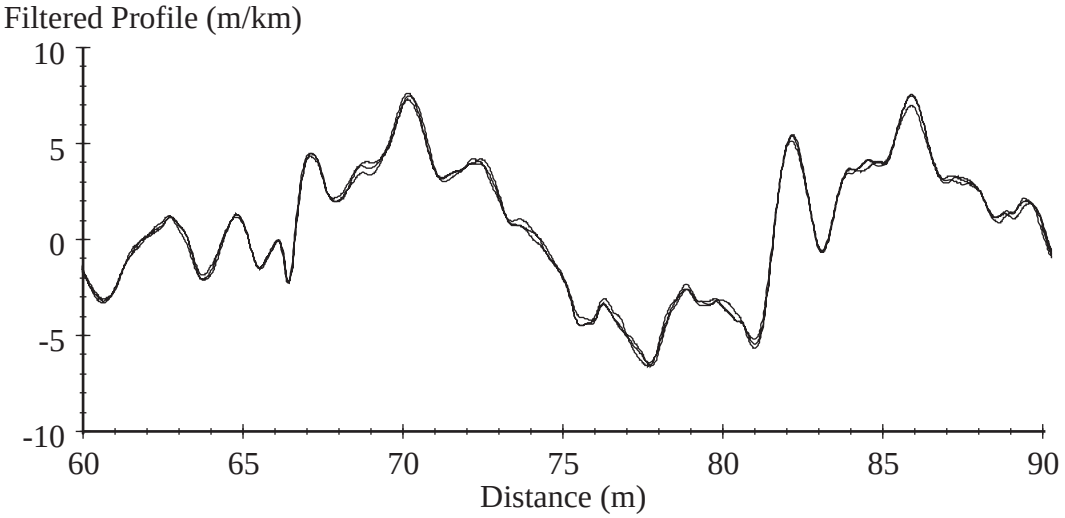


Figure 23. Three highly correlated repeat measurements.

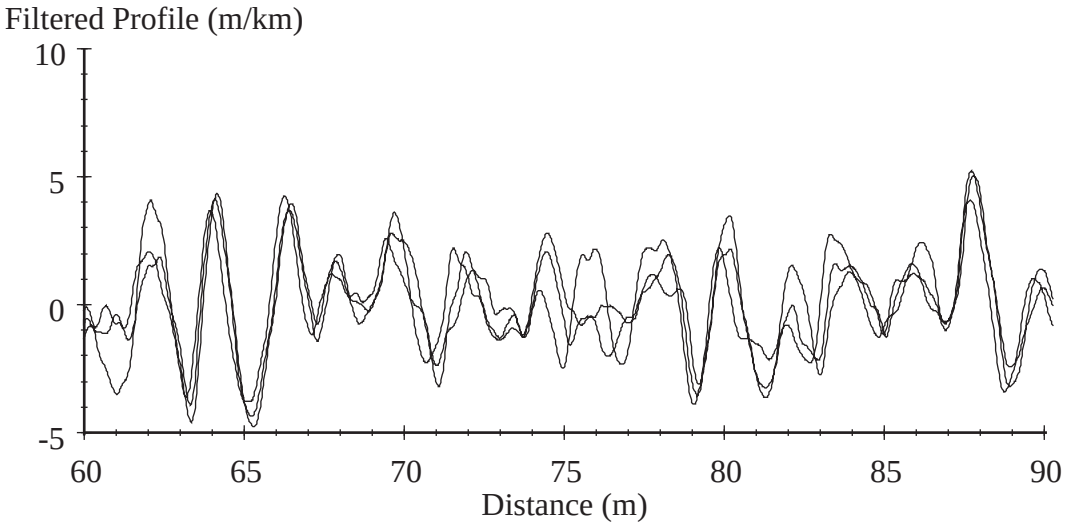


Figure 24. Three moderately correlated repeat measurements.

Step 3: Apply a negative offset (δ_0) to the correlated profile so that the first point in it is also the first point in the reference profile. This value of offset is equal to X_{sQ} - X_{sp}, where X_{sQ} is the longitudinal position of the start of the broader reference profile (Q), and X_{sp} is the longitudinal position of the start of the correlated profile.

Step 4: Extract the portion of the reference profile (Q) that is covered by the correlated profile ($\hat{p}$). The extracted segment, q, will cover the same number of samples as $\hat{p}$.

Step 4a: Filter the extracted profile (q).

Step 4b: Offset the filtered profile vertically so that the mean is zero. The result is $\hat{q}$. Note that this signal must be conditioned *after* it has been extracted from the broader reference profile. This ensures equal application of end conditions in the two signals that will be correlated in equation 44.

Step 4c: Calculate the variance of the filtered and shifted profile over the range of interest (σ_q).

Step 5: Cross-correlate the signals. In this application, the variance must be calculated over the segment of interest only to account for the common situation in which the broader profile is not stationary.

$$\rho_m = \frac{1}{\sigma_p \sigma_Q} \sum_{i=1}^{N_p} \hat{p}_i \, \hat{q}_{i+m}$$

$$\delta_m = X_{sQ} - X_{sp} + m \bullet \Delta \qquad (44)$$

In equation 44, the value "m" is the number of samples that are skipped at the start of the long profile Q to create the shorter profile $\hat{q}$. For each value of ρ, there exists an associated value of longitudinal offset, δ. In the first application, m is zero, and the offset between profiles is X_{sQ} - X_{sp}. (The value of m is incremented from 0 to N_Q - N_p.)

Step 6: Shift the offset of the correlated signal by a distance equal to the sample interval of the reference profile. This amounts to shifting ahead one sample on the reference profile. (Each time this is done, increment the value of "m.")

Step 7: If the end of the reference profile has not been reached, return to step 4.

The offset that corresponds to the highest value of ρ is the proper offset for synchronization. Note that the choice of a reference profile in this process does not necessarily mean that it is correct. Often, this process is simply a way to make the location referencing consistent between measurements.

Steps 2a and 4a require that the profiles are filtered. It is essential that both filters are equivalent. Further, precise synchronization requires that the filters must remove enough of the waveband of each profile to eliminate differences in the filtering used to produce the original measurements. In other words, when the profiles are entered into equation 44 their expected wavelength content must be equal. If the filters are chosen carefully, they will obscure differences in long and short wavelength cutoff and filter shape used by the device. Note that an equivalent filtering history can not always be achieved, particularly when the filtering done at the time of the measurement is not equivalent between the two profiles, and the measurement process that produced one of them imposes a phase shift over a broad range of wavelengths. In this case, synchronization over one waveband may yield a slightly different offset than synchronization over other wavebands.

If the profiles are to be used strictly for the calculation of IRI, the synchronization should be done using the output of the filters from the IRI algorithm. These filters produce a slope profile that covers a wavelength range from about 1.3 to 30 m (4.27 to

98.4 ft). This is well within the intended valid waveband of most profilers. Several other filtering options are possible.

The interpolation of the "correlated" profile in step 2b must be performed with care. If the sample interval of the correlated profile is similar to the sample interval of the reference profile or much larger, apply direct linear interpolation. However, if the sample interval of the reference profile is much larger than that of the correlated profile, direct interpolation is not sufficient. Conditioning must be applied to the correlated profile that is equivalent to that of the reference profile. This could include direct application of an anti-aliasing filter. It may also require modeling of the physical attributes of the reference device. For example, the application of a tire bridging or enveloping filter that reproduces the manner in which the reference device contacts the pavement.

The process outlined above provides a rating of agreement between profiles as a function of offset distance. Often, measurements differ in their distance measurement accuracy as well as their longitudinal referencing. Even small errors in measurement of longitudinal distance may compromise the correlation level. This occurs when the ratio of the smallest wavelength of interest to the overall length of the profile is on the same order of magnitude as the longitudinal distance measurement error level.

Cross correlation can also be used to quantify linear distance measurement error. This requires that correlation level is expressed as a function of both offset distance and distance measurement error level. The combination of offset distance and sample interval correction factor that produce the highest correlation to the reference are then considered "correct."

Rating of Agreement

The same process described above can be used for rating of agreement between profiles. Repeatability is rated by comparing two measurements by the same profiler on the same segment of road. When this is done, it does not matter which of the measurements is considered the "reference." This is because the sample intervals will be equal, and the process has reciprocity. (That is, the same result is obtained if the reference and correlated profiles are switched.) When profiles of unlike sample interval are compared, as will usually be the case for rating agreement between two profilers, the choice of which measurement is considered the reference can be important. This is because the candidate profile measurement will be interpolated to have the same sample interval as the chosen reference. This will have a smoothing effect on the candidate profile. In addition, the method used to measure a road datum plane (i.e., the height sensor footprint) and sampling practices are deemed correct in the reference measurement.

The method of cross correlation described above for synchronization can be used directly, with the exception that the output is the correlation level (ρ_m). Typically, rating of agreement and synchronization are performed concurrently with this method. It is important to allow for a modest range of longitudinal offset between two profiles under comparison, even when synchronization is already done by some other method. This is because profiles may exhibit optimal synchronization at slightly different offsets when

different wavebands are considered. This depends on the phase shift of the filtering done by each profiler.

When rating agreement between profiles, the output of the cross correlation method is the correlation level at the optimum longitudinal offset (and sample interval correction, if it was included). This can be calculated using equation 44, but the scale factor of equation 43 must be applied to the value of ρ_m:

$$\text{Agreement Level} = \rho_m \bullet f \tag{45}$$

This penalizes the correlation level by the ratio of the variance of each signal, so two profilers must have the same level of roughness, in addition to the same shape.

The method described here is only valid when no frequency offsets exist between profiles. Although the method has been used successfully under small frequency offsets caused by small linear errors in longitudinal distance measurement, large errors in longitudinal distance measurement would invalidate the results. Thus, the shortest wavelength that can be evaluated by the method must be an order of magnitude larger than the error in overall longitudinal distance the builds up over the length of the profile under evaluation. Often, this renders the correlation of very short wavelength content suspect. Further, it typically imposes a limit of the length of profile that may be compared.

The method has been extended to search for longitudinal distance measurement errors by searching for the optimal adjustment in sample interval that results in the highest rating of agreement. Under this strategy, the linear portion of error in longitudinal distance measurement is removed before the final correlation coefficient is calculated. This way, the linear error in longitudinal distance measurement is quantified in percent, and the correlation coefficient represents the outcome of all of the other error sources.

THRESHOLD DEVELOPMENT

Cross correlation of IRI filter output is meant to represent the agreement in the relevant aspects of profile shape, weighted by the IRI filter itself. It will not have a direct relationship to agreement in the overall IRI value on a segment of road. This is an important aspect of the method, because it seeks to provide a rating of the agreement on measurement and placement of localized roughness. Compensating error that may not show up in direct IRI comparison is penalized. Nevertheless, it would be very useful to know what threshold values of cross correlation provide a reasonable expectation that IRI will be measured within some desired tolerance. Measurements from a major profiler comparison experiment conducted in 1993 by the Road Profiler User's Group (RPUG) are used for this purpose.

The 1993 RPUG experiment took place in four regions in the U.S. In each region, a State DOT prepared up to eight test sections 160.9 m (528 ft) long. These sections were selected to cover range of surface type, roughness, and surface texture. Each profiler that participated in the experiment measured the sections in the region in which it operates. In most cases, the profilers measured each section 10 times. The sections were also measured using a DipStick to provide a reference roughness value. Overall, 34 profilers

took part in the study and more than 2,400 measurements were made. The experiment is described in detail elsewhere.[4]

A major finding of the study was that profilers with ultrasonic height sensors were not able to measure the IRI within sufficient tolerance for practical use. Since then, most ultrasonic sensors have been replaced. The analyses reported here, therefore, exclude measurements made with ultrasonic height sensors.

The remaining 16 profilers from the RPUG experiment made 937 measurements. On each site, this permits a large number of IRI comparisons. For example, on a site measured in the northeastern region a total of 50 measurements were made. Comparison of each measurement with all of the others generates a total of 2,450 comparisons for each wheel track. For each comparison, a percentage difference in IRI can be matched to the cross correlation of IRI filter output for those two profiles. Note that most pairs were compared twice, so that one of the profiles could take the role of reference measurement in each comparison. (See equation 44.) This was needed because the process does not have reciprocity when the sample interval values are not equal.

For the site described above 2,230 unique comparisons were possible. Figure 25 shows the absolute percentage difference in IRI versus cross correlation level for all of these measurements. The figure shows that a broad range of error is possible for a given level of cross correlation. On the other hand, each correlation level seems to have a maximum possible error in IRI associated with it. Some part of this maximum error is associated with the “amplitude” term in equation 43, and the rest is caused by differences in profile shape. Values on the lower left portion of figure 25 represent cases where the overall IRI was in agreement, but the profiles were not. These are cases of compensating error in IRI that are not rewarded by the cross correlation method.

The 1993 RPUG data were used to relate cross correlation level to the 95th percentile of IRI error level over the entire dataset. This includes every measurement on every test section, and covers 129,812 pairs of IRI error and cross correlation level. These pairs were assembled into bins by their cross correlation level. Each bin covered a range of 0.01 (out of 1) along the scale. For example, the bin that ranged from 0.93 to 0.94 included 2,302 pairs. The set of values for each (well populated) bin closely approximated a Gaussian distribution, and were summarized by the average, RMS, and 95th percentile difference in IRI. Figure 26 shows the results for cross correlation levels of 0.85 and above. A clear relationship exists between cross correlation of IRI filter output and the 95th percentile level of error in IRI that may be expected on a site of similar roughness and surface texture.

It is proposed that cross correlation function as the standard method of rating profile agreement within profiler certification testing programs. Cross correlation has the potential to provide a rating of agreement between profiles in a given waveband, and may be used successfully over a broader band of wavelengths if the filtering is done properly. In particular, overall profile agreement should be judged using filtered profile slope, and expected agreement in overall IRI and spatial distribution of IRI can be judged by comparing IRI filter output. Since the method is indifferent to which type of profiler makes each measurement when two profiles are compared, threshold limits on cross correlation level may be set that pertain to repeatability as well as accuracy.

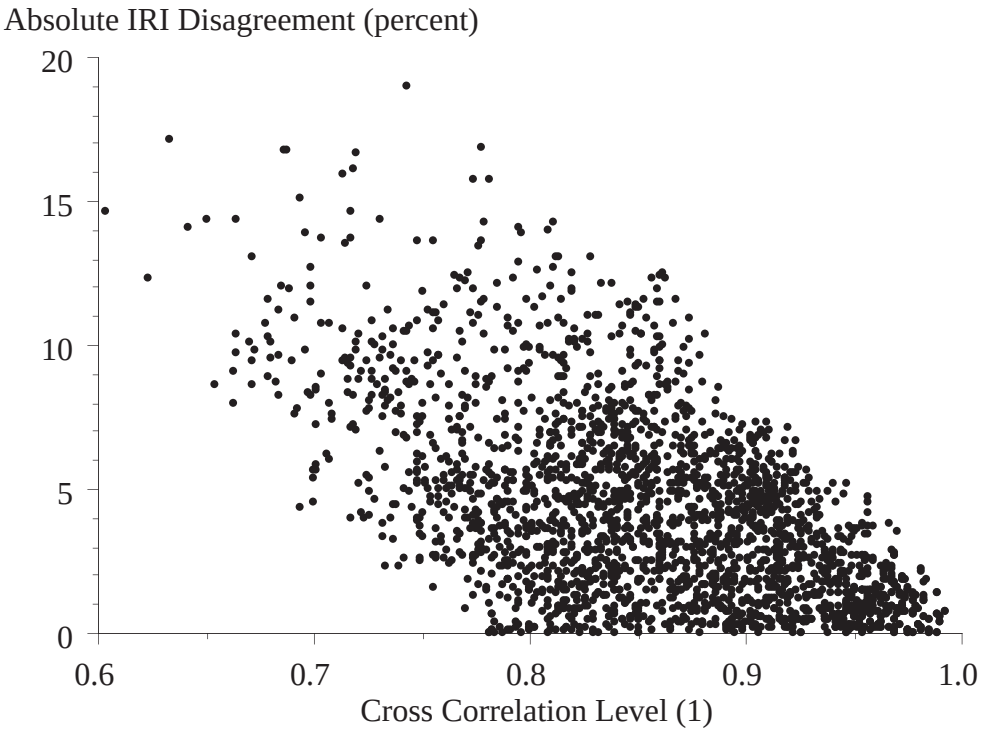


Figure 25. IRI agreement versus cross correlation level.

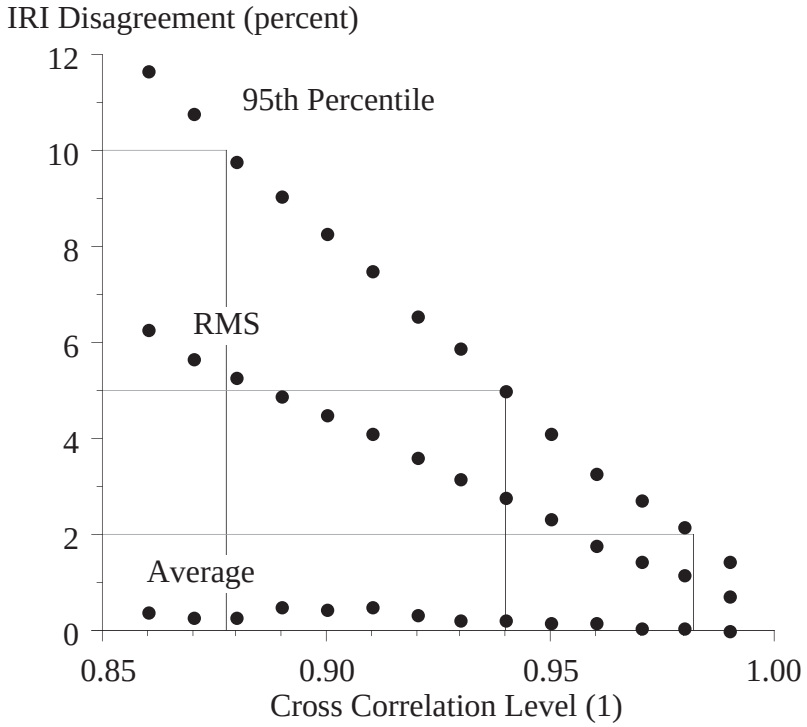


Figure 26. IRI agreement associated with cross correlation level.

Data from the 1993 RPUG experiment were used to establish a relationship between cross correlation level of IRI filter output and agreement in overall IRI over 160.9 m (528 ft) of road. The following thresholds are proposed for various "classes" of profiler:

- **Reference Class**: At a cross correlation level of 0.98, you may expect your overall IRI measurements to agree within 2 percent of each other 95 percent of the time.
- **Project Class**: At a cross correlation level of 0.94, you may expect your overall IRI measurements to agree within 5 percent of each other 95 percent of the time.
- **Network Class**: At a cross correlation level of 0.88, you may expect your overall IRI measurements to agree within 10 percent of each other 95 percent of the time.

Further, a value of 0.94 could also be used as a threshold for construction quality control. This must be verified by testing several more modern profilers on new or very smooth pavement with the appropriate surface texture of each pavement type to establish that the limit is correct. The 2004 FHWA profiler round-up provide these data, and the results should be used to verify or re-establish the thresholds listed above.[6] In addition, the analyses must set an independent threshold that will guarantee repeatable and accurate output of the prevailing method of locating must-grinds or isolated rough spots.

Please note that the threshold correlation values were set somewhat conservatively. The data shown in figure 26 are the basis for the recommended threshold values. In figure 26, a given value of cross correlation actually represents the upper limit of a range that is 0.01 units wide. The "Project Class" threshold of 0.94, therefore, is established because values from 0.93 to 0.94 exhibited the desired performance.

The cross correlation method must be applied very carefully. Analysis of the 1993 RPUG data, and other recent studies, show that profilers will exhibit a different level of repeatability and accuracy on different types of pavement.[28,75] Achieving one of the class levels listed above on a given pavement type only implies that good performance is expected on pavement of the same type and level of roughness, and of the same surface texture. Therefore, selection of test sites for profiler verification and classification is very important.

WAVEBAND ANALYSIS

Four filtering options for rating repeatability and accuracy are recommended:

1. The output of the IRI algorithm: This is a slope profile with frequency weighting determined by the quarter-car filter using the Golden Car parameters.
2. Long waveband: The profile, passed through a high-pass filter with a cutoff wavelength of 40 m (131.2 ft) and a low-pass filter with a cutoff wavelength of 8 m (26.2 ft).
3. Medium waveband: The profile, passed through a high-pass filter with a cutoff wavelength of 8 m (26.2 ft) and a low-pass filter with a cutoff wavelength of 1.6 m (5.25 ft).

4. Short waveband: The profile, passed through a high-pass filter with a cutoff wavelength of 1.6 m (5.25 ft) and a low-pass filter that is customized to reproduce the bridging and filtering applied by the reference or benchmark profiling device.

Typically, conversion to slope is an important aspect of the filtering process. This is because most profiles exhibit much less variation in slope amplitude than elevation amplitude over the wavelength range of interest. Thus, preprocessing for cross correlation analysis should either include conversion to slope, or the use of relatively narrow wavebands, such as the long, medium, and short wavebands described above.

The first item above emphasizes content in the profiles that is relevant to accumulating contribution to the IRI. The other three filters cover the waveband of interest for broad applications of profilers that are linked to vertical vehicle dynamic response to road roughness. Correlation results in these three bands also helps diagnose the source of disagreement between devices.

The low-pass filter used to isolate the short waveband must reproduce the filtering and bridging applied when the "true profile" is measured. Chapter 6 and 7 recommend two alternative methods for smoothing measured profiles in a manner that reproduces tire bridging and envelopment. If the candidate reference device inherently filters out very short wavelengths in a manner that provides the same enveloping and bridging response as the benchmark measurement, no additional low-pass filter is needed. If the candidate reference device does not apply any low-pass filtering, be it digital or by virtue of the device's footprint, the directional filter described in chapter 6 should be applied to isolate the short waveband for cross correlation analysis.

Each waveband will be isolated using a third-order high-pass and low-pass Butterworth filter, with the exception of the low-pass filtering for the short waveband. The filters shall be applied once in the forward direction and again in the reverse direction. This will cancel the phase shift. The cutoff values are set so that when the filters are applied the remaining content is primarily sensitive to the wavelength range of interest.

CHAPTER 6. SAMPLING AND FOOTPRINT REQUIREMENTS

This chapter defines the sampling and footprint requirements for a reference profiling device. The chapter covers three important aspects of the profile sampling process: (1) the longitudinal sample interval, (2) the footprint length and width, and (3) the bridging and enveloping that should occur within the footprint. Each of these sampling qualities needs further study to verify or improve the recommendations for them that are made here. Nevertheless, this chapter seeks to recommend practices that are based on the best available information. The recommendations are also expected to steer the profiling industry toward better practices, so that when more information becomes available the technology has already moved in the proper direction.

An important theme of this project is the use of performance based requirements instead of method based requirements. In that sense, the major recommendation of this chapter is that a reference profiler should sense the pavement as much like a common automobile tire as possible. Further, profile sampling practices should not preclude the same level of relevance to truck tire response. Unfortunately, these recommendations are too vague to be useful for the specification or procurement of a reference device.

Specific footprint dimensions, a maximum sample interval, and filtering methods are recommended here, but not mandated. These specifications will be applied when the measurements are made as a benchmark for the accuracy of candidate reference devices, as described in chapter 7. The candidate reference device itself need not use the same sampling practices. However, candidate reference devices will be expected to reproduce benchmark profile measurements made using these sampling practices. Reproduction of the benchmark profiles will be established by the profile comparison methods and accuracy thresholds described in chapter 4 and 5.

Longitudinal recording interval is a critical aspect of the sampling process.

Recommendation: *Profile should be recorded at an interval no larger than 70 mm (2.76 in).*

When profile is recorded at a larger interval, too much potential exists for aliasing error. Further, at larger values of profile recording interval the moving average filter used in the IRI and RN calculation algorithms cease to provide the expected short wavelength cutoff.

A recording interval of 70 mm (2.76 in) or less is also needed for profilograph simulation, particularly when PI under a null blanking band is of interest. This is because most profilograph simulations apply a third-order Butterworth filter with a cutoff wavelength of 0.6 m (2 ft). As the recording interval increases, the gain response of the filter departs from the intended shape. The difference is significant when the recording interval is greater than 70 mm (2.76 in).

The profile recording interval may be much larger than the profile sampling interval (or sampling rate), depending on the footprint of individual readings. For example, a profiler may sense the pavement surface with a laser that takes thousands of readings per

second. In this case, each recorded profile point must be based on multiple readings within the footprint, using the filtering method described below.

Recommendation: *When data are collected at a high sampling rate, proper anti-alias filters must be applied before decimation to the recording interval. The low-pass filter should have a cutoff wavelength equal to twice the recording interval.*

Alternatively, the profiler may sense the pavement with a very large footprint within each reading, often by contact with the surface. In this case, the length of contact should be equal to the recording interval.

Recommendation: *When the sampling rate and recording interval are the same, the footprint of the device should have a length that is equivalent to the recording interval.*

For example, a contacting device with a recording interval of 70 mm (2.76 in) is also expected to contact the pavement over a length of 70 mm (2.76 in) for each reading. When the pavement is in contact with the device over the entire footprint, and all of the features within the footprint are full enveloped, the overall elevation reading is equivalent to the average height within that area. The anti-aliasing quality provided in this case is similar to a filter with a cutoff wavelength of twice the recording interval.

The profile sampling interval may not be larger than the profile recording interval. In other words, measurement of profile with lesser detail, and interpolation to the required recording interval is not permitted. Further, the footprint within each recorded sample must include the anti-aliasing measures described here.

Relevance to vehicle response of a profile also requires a minimum footprint width. The optimal width is not known. For this study, the footprint width is set to a value that is at least three times larger than the characteristic length of transverse textural features. In particular, three times larger than: (1) most types of aggregate that appear on pavement surface, and (2) the most common spacing of longitudinal tines.

Recommendation: *Sense the pavement with a footprint that is at least 70 mm (2.76 in) wide.*

In many cases, a contacting footprint provides a way to bridge over narrow features that do not affect vehicle response, because the tire does not contact them either. When a device measures the road with a very small sampling interval, then applies a low-pass filter to the signal, some surrogate form of tire bridging is needed.

Recommendation: *When data are collected at a very rapid sampling rate, apply a low-pass filter with bridging qualities.*

Chapter 7 recommends methods of measuring a benchmark profile as a standard for the accuracy of candidate reference devices. One of the methods senses the pavement at a very high sampling rate, then applies a low-pass "bridging" filter. The filter seeks only the highest features within a given baselength, until they displace an area that implies an average depth of 1 mm (0.04 in). (This filter is described in more detail within this chapter.) The other method of measurement contacts the pavement over a length (and width) of 70 mm (2.76 in).

All of the recommendations in this chapter are based on the best available information. However, they have such important consequences that further study is recommended. In particular, the theoretical study of longitudinal sampling interval should be augmented with a numerical study using very detailed short-interval profiles. This is needed to capture influences of texture that are not represented accurately in the spectral models studied here. In addition, a direct connection to vehicle response is needed. Two types of study are recommended:

1. Make direct observations of the manner in which texture and short-duration surface features protrude into the tread of standing or slowly rolling tires. This would provide the basis for designing a non-linear filter, which attempts to assign weighting to textural features in proportion to their influence on vertical forces at the tire contact patch.
2. Perform a statistical study of the link between measured vehicle response and key aspects of very detailed, simultaneously measured profiles. To support the study, measure the profile at a very small interval in the longitudinal direction, and measure several densely spaced side-by-side profiles within the zone of tire contact. With coherence to spindle response as a correlation standard, parse the profiles to find the optimal trade-off between the level of detail needed in the measurement, and prediction of spindle response.

LONGITUDINAL SAMPLING

Karamihas provided background and analyses of longitudinal sampling procedures in a recent study of profile measurement errors.[28] Parts of that discussion are repeated here, and augmented with more recent information and additional calculations.

Background

A true road profile represents the height of the road along a continuous imaginary line on the surface. Since profiles are usually stored as digital signals, they must be reduced to a discrete collection of "sampled" points. In this process it is very important to accurately measure the components (that is, the wavelength range) of the true profile of interest. It is also important, for economic reasons, not to attempt to store more detail than is needed. This motivates the need for proper filtering and decimation practices.

All profile measurement devices have an inherent sampling interval or sampling rate. For example, most inertial profilers use digital height transducers, so they can only make a measurement a finite number of times in a second. These sensors typically provide readings at a constant time step, which often produces 32,000 readings per second. This is a *sampling rate* of 32 kHz. However, these signals are usually filtered (in the time domain) and decimated to a constant distance step before they are used within the profile calculation algorithm. This distance step is the *sample interval*. Once the profile is calculated, it is typically saved for eventual analysis. In some cases, the profile is filtered again (in the spatial domain) and further decimated before it is stored. In others it is not. Whatever the case, the *recording interval* is the distance step at which the profile is stored.

Slower speed profiling devices usually contact the pavement with a pre-determined spacing between readings. For example, in an evaluation of profile equipment, Fernando used rod and level measurements at an interval 152.4 mm (6 in) as a standard for accuracy.(61) This is both the sample interval and recording interval of the profile. In the same work, two devices were evaluated that use an inclinometer to measure the slope between supporting feet or wheels. A reading is typically recorded each time the trailing support is shifted forward to the position of the leading support from the previous measurement. As a result, the recording interval is equal to the wheelbase of the device.

A profiler may use any combination of sampling rate, sample interval, and recording interval, depending on its sensor capabilities, configuration, electronics, and calculation algorithm. For the rest of the discussion, it is assumed that a single low-pass filter is applied before decimation to the recording interval in lieu of studying each step in the sampling process individually. Relevant and reproducible measurements of profile depend on these filters to eliminate aliasing errors. Aliasing occurs when, as a consequence of decimating to a finite interval, the short wavelength content of the true road profile contaminates the measurement of the longer wavelength content.

Figure 27 shows a simple illustration of aliasing. A sine wave is sampled at an interval, Δ, which is slightly longer than its wavelength, 1.1Δ. As a result, output readings miss the peak of the sine wave by a progressively larger margin. The only information that is available after the measurement is the set of sampled values. When the sampled points alone are considered, they appear to define a sine wave with a much longer wavelength of 11Δ.

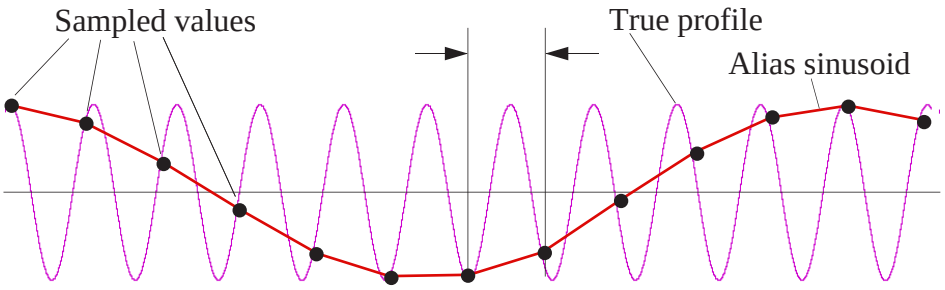


Figure 27. Simple example of aliasing.

Aliasing contaminates a signal for wavelengths above twice the recording interval. When a signal is digitized, no information is available above wave numbers that correspond to twice the recording interval:(47)

$$\nu_f = \frac{1}{2\Delta} \tag{46}$$

This is called the *folding wave number*. In the absence of the proper filters, content at a wave number lower than the folding wave number (i.e., a wavelength longer than twice the recording interval) is contaminated by content at higher wave numbers. A wave number, ν, is contaminated by aliased content at wave numbers of:(47)

$$(2\nu_f - \nu),(2\nu_f + \nu),(4\nu_f - \nu),(4\nu_f + \nu),....,(2n\nu_f - \nu),(2n\nu_f + \nu),..... \tag{47}$$

Consider the example above. Measurement of the content at a wave number of $1/(11\Delta)$ was contaminated by a feature with a wave number of $10/(11\Delta)$ when the folding wave number was $1/(2\Delta)$. This corresponds to the first item in equation 47.

If perfect anti-alias filtering were applied to the signal before it was recorded, all content for wavelengths shorter than 2Δ would be eliminated, so no erroneous content would be "folded in." Of course, aliasing error is very difficult to eliminate entirely, because most low-pass filters do not eliminate all content beneath the wavelength range of interest. On the other hand, the "filtering" done within the sensor footprint of most profiling devices helps remove the very short wavelength content. This limits the number of terms in equation 47 that may be important.

From a more practical standpoint, imagine a height sensor with a very small footprint measures a few centimeters deep into a narrow crack. This is a feature in the road that is likely to be ignored by a tire passing over it, and should also be ignored by the roughness measurement. If the profiler is operating with a very short sample interval, the dip will be recognized in the profile as very narrow. Then, a proper filter can eliminate much of its influence on the measured roughness. However, if the sample interval is very long, the crack will erroneously appear to be a dip a few centimeters deep and twice as long as the sample interval. This will artificially increase the roughness of the section because there was not enough information available to recognize it as a narrow crack after sampling.

The potential for this type of error in the measurement of road profile is enormous. Distress such as cracks and spalls can easily lead to aliasing error. Many features that can cause aliasing errors are intentionally built right into pavement. Keep in mind that profile content in the wavelength range from 1 to 50 mm (0.04 to 2 in) leads to coarse surface macrotexture and is desirable from the standpoint of safety. Tining, large exposed aggregate, and many types of coarse seal coat are all features that have caused aliasing errors in common profiling equipment.[4,5,28,75]

Fortunately, aliasing can be avoided. Refer once again to the example pictured in figure 27. Assume that the original sine wave has a wavelength that is outside our range of interest, but the aliased sine wave does not. In the original example, a single point was measured every Δ. As an alternative, consider a case in which a sampling rate was used that allowed 10 measurements to be made over the distance Δ, as shown in figure 28. Then, before the sensor readings were digitized, each set of 10 measurements were averaged to a single value. (Note that the average over a distance Δ of the original sine wave is less than 10 percent of its original amplitude.) These averaged values could then be digitized at a sample interval of Δ. This procedure leads to a much higher level of quality in the measurement. The original sine wave still does not appear in the final measurement. Figure 28 shows that the (artificial) longer, aliased sine wave is also virtually eliminated.

Specifications for sample interval, recording interval and anti-aliasing have been established in the past. The original definition of a Class 1 profiler by the World Bank required a sample interval (and recording interval) no greater than 250 mm (9.84 in).[25] This was written with measurement of the IRI with a rod and level in mind, and for a very large range of roughness. Note that 0.9 m (2.95 ft) was established in this report as the short wavelength boundary for profile measurement when the IRI is of interest. (See

chapter 3.) A recording interval of 250 mm (9.84 in) corresponds to roughly four points within the shortest wavelength of interest. In one of the earliest evaluations of inertial road profiling equipment, Darlington recommends the use of four points within the shortest wavelength of interest, rather than the typical standard of two.(34) The World Bank publication also suggests a sample interval of 50 mm (1.97 in) for high-speed devices.

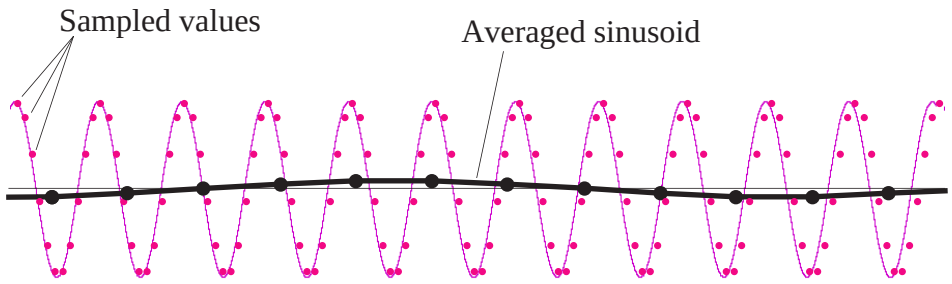


Figure 28. Use of filtering to reduce the influence of aliasing.

ASTM requires a sample interval of 25 mm (1 in) for Class 1 status among inertial profilers.(59) No specific specification is given for the recording interval, except that it shall be "adequate...for the intended use." Further, anti-aliasing filters are mandated for cases in which the folding (spatial) frequency is close to the upper frequency of interest (i.e., when the shortest wavelength of interest is not much longer than twice the sample interval).

AASHTO MP 11-03 requires a sample interval and recording interval of 50.8 mm (2 in) for inertial profilers, but does not specify the use of anti-alias filters.(7) AASHTO PP 49-03 specifies a sampling and recording interval of 120.7 mm (4.75 in) for reference profiles, again with no requirement for anti-alias filters.(64) In the case of PP 49-03 the lack of anti-alias filters is not a critical problem, because the method of comparison to the reference profile is primarily sensitive to long wavelength content.

Theoretical Study of IRI

This section theoretically examines the effect of longitudinal recording interval on IRI with two examples of low-pass (anti-alias) filtering. First, it is assumed that the longitudinal sampling rate is extremely high, and a "perfect" low-pass filter is applied to the data. With this filter, all content for wavelengths below twice the recording interval is eliminated so no aliasing is possible, and all content for wavelengths longer than twice the recording interval is left unmodified.

Second, the analysis is repeated using a moving average with a baselength equal to the recording interval. In this case, content for the wavelengths eliminated by decimation are allowed to "fold in," after they have been attenuated by the moving average. This represents a crude model of a rod and level with a large flexible rubber footpad. The moving average represents the enveloping action of the footpad, and its baselength derives from the assumption that the length of the footpad is equal to the recording interval. These two filtering possibilities correspond to the two benchmark profile measurement methods proposed in chapter 7.

Profile measurement often involves multiple filters. Some of the filters are applied digitally, some are applied using analog circuitry, and some are "mechanical" filters that are applied by virtue of the footprint that is used to contact the pavement. No attempt is made to study these intermediate steps. Instead, the net effect of all low-pass filtering steps is represented as a single, equivalent process.

"Perfect" Anti-alias Filter

Recall that, in the spatial frequency domain, the IRI may be estimated by:

$$\text{IRI} = \sqrt{\frac{2}{\pi}} \bullet \sigma \tag{48}$$

where σ is the root mean square, and the mean square is:

$$\sigma^2 = \int_0^\infty \left|H_{IRI}(\nu)\right|^2 \bullet G'_{in}(\nu) \bullet d\nu \tag{49}$$

H_{IRI} is the transfer function of all of the IRI filters together as depicted in figure 4, and G'_{in} is the (Gaussian, random, and stationary) input slope profile spectral density. For the "perfect" low-pass filter, all content for wavelengths shorter than twice recording interval is eliminated. This effect on the input profile can be represented by changing the upper limit of integration in equation 49. (The upper limit of integration would change from infinity to $1/(2\Delta)$.)

The choice of recording interval also affects the IRI calculation in three ways. First, the numerical solution to the equations of motion loses stability as the recording interval increases. This has a negligible effect on the IRI until the recording interval becomes extremely large.(32) Second, as the sample interval grows, more and more of the spatial frequency range is left out of the calculation. Chapter 3 concluded that wavelengths up to 0.9 m (2.95 ft) can be ignored before the IRI is underestimated by more than 1 percent. With perfect anti-aliasing, the recording interval would have to be 450 mm (17.7 in), which is half of 0.9 m (2.95 ft), or larger to cause a 1 percent error by this mechanism. Third, the recording interval affects the performance of the moving average used in the IRI algorithm by altering the effective baselength. This mechanism is significant at recording interval values used in common practice.(28)

The IRI is calculated in several steps. First, the profile is converted to slope. Second, a moving average is applied to the result.[4] Finally, the Golden Car filter is applied. This alters equation 49 to:

$$\sigma^2 = \int_0^\infty \left|H_{GC}(\nu)\right|^2 \bullet \left|H_{ma}(\nu)\right|^2 \bullet G'_{in}(\nu) \bullet d\nu \tag{50}$$

[4]In the recommended implementation, the moving average and slope conversion are applied simultaneously.

where G'_{in} is the spectral density of input slope profile, H_{ma} is the square gain for the moving average, and H_{GC} is the squared gain for the Golden Car filter.

Theoretically, the gain function for the moving average is:[67]

$$H_{ma}(\lambda) = \frac{\sin(\pi B/\lambda)}{\pi B/\lambda} \tag{51}$$

Where B is the baselength of the average and λ is wavelength. The intended baselength for the moving average in the IRI calculation is 250 mm (9.84 in), but the average can only be applied for an integer number of points. The number of points is computed as follows:

$$I_B = \text{NINT}(B/\Delta) \tag{52}$$

Where I_B is the number of points used in the moving average, NINT stands for "nearest integer," B is the baselength, and Δ is the recording interval. (The value of I_B must be at least one.) Of course, the fraction in the brackets will rarely produce an integer exactly, so the effective baselength, which is $I_B \bullet \Delta$, is rarely 250 mm (9.84 in).

Table 6 lists some examples of the calculation in equation 52. The fluctuations in effective baselength cause the wavelength content of the moving average to shift, and introduce a small bias into the resulting IRI. The effective baselength is at its lowest value when the recording interval is about 167 mm (6.58 in). This is because a value of 167 mm (6.58 in) is just high enough to produce a value for I_B of 1, so no averaging is applied. A recording interval of 166 mm (6.54 in) is just small enough to produce a value for I_B of 2. This makes the effective baselength equal to 332 mm (13.07 in).

Table 6. Effective moving-average baselength.[28]

Recording Interval Δ (mm)	B/Δ	I_B	Effective Baselength (mm)
25	10.00	10	250
50	5.00	5	250
75	3.33	3	225
100	2.50	3	200
125	2.00	2	250
150	1.67	2	300
175	1.43	1	175
200	1.25	1	200
225	1.11	1	225
250	1.00	1	250
275	0.91	1	275
300	0.83	1	300

In addition to the change in effective baselength, the gain function of the moving average is also affected by the discrete nature of the calculation. When I_B is an odd number, the gain function for the moving average is:

$$H_{ma}(\lambda) = \frac{1 + 2 \bullet \sum_{k=1}^{(I_B - 1)/2} \cos(2\pi k \Delta / \lambda)}{I_B} \tag{53}$$

When I_B is even, the gain function is:

$$H_{ma}(\lambda) = \frac{2 \bullet \sum_{k=1}^{I_B/2} \cos\left[2\pi(k - 0.5)\Delta / \lambda\right]}{I_B} \tag{54}$$

These expressions converge to a gain function that is very much like equation 51 when I_B is greater than 10. When I_B is less than 10, the discrete nature of the moving average calculation affects the shape of the transfer function for wavelengths shorter then the effective baselength significantly.

Together, equations 48, 50, and 51 provide the expression for the "correct" IRI value that is calculated from a profile with an infinitely small recording interval. The expected IRI values for a given recording interval are calculated by: (1) changing the upper limit of integration in equation 50 to $1/(2\Delta)$, and (2) replacing equation 51 with either equation 53 or 54, whichever is appropriate. When these two calculations are compared, the error in IRI caused by the second and third mechanism described above may be estimated.

Figure 29 shows the error in IRI as a function of recording interval for Road 1. (The example roads were defined in chapter 3.) This is a road of white noise slope. The error changes smoothly with recording interval until the number of points in the moving average transitions from one integer to another. When the number of points in the moving average changes the effective baselength changes abruptly. In turn, the expected error in IRI changes abruptly. The largest jump occurs near a recording interval of 167 mm (6.58 in). In this case, the downward bias in IRI of about 0.7 percent changes sharply to an upward bias of 2.1 percent. The upward bias for recording intervals above 167 mm (6.58 in) occurs because no moving average is applied. (When Δ is greater than 167 mm (6.58 in), I_B has a value of 1.) As recording interval increases beyond 167 mm (6.58 in), the IRI gets steadily smaller as more and more of the wavelength range of interest is ignored.

The results in figure 29 differ from those reported by Karamihas for a similar theoretical study.[28] This is because the (earlier) study by Karamihas accounted for the change in effective baselength, but failed to include the "discrete" version of the moving average transfer function gain.

Figure 30 shows the error in IRI versus recording interval for Road 4. Sample Road 4 is the most sensitive to recording interval among the four samples, because it includes the most significant short wavelength roughness. The error nears an upward bias of 1 percent at a recording interval of 71.5 mm (2.81 in), and reaches an upward bias of 1.45 percent at a recording interval of 100 mm (3.94 in). Figure 30 also shows data from a numerical study using a measured profile with spectral qualities that are similar to Road 4.[28] Agreement is excellent between the numerical study and the theoretical predictions.

A comprehensive numerical study is needed that uses very detailed measurements of real profiles on a set of smooth roads with diverse macrotexture and megatexture. This would be much more relevant than the study presented here, because smooth roads with coarse texture are likely to require the most stringent sampling criteria. Further, the spectral models used in this study are not valid into the texture range, particularly for open-graded surfaces and "periodic" textures that result from tining.

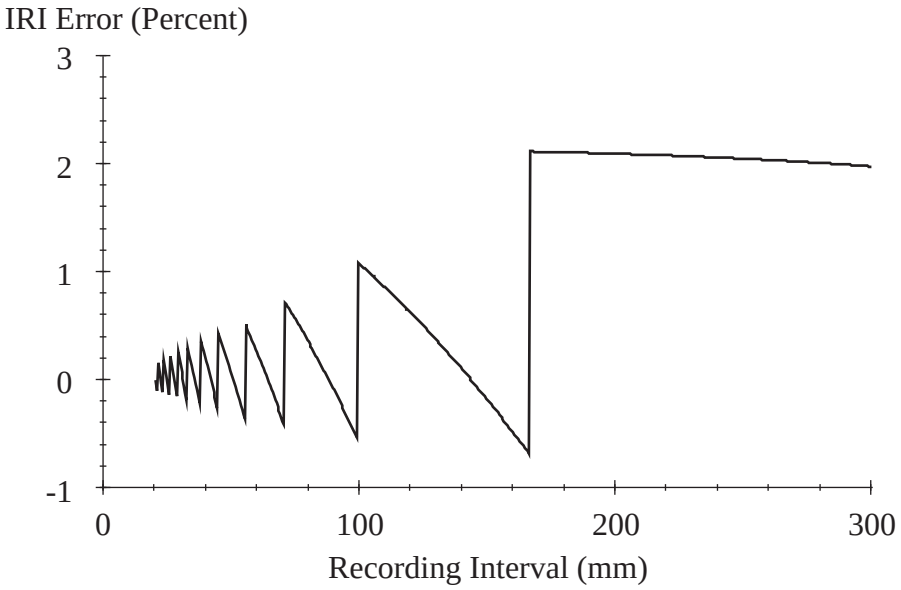


Figure 29. IRI error versus recording interval, Road 01.

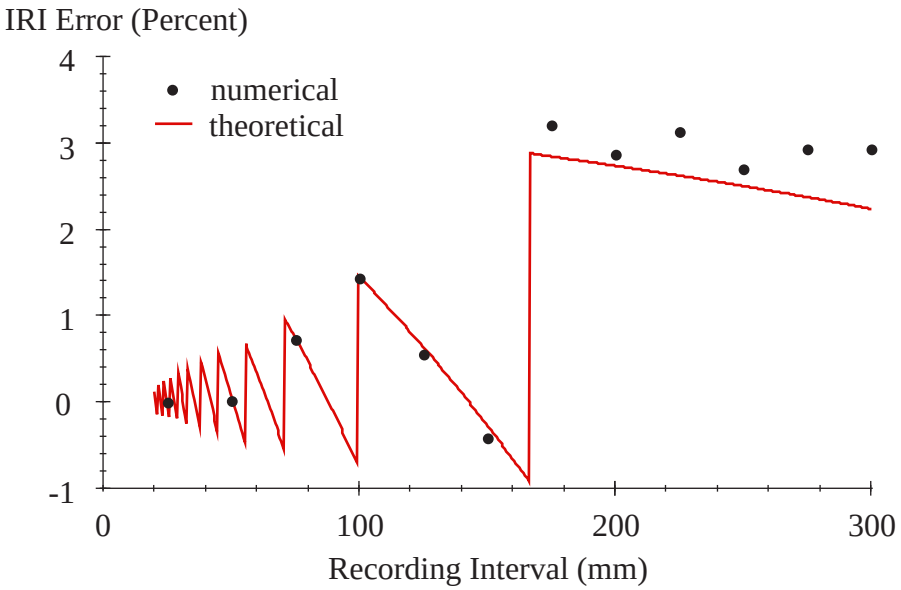


Figure 30. IRI error versus recording interval, Road 04.

Moving Average Anti-alias Filter

The study above was repeated using a moving average in place of the "perfect" anti-alias filter. The moving average represents a more realistic case of digital anti-aliasing than the perfectly sharp cutoff used above. A moving average is also a crude model of the way a tire may envelop small surface aspirates such as macrotexture, or the way some current reference devices that contact the pavement envelop texture.

When the moving average is used for anti-aliasing, the sampling process is modeled as follows:

Step 1: Calculate the slope PSD using equation 14 and the appropriate coefficients for the sample road of interest.

Step 2: Apply a moving average with a baselength equal to the recording interval. It is assumed that the original measurement was made with an extremely small sampling rate. This is analogous to a contacting device, which contacts the pavement over the entire recording interval. The moving average is approximated by:

$$H_{ma}(\lambda) = \frac{\sin(\pi\Delta/\lambda)}{\pi\Delta/\lambda} \tag{55}$$

This step produces the "averaged PSD."

Step 3: Decimate the profile to the recording interval of interest. This is done by "folding" all of the spectral content for wavelengths shorter than 2Δ to the range longer than 2Δ.

After this step, the folded PSD only covers a range of wave numbers from 0 to $1/(2\Delta)$, or wavelengths from infinity down to 2Δ. At a given wavelength between 2Δ to infinity equal to λ, the value of the folded PSD is the sum of the mean square values from the averaged PSD at wavelengths of:

$$\frac{1}{\frac{n}{\Delta} \pm \frac{1}{\lambda}}, n = 1, \infty \tag{56}$$

Steps 1 through 3 generate a slope input PSD that is modified by the sampling process.

Step 4: Calculate the expected value of IRI using equation 48 and 50, with the appropriate transfer function for the moving average from either equation 53 or 54. The limits of integration need not extend past $1/(2\Delta)$, because folding has removed all content for higher wave numbers.

These steps provide the expected value of IRI for a given recording interval. Once again, this may be compared to the value for a very small recording interval to study the error.

The relationship between IRI error and recording interval was very similar, qualitatively, to the case of "perfect" anti-aliasing filters, above. The error levels were slightly higher, because of the aliased short wavelength content that folded in to the range

of interest. Road 4 was the most sensitive. The error on Road 4 changed from a value just above -1 percent to a value just below 1 percent at a sample interval of 55.6 mm (2.19 in). Road 4 also exhibited an absolute error level above 1 percent when the recording interval passed above 70 mm (2.76 in).

Error in PTRN was extremely sensitive to recording interval with either example of anti-alias filtering. The sensitivity is so high that it is not considered practical to make a reference measurement at a sufficiently small recording interval to eliminate the error. This is, instead, considered a weakness in the algorithm. The study of RN in this manner showed that the 250-mm (9.84-in) moving average interacts so strongly with the wavelength range of interest of the primary filter that it must be replaced by a low-pass filter that is not so heavily influenced by the recording interval.

Filtering for Simulated Profilograph Index

In manual reduction of profilograph traces, short narrow deviations are eliminated by outlining.(76) The influence of texture, cracks, and narrow joints are also greatly reduced by the broad contact made by the measuring wheel. When profilograph response is simulated from measured profile, the trace is typically smoothed using a third-order Butterworth low-pass filter.(45) In part, this takes the place of the tracing operation, but the use of a minimum scallop width is also necessary.(46,77,78)

The most common choice of a cutoff wavelength for the filter is about 0.6 m (2 ft), although a range of values up to 0.76 m (2.5 ft) have been reported.(79) The third-order Butterworth filter offers the following gain characteristics:

$$\left|H_{BW}(\lambda)\right| = \frac{1}{\sqrt{(\lambda_c/\lambda)^6 + 1}} \tag{57}$$

Where λ is wavelength, and λ_c is the cutoff wavelength.

This is the theoretical performance of the filter. In practice a third-order Butterworth low-pass filter is performed using a recursive summation, in which an output value at a point depends on a linear combination of four values in the original signal leading up to that point and three points preceding it in the output signal. The coefficients on each term depend on the recording interval and the desired cutoff wavelength.

As the recording interval approaches the cutoff wavelength, the behavior of the filter begins to degrade. Figure 31 shows the gain characteristics of a third-order Butterworth low-pass filter for three cases: (1) a very small interval, (2) an interval of 70 mm (2.76 in), and (3) an interval of 150 mm (5.91 in). At a very small interval, the gain characteristic is very close to the desired theoretical performance. At a recording interval of 70 mm (2.76 in), the performance of the filter is degraded somewhat, and at a recording interval of 150 mm (5.91 in) the performance of the filter has degraded significantly. Since PI with a null band is intended to capture the influence of short wavelength content within the profile, a signal with a recording interval greater than 70 mm (2.76 in) should not be input to this filter.

This discussion did not cover the effect of folding on the filter response, which would increase the problems with performance at large recording intervals when no other anti-aliasing filters are applied.

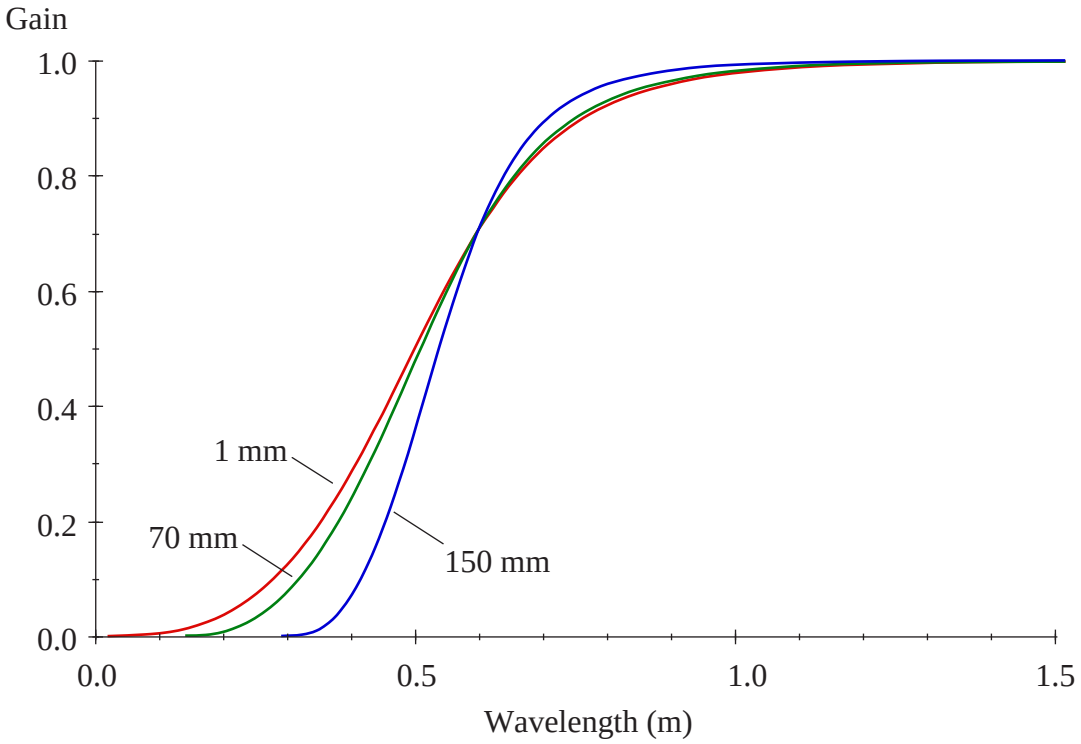


Figure 31. Third-order Butterworth low-pass response at various intervals.

TIRE ENVELOPMENT

Reproducible road profile measurements depend on appropriate sampling procedures, including a sufficient recording interval and proper anti-aliasing, as described above. This section extends the discussion to relevance. Relevant road profile measurements sense the pavement as much like a vehicle tire as possible. In particular, the profiler should seek to duplicate the way tires envelop macrotexture and megatexture and bridge over concave features with characteristic dimensions that are much smaller than the tire footprint. This can be done in two ways. First, a profile may include tremendous detail about the road surface, so that the bridging and enveloping action of a tire may be calculated from it using the proper filters or simple tire models. Second, the profile may be measured using a large footprint that is designed to reproduce quasi-static tire bridging and envelopment.

This section reviews the tire envelopment and bridging offered by vehicle dynamics models that appear in the literature. A simple enveloping and bridging strategy is suggested. This strategy may be implemented as a digital or analog filter, or as an aspect of the footprint design of a reference device.

Vehicle Dynamics Models

This section reviews the mathematical models of tire envelopment. They typically exist within simulation models of vehicle ride or durability. The tire models cover a large range of complexity, because each was conceived for a specific purpose, and corresponds to unique trade-off between accuracy, bandwidth, and efficiency requirements. Some models of tire envelopment may be applied as an equivalent profile processing filter. These are the most useful for application to road evaluation, because they can be applied to the profile without coupling to a specific vehicle model. Other models can not be reduced in this manner, and are reviewed here simply to help explain the complicated physical phenomena that occur when a tire interacts dynamically with the road.

This section discusses six categories of tire model that are used for prediction of vehicle ride and durability. (See figure 32.) Zegelaar provides an excellent review of tire models that provides more technical detail than this report.[80]

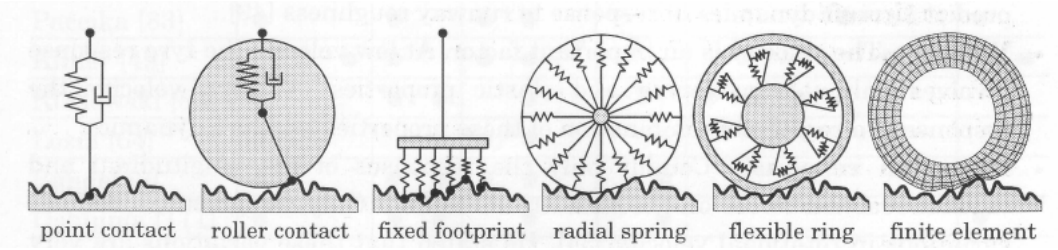


Figure 32. Tire models for response to road roughness.[80]

Point Contact

In a point contact model, the compliance of the wheel is represented by a single vertical spring and damper. (See figure 32.) The tire footprint is reduced to a single point of contact, which "follows the contour of the road faithfully."[81] This model has been used in several early studies of vehicle response to road and terrain roughness with varying degrees of success.[82,83,84,85] Rasmussen concluded that, for most applications, tire damping can be neglected.[83] The tire compliance is then represented by a vertical spring only. Jurkat made some improvements to the model for response to large obstacles by adding elastic stops for large deflections, and preventing the tire from pulling the vehicle back to the road if it loses contact (i.e., letting the tire leave the ground).[85]

Most studies of tire models are validated only for response to large obstacles. On large obstacles the point follower typically over predicts tire response, because it follows the contour of the road for rapid changes in elevation when a real tire would lose contact. No study was found that examined the consequences of using a point follower model over a coarse-textured road, or even a natural road profile. However, several studies reported the response of a point follower model to a "cleat." The response to a cleat is usually quite severe, depending on the height of the cleat and the traveling speed. If one of these cleats were inverted, it would take on a shape that is very much like a saw-cut joint with no net change in elevation across it (i.e., no faulting), as shown in figure 33. The response of an actual tire to the inverted cleat would be very small. The point

follower model, however, would produce a response on the cleat that is as severe whether it is inverted or not.

Indeed, it was recognized early in the development of these models that tires do not respond the same way to protruding road features as they do to indented features of the same size and shape. Lippmann acknowledged this non-linearity, and cited two causes: (1) "discontinuous buildup and release of tread compression," and (2) "bridging."[86] Schuring, states that "...traversing a small, sharp obstacle, an actual wheel bridges and filters harsh contour changes."[81] *Bridging* is the mechanism by which the tire contact patch never makes contact with small, concave features in the road. It is the lack of proper filtering and bridging that disqualifies the point contact model for use on natural road profiles.

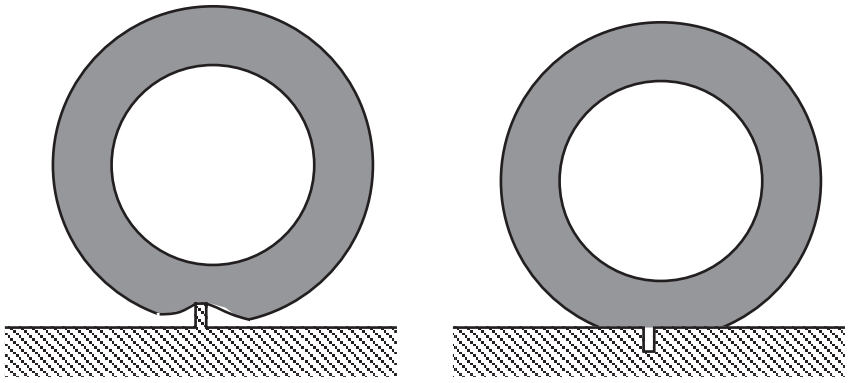


Figure 33. Tire response to a cleat.

Rolling Contact Models

A rolling contact model contacts the road using a rigid disc. The disc is constrained to move vertically beneath the axle, and is "connected" to the axle by a spring and damper.[87,88] As shown in figure 32, contact with the road no longer occurs directly below the axle, and may occur at two points. The rigid disc used in this model alters the effective road profile by removing dips that the never contact it. While this model does provide for bridging over narrow concave road features, it allows for no envelopment of short wavelength features.

Parallel Spring Models

A parallel spring, or fixed footprint, model represents the tire using several uniformly spaced springs across a finite contact length.[89,90,91] The parallel spring model acts much like the point follower model for responses to wavelengths greater than 10 times the contact length, but it offers a distinct improvement over the point follower for wavelengths shorter than 1.5 times the contact length.[81,89]

The parallel spring model applies one spring over each profile point, and the force on each spring element is proportional to the profile height, the model acts very much like a moving average. This is because the average spring force is proportional to the average

profile height. Of course, this requires the use of linear springs that are not permitted to lose contact with the profile. In fact, a simple method of implementing the parallel spring model is to perform a moving average on the profile as a pre-processing step, then run the simulation on the filtered profile using a point follower. This has produced excellent predictions of vertical spindle acceleration to frequencies up to 30 Hz on very rough roads.[92] When the model is further restricted to use a bed of springs over 250 mm (9.84 in) of profile, the parallel spring model provides enveloping properties that are equivalent to the IRI.

The main drawback of this model is the inability to bridge over narrow, concave features. When a deep gap appears in the profile, such as the inverted cleat shown in figure 33, the springs above the gap will stretch into them and try to make contact with the bottom. A tire does not behave in this manner, because it is supported by contact between the tread and the road outside the edges of the dip. The moving average works the same way. No matter how narrow or deep a dip is, it will influence the average in proportion to the depth and the width.

Radial Spring Models

A radial spring model uses springs that are distributed around the tire circumference to represent tire compliance.[93] (See figure 32.) In many applications, the radial springs are replaced by radial segments, and the force on the tire is proportional to the displaced area (in the pitch plane). The line of action of the force coincides with a line that runs from the centroid of the displaced area through the tire center.[81,94]

Radial spring models provide an improvement over the parallel spring model for vehicle dynamics studies in two ways. First, the tire contact length is allowed to change with time as it is affected by the road profile and axle dynamic motions. This is why radial spring models are often called "adaptive footprint" models.[95] Second, they are able to compute the protrusion of the road into the tire with much greater accuracy. This allows the model to account for "both the elevation and slope characteristics of the original terrain (or road) contacting the tire."[96] As a result, radial spring models provide a more realistic prediction of longitudinal tire forces.

Radial spring and radial segment models represent tire envelopment with acceptable accuracy when the modal responses of the tread band are not of interest. Like parallel spring models, radial spring and radial segment models do not provide an accurate representation of the bridging effect on features like an inverted cleat. This is because, like parallel spring models, the radial springs do not account for the bending stiffness of the tread band. Further, radial spring models are only effective when they are part of a coupled dynamic model of vehicle response. (In other words, they are only accurate when the motion of the axle is known at every instant.) As a result, a radial spring model can not be simplified as a pre-processing filter to a profile index calculation.

Ring and Finite Element Models

Several other models for prediction of tire dynamic response to road irregularities have been developed. Some models represent the tread as a circular ring (the tread band), which is connected to a mass at the tire center (the wheel) by radial and tangential

springs. The tread is then represented by distributed radial and tangential stiffness. In many of these models, the tread band is a rigid ring.[97,98,99,100] In others, the tread band is represented as a cylindrical shell.[101,102,103,104,105] Even more complicated models are available that use finite elements.[10] These models predict the response of tires to road obstacles very accurately, and many of them provide for tire bridging. However, they are not well adapted to deal with small road asperities. Further, they use too much computation time for practical application in road roughness index calculations. They also require mechanical tire properties that are very specific to a given tire. As such, they would be difficult to generalize into a standard tire model.

Profile Envelopment Filters

The 250-mm (9.84-in) moving average in the IRI algorithm approximates tire envelopment. Appendix A of NCHRP Report 228 describes slow-speed tire enveloping tests that provided the basis for selecting the moving average.[48] These tests measured the response of tires to impulse-like road disturbances, such as a 2x4, a piece of angle iron, and welding rods, at various test speeds and tire pressures. The analysis of these data sought a pre-processing filter for a profiler that best duplicated the effect of tire enveloping. The processed profile serves as input to a simple vehicle model, which represents tire contact using a point follower.

Figure 34 shows an axle vertical load signature that may be expected when a tire rolls at low speed over a cleat. The force is highest when the cleat just enters the tire contact area, and when it is just about to exit. This suggests that a proper tire envelopment filter for profile should assign the highest weighting to features at the edges of the contact length.

In the experiments for the NCHRP, the artificial disturbances provided impulsive inputs to the tire. When these artificial features were very narrow, they approximated white noise elevation. The 2x4 represented two step inputs, one upward step and one downward step. Step changes in elevation have the same spectral amplitude content as white noise slope. Sayers used these data to derive the transfer function from input profile to axle response. (More than 40 pen-recorded response functions were collected.) Most of these response functions exhibited a “node” at one or more frequency. A node is defined as a frequency at which the transfer function approaches a minimum, or approaches zero. This occurs when the system responds very little to profile input at a given frequency.

Figure 35 provides an example of a node in the frequency response for tests of a popular sport utility vehicle on fairly rough road. The figure shows the transfer function of road profile acceleration input to vertical spindle acceleration for a vehicle traveling 4 m/s (10 mph) over a large triangular bump. Since the test was done at low speed, most of the response is expected to result from quasi-static tire envelopment. At low wave numbers (or long wavelengths), the tire simply follows the vertical path of the road, and the “gain” is close to 1. In other words, the spindle follows a path that is parallel to the road for those wavelengths, and does not exaggerate or attenuate the road shape. (The deviation away from 1 at very low wave numbers is due primarily to measurement procedures, rather than vehicle motion.) At a wave number of 4.15 cycles/m (1.26

cycles/ft), the ratio of response at the spindle to the acceleration at the road surface (for that speed) reaches a local minimum, and is very low. This corresponds to a frequency of about 16.6 Hz at the 4 m/s (10 mph) test speed.

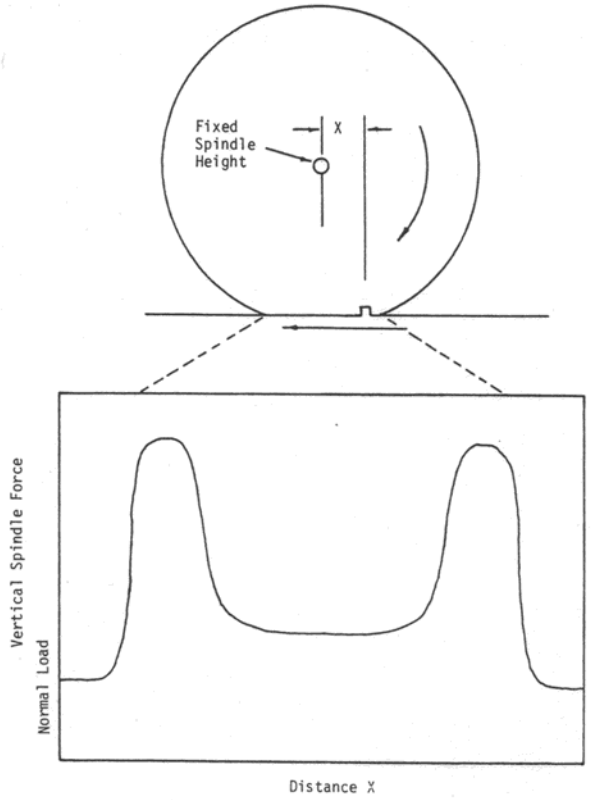


Figure 34. Force at the axle in response to an impulse.(48)

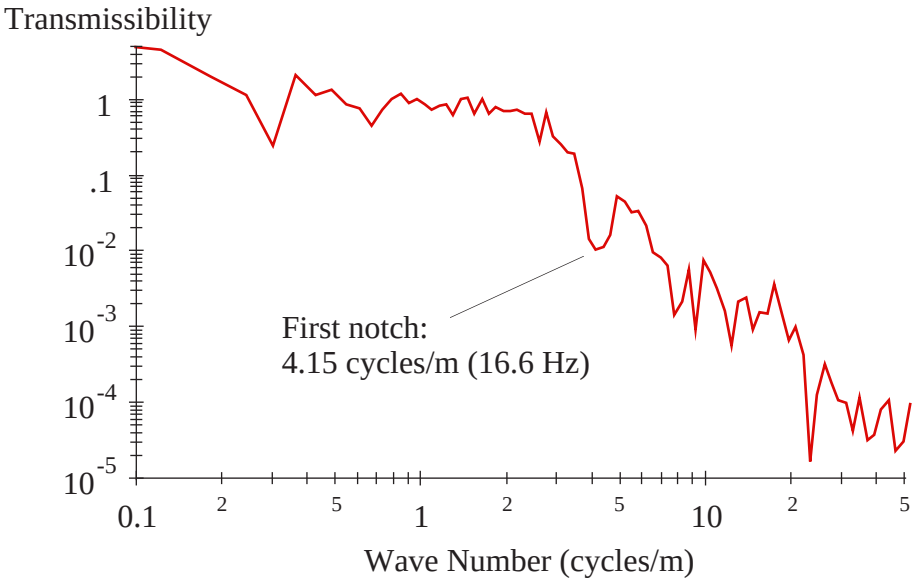


Figure 35. Road to spindle transmissibility over an impulse at low speed.

Figure 36 shows frequency response when the test was repeated at 8 m/s (20 mph). In this case, the transmissibility between the road profile and vertical spindle acceleration is much greater than 1 for parts of the low wave number (long wavelength) range. This is because, at higher speed, the spindle response includes the dynamics of the vehicle in addition to the effect of tire envelopment. The peak response occurs at a wave number of 1.47 cycles/m (0.49 cycles.ft), which corresponds to a frequency of 11.7 Hz. This is axle hop motion that was excited by the triangular bump. In this response function the first local minimum, or first notch, occurs again at 4.15 cycles/m (1.26 cycles/ft), which corresponds to a frequency of 33.2 Hz. The notches for the two tests depend on wavelength, rather than frequency. This verifies that they are caused by tire envelopment.

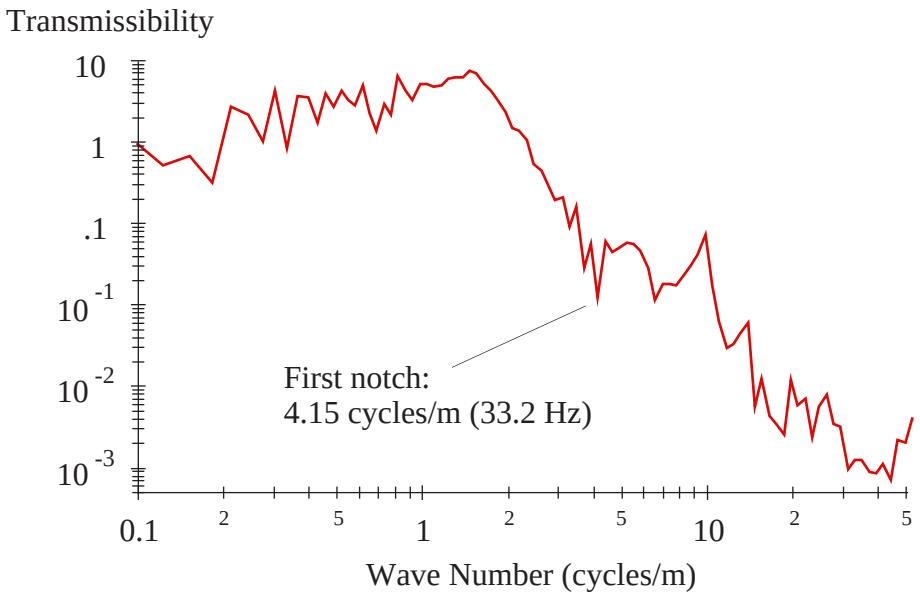


Figure 36. Road to spindle transmissibility over an impulse at higher speed.

Figure 37 summarizes the outcome of a more detailed tire envelopment study done by Sayers for the NCHRP. In the tests conducted by Sayers, the frequency at which the node occurred was proportional to speed, but the wave number (and hence, the wavelength) corresponding to the node was consistent over a broad speed range. This also verified that the node, and the roll-off in response approaching the node, was caused by tire envelopment. The tests by Sayers also found that the nodal wave number increased as tire pressure increased. In other words, the nodal wavelength decreased as tire pressure increased. This suggests that the nodal wavelength was related to the length of tire contact area.

Figure 37 shows three candidate profile weighting functions that were considered for modeling tire envelopment. The "representative tire" weighting function was reported in the literature from laboratory tire tests using a cleat.(106) The "complex model" was an approximation used by Sayers to reduce the representative tire model to three parameters. (This symmetrical weighting function could be described as the difference between two box-type functions with different widths and heights.) Note that the complex model has a weighting function that is similar to the representative tire. More importantly, it has a

wave-number response function that is exceptionally close to that of the representative tire.

Figure 37 also shows a very simple model. This model is a simple box-type weighting function that is described by a single parameter—the length. For this weighting function, the first node in the wave-number response will appear at a wave number that is the inverse of the length. When this length is set so that the node appears in the same place as in the other models, the response is very similar to the other models up to the nodal wave number. Sayers measured nodal wave numbers corresponding to wavelengths ranging from 0.24 to 0.33 m (0.79 to 1.08 ft). Thus, all of the wavelength range of interest for the IRI appears in the range where the simple model approximates the others well.

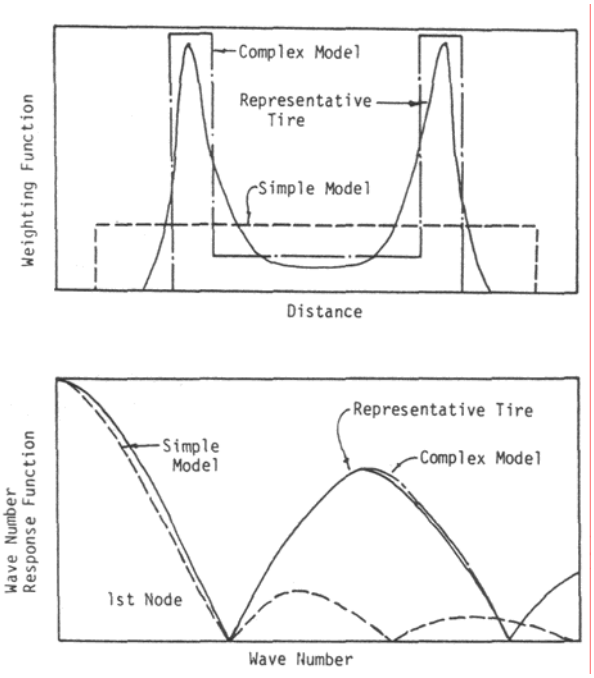


Figure 37. Comparison of tire envelopment weighting functions.[48]

The simple model was selected to represent tire envelopment in the IRI algorithm. The model offered three positive qualities:

1. It was implemented as a simple calculation (the moving average).
2. The weighting function was defined by a single value, which was simple to derive from tests. The moving average length simply needs to have a length that places the notch in response to the proper wave number. (For the SUV tire discussed above, this would be 0.24 m (0.79 ft). This is very close to the 250 mm (9.84 in) baselength used by the IRI algorithm.)
3. Because of its simplicity, this model is very general. A more complicated weighting function would offer more accuracy for higher wave numbers (very short wavelengths), but it would be more sensitive to tire type.

Note that the appropriate moving average baselength is greater than the contact length of typical automobile tires.

TIRE BRIDGING

The discussion above showed that a moving average is a reasonable approximation of tire envelopment for typical road features. Indeed, the moving average affects a profile in much the same way as a set of distributed linear springs. Unfortunately, the moving average does not provide a sufficient model of tire bridging. This section proposes a modification to the moving average that will help increase the relevance of profile measurements by incorporating a crude representation of the bridging effect. The filter is an approximation of a set of parallel springs, where each "spring" is allowed to reach a maximum extension and lose contact with the road if it is over a low point. Since the filter is applied to profile, it acts as if a single spring acts on each profile point within the averaging length. If the needed tire force (or, in effect, the protrusion above a datum plane) is accounted for by the high points, then the low points are ignored. Since this filter ignores narrow dips, it is referred to as a *bridging filter*.

The modified filter should not replace the moving average as a standard aspect of the IRI and RN calculation procedures. The relevance of this filter has not been experimentally verified, nor has the filter been used in practice. More testing of the algorithm and a validation experiment would be needed first. Rather, the filter is proposed in this project for a single application: benchmark profile measurement. When a benchmark profile measurement includes a high level of detail about the pavement surface, the bridging filter is recommended as a way of smoothing the profile and eliminating narrow dips that would be ignored through the bridging action of a tire.

Two strategies are recommended in chapter 7 for the purpose of making benchmark profile measurements. One contacts the pavement with a footprint that is 70 mm (2.76 in) in diameter. The other measures a high level of detail along the pavement, and over a 70-mm (2.76-in) wide track. The bridging filter described here serves the secondary purpose of making the detailed profile measurement equivalent to the contacting profile measurement.

The recommended filter is based on the expectation that the only features on the road that are relevant to vertical dynamic response are those that penetrate into the tire tread. An exaggerated diagram of this effect appears in figure 38. The filter described here makes the assumption that, in the side view, the average penetration into a tire tread is fixed. If a block of tire tread maintains contact with the road over its entire length, the average height of the tread-pavement contact would be the average profile height over its length. When gaps appear between the tire tread and the pavement, the protruding features in the profile must penetrate more deeply into the tread to achieve the same displaced area.



Figure 38. Penetration of macrotexture into a tire.[107]

The assumption of a constant tread penetration depth is only an approximation of real tire tread behavior. First, the level of indentation into a tire tread depends heavily on its material properties, and the vertical force on it at a given instant. The filter recommended here represents a standard tire tread block, and a quasi-static approximation of its behavior. Second, the manner in which macrotexture protrudes into a tire tread depends heavily on the shape of the highest portions of the texture profile. In particular, sharp upward features affect tire tread differently than blunt features.[108] Nevertheless, the "model" of a constant average tread penetration provides a way to treat narrow downward profile features more realistically.

Little information is available in the literature to help specify an average tread penetration depth. The most heavily cited work is a study that calculated the stress and contact conditions for measured texture profiles using a contact mechanics model and tire tread fundamental properties.[109] In this study, the displaced tread volume implied an average penetration of about 0.5 to 1.0 mm (0.02 to 0.04 in). (This is a difficult parameter to select, since it depends heavily on the tire inflation pressure and tread elastic modulus. The value is set conservatively here, and is biased toward a greater depth of contact.)

The recommended average penetration depth for the bridging filter is 1 mm (0.04 in). This is large enough to absorb the macrotexture for many pavements, but gaps between the tire and pavement are expected on very coarse textures. For example, the mean texture profile depth on pavement with a permeable friction course or an open-graded friction course usually exceeds 1 mm (0.04 in).[110,111] In addition, nearly all tined pavements are specified with a channel depth much greater than 1 mm (0.04 in).[112]

At an average depth of 1 mm (0.04 in), the filter will help ignore undue influence from narrow downward features. Consider a short length of profile that is perfectly smooth, with the exception of a single point that is 24 mm (0.94 in) below the surrounding elevation. This "narrow dip" would affect a passing tire very little. If the profile is smoothed using a moving average over a length that corresponds to 12 profile points, the filtered profile will include an area 12 points wide that is 2 mm (0.08 in) below the nominal road height. This is because the dip was within the range of the average at 12 different positions, and affected the average equally at each position.

The proposed bridging filter seeks to replace the moving average with a calculation of the depth into the pavement needed to displace an area with an average depth of 1 mm (0.04 in). Consider again the sample dip. When all 12 points have the same elevation, they all contribute equally to the displaced area, and the tread simply moves downward 1 mm (0.04 in) into the pavement. However, when any area is examined that includes the single low point; only 11 of the 12 points under consideration displace any area. As a result, the tread must move downward into the pavement 1 mm (0.04 in) times 12/11 to maintain an average penetration of 1 mm (0.04 in) over the considered width. After the filter has run the length of the profile, it is shifted back upward 1 mm (0.04 in) across the entire length. The net result of the narrow dip and the filter together is a dip that is 12 points wide and 1/11 mm (0.0036 in) deep. This is much less severe than the 2 mm (0.08 in) depth by the moving average.

Note that, as long as the dip is more than 12/11 mm (0.043 in) deep, its effect on the bridging filter does not change, whereas the response to the moving average is proportional to the dip no matter how deep it is.

At each point, the filter works as follows:

Step 1: Over the N samples covered by the filter, sort the elevation values (in mm) from highest to lowest. Store the result into an array, P. Set P(N+1) to be P(N) – D. ("D" is the target penetration depth of 1 mm (0.04 in).)

Step 2: Set the number of points enveloped (m) to 0. Initialize the total displaced area (A_D) to zero. Initialize the target displaced area (A_T) to N•D.

Step 3: Increment (i.e., add 1 to) the value of M.

Step 4: Accumulate the incremental displaced area (A_I) as follows:

$$A_I = m \bullet (P(m) - P(m+1))$$

Step 5: Compare the total displaced area to the target displaced area.

Step 5–1: If $A_D + A_I$ is less than A_T:

Add to the total displaced area: $A_D = A_D + A_I$

Return to step 3.

Step 5–2: If $A_D + A_I$ is greater than of equal to A_T:

Compute the fraction of the incremental area that was needed:

$r = (A_T - A_D)/A_I$

Step 6: Calculate the filtered elevation (F):

$$F = P(m) - r \bullet (P(m) - P(m+1)) + D$$

For efficiency, the sorted profile points may be inspected after step 1. If the lowest point over the length of interest, P(N), is less than 1 mm (0.04 in) below the highest point, F is simply the average of the value in array P.

Figure 39 shows how the filter affects the profile in the vicinity of some deep joints on a concrete pavement measured in McFarland, Kansas. The same profile is shown three times: (1) raw data, (2) after a moving average with a baselength of 70 mm (2.76 in), and (3) after application of the bridging filter over a baselength of 70 mm (2.76 in), with a depth of 1 mm (0.04 in). The raw profile was collected at a sample interval of about 6.5 mm (0.26 in). At such a short interval, the narrow dips at the joints appear in the profile, as well as some influence from the surface macrotexture. A 70-mm (2.76-in), 11-point, moving average removes much of the texture influence, but the downward spikes at the joints are still present. They are just wider and shallow. After the bridging filter is applied, dips at joints are still present, but much more shallow than after the moving average. A useful property of the bridging filter is that it duplicates the behavior of the moving average in areas where no large dips appear.

On profiles with significant grade, the trend over the entire profile must be removed before the filter is applied. (It may be added back in after the filtering.) Do not remove

the trend within the length of interest at each step. Note that this filter has not been verified through experimental comparison the vehicle response. As described in the introduction to this chapter, more research is needed to develop a standard bridging filter.

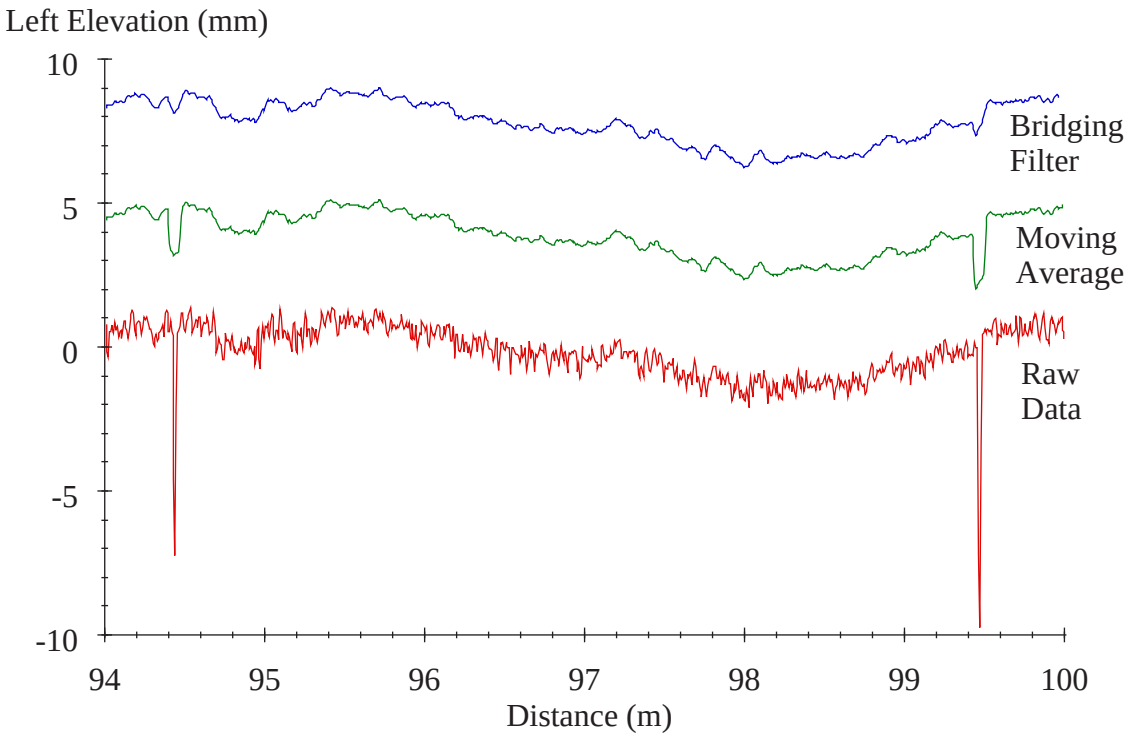


Figure 39. Filter comparison.

FOOTPRINT WIDTH

Very little data were available to support the establishment of a minimum footprint width. For this study, the recommended minimum footprint width is set to 70 mm (2.76 in). This value is at least three times larger than the characteristic length of transverse textural features. For example, it is more than three time larger than the most common longitudinal tine spacing of 19 mm (0.75 in).[112,113] The 70 mm (2.76 in) width is also many times larger than the most common asphalt surface aggregate sizes, and at least twice as wide as the largest common surface aggregates.[114,115,116]

To establish a minimum footprint width, an experiment is recommended in which multiple side-by-side profiles are measured within a tire contact zone. Simultaneously measure the vertical response at the wheel spindles of the host vehicle. Through empirical correlation, find the minimum number of profiles and the optimum spacing that yields the most coherent relationship to spindle response. Using only three profiles spread out across the tire contact zone, Ahlin was able to improve the relevance of profile measurements significantly.[117]

CHAPTER 7. BENCHMARK TESTS

This chapter recommends a set of tests for qualifying candidate reference devices as valid. Three types of testing are recommended: (1) profile measurement accuracy, (2) profile repeatability, and (3) longitudinal distance measurement accuracy. The testing program and analysis methods described here build on the findings and engineering decisions that have appeared in all of the previous chapters.

The recommended testing program will take place on six pavement sections of diverse texture, pavement type, and roughness.

Recommendation: *Test candidate reference device performance on: (1) dense graded asphalt with small aggregate, (2) a fresh chip seal, (3) stone matrix asphalt/open graded asphalt, (4) transversely tined jointed concrete, (5) longitudinally ground concrete, and (6) longitudinally tined concrete.*

Recommendation: *Test sections should cover a range of roughness from 0.5 to 4.0 m/km (31.7 to 253.4 in/mi). They should not include significant distress or transverse roughness variation.*

Recommendation: *On each section testing will cover one well-marked wheel path. At least one section will be 321.8 m (1056 ft) long, and the rest will be about 160.9 m (528 ft) long.*

The rationale for these selections appears within this chapter. The long section is needed to perform a proper test of long wavelength repeatability and accuracy. The range of roughness and texture are meant to help cover features that are likely to occur in common practice. However, the selection of surface textures is not meant to reproduce the "population" of textures found in practice. Rather, it represents a range of textures, selected to challenge a candidate reference device with the same diversity as the domestic road network.

Repeatability tests will be performed on all 6 sections, using 10 measurements of each section.

Requirement: *A candidate reference device must demonstrate adequate repeatability on all 6 test sections over a minimum of 10 runs each.*

Adequate repeatability is defined by a minimum level of composite cross correlation in four wavebands, as described in chapter 5. "Composite" cross correlation for the 10 runs is defined as the average correlation level for the 45 possible pairs of profiles.

Devices that have gaps in contact with the pavement, or a recording interval greater than 70 mm (2.76 in) will be asked to stagger the starting point of their runs. In this instance, 10 runs will be required: 5 with the original starting point, and 5 others with the device offset upstream by half the spacing of the supports. Note that the repeatability of all 10 runs will be tested as a single group.

Accuracy tests will be performed on all six sections, using the same profiles from the repeatability study.

Requirement: *A candidate reference device must demonstrate adequate agreement to a benchmark profile measurement on all 6 test sections over a minimum of 10 runs each.*

Adequate agreement is defined by a minimum level of average cross correlation in four wavebands, as described in chapter 5. Adequate agreement also requires that the composite gain between the benchmark profile measurement and the 10 candidate profiles meet the criterion described in chapter 4. The gain method has never been applied in this manner, and the cross correlation requirement alone should be thought of as a fall-back.

The benchmark profile shall be measured on each section by one of two possible methods, described in this chapter. One method seeks to measure the pavement surface with a very short longitudinal distance interval, and a high level of detail over a width of 70 mm (2.76 in). The profile data are then reduced using a bridging filter in the lateral direction with a baselength of 70 mm (2.76 in) and a "depth" of 1 mm (0.04 in). (See chapter 6.) Subsequently, apply the same bridging filter in the longitudinal direction. The other method measures the pavement with a specialized rod and level. This device should contact the pavement with a pivoting circular pad, 70 mm (2.76 in) in diameter. The underside of the pad must be fitted with rubber that envelops texture in a manner that is similar to common tire tread, but is as insensitive to temperature as possible. Both measurement methods present potential problems, as described below.

Longitudinal distance measurement accuracy will be tested on all six sections.

Requirement: *The measured length of all six test sections must agree with a steel tape to within 0.1 percent on all runs.*

It is recommended that the starting and ending location of the test sections are well marked. However, the sections should not be precisely 160.9 m (528 ft) long. Instead, each section should be a unique, predetermined, and undisclosed, length that is within about 8 m (25 ft) of 160.9 m (528 ft). This will help ensure that operators do not correct longitudinal distance measurement errors during the experiment.

When the testing program is complete, compile a "report card" for each device. This should include the IRI, PI with a null band, and longitudinal distance measurement error for each run. In addition, report the composite cross correlation for repeatability and the composite cross correlation to the benchmark profile in the four wavebands of interest on each section. Finally, include a plot of composite gain error for each test section. The test report for each device should also cover aspects of its operation and performance that may be of interest to an agency that is establishing a profiler verification site. Examples include: (1) speed of operation, (2) ease of operation, (3) transport procedures, (4) calibration and other pre-test procedures, and (5) troubleshooting procedures. Report these aspects of performance by direct observation of the operators, and through communication with the manufacturer. (Report both.)

If a candidate reference device is found to qualify in all aspects of performance on some test sections, but not on others, it may be granted conditional status as a reference device. The qualification would cover only the type of texture for which it succeeded, and only pavements of equal or greater roughness.

TEST SECTIONS

This section recommends a set of pavements for testing the accuracy and repeatability of candidate reference devices. The test sections must include a broad range of surface textures, including diverse levels of texture and directionality. This is needed to ensure the success of a candidate reference device's sampling practices, footprint, and low-pass filtering scheme in providing profile that is equivalent to the behavior of a vehicle tire. The test sections must also cover a range of roughness. However, measurement of smooth pavement will be emphasized, because the most common application for a reference device is verification of profilers for construction quality control. Further, smooth pavement with coarse macrotexture poses the greatest challenge to profiler accuracy and repeatability.[63,75]

A minimum of six test sections is needed to provide a broad range of conditions. Each test section should have a different texture type. While this does not provide enough test pavements to cover all of the common texturing alternatives, it does allow for coverage of major categories of texture, including a transverse texture, a longitudinal texture, and an isotropic texture. Test sections should include the following six surface textures:

1. Dense graded asphalt with small aggregate: This provides a section with very little macrotexture. The diameter of the aggregate should be 9.5 mm (3/8 in) or less.
2. A fresh chip seal: This provides a section with isotropic texture, with emphasis on the short wavelength end of the macrotexture range. A fresh chip seal also contains "positive texture," in that the excursions from the nominal road elevation are upward. It is also a very common surfacing alternative among secondary roads.
3. Stone matrix asphalt (SMA) or open graded asphalt at a maximum aggregate size: This provides a section with isotropic texture, with emphasis on the long wavelength end of the macrotexture range. As an alternative, a permeable friction course may be used in place of the SMA surface. A permeable friction course is unique in that it may contain a high level of both macrotexture and megatexture. If SMA is selected, it should have aggregate with diameter of 12.7 mm (1/2 in) or larger. If on open graded asphalt is selected, aggregate with diameter of 25.4 mm (1 in) or less is preferred.
4. Transversely tined jointed concrete: Transverse tining provides the most a common example of transverse texture. Any typical spacing scheme is permitted, but the section must include saw-cut joints without protruding sealant. The tining

and joints provide examples of "negative texture," which pose a challenge to the bridging qualities of a device's footprint.

5. Longitudinally ground concrete: This provides an example of longitudinal texture. The entire section should be ground, which is likely to also provide a very smooth surface. In place of a ground section, the experiment may include a concrete pavement with a drag texture.
6. Longitudinally tined concrete: This provides another example of longitudinal texture, with depth and lateral dimensions that are unique compared to longitudinal grinding. Longitudinal tining has also posed the greatest challenge to modern profilers.(75)

The test pavements should also provide multiple levels of roughness. Ideally, the six sections would include at least one example between 0.5 and 1.0 m/km (31.68 and 63.36 in/mi), one between 1.0 and 1.5 m/km (63.36 and 95.04 in/mi), one between 1.5 and 2.5 m/km (95.04 and 158.40 in/mi), and one between 2.5 and 4.0 m/km (158.40 and 253.44 in/mi). If it is possible, select another pavement that is smoother than 1.0 m/km (63.36 in/mi). None of the sections should include significant surface distress. In particular, sections with very aggressive transverse roughness variations should be avoided. For example, avoid sections with significant rutting or any longitudinal or alligator cracking. If possible, the section with longitudinal texture should be a continuous reinforced concrete pavement, to avoid diurnal variations associated with jointed concrete. Further, the transversely tined concrete pavement should exhibit negligible diurnal variations in roughness. This must be verified through careful consideration of the design and support conditions, as well as inertial profiler measurements throughout a day in which the weather would promote changes in roughness.

Five of the test sections shall be about 160.9 m (528 ft) long. To provide a more valid test of long-wavelength measurement capability, the dense-graded asphalt section should be 321.8 m (1056 ft) long. Sayers called for a 320-m (1050-ft) long section in the Ann Arbor Road Profilometer Meeting for the same purpose.(63) The long measurement is recommended on the section with the finest texture to help study long-wavelength measurement capability in the absence of footprint and sampling issues. At least two of the test sections should appear on pavements with less than 2 percent grade. However, a grade change of at least 2 percent is preferred on one of the sections. All test sections shall lack horizontal curvature. (That is, they should all be tangent sections.)

Only one wheel path will be tested on each section. No preference is given to the left or the right side, but profile should be measured about 0.9 m (2.95 ft) from the lane center to cover a "central" wheel path. It is anticipated that the wheel path will be marked with a chalk line. This is sufficient for walking speed devices and very slow speed devices. For higher speed devices, or devices with special lane marking needs, the markings will be placed as specified by the operating agency. However, markings required by a candidate reference device will be considered part of the expense and labor associated with it.

REPEATABILITY

Repeatability tests provide great value when evaluating the quality of a profiling device, with minimal cost. Rating of repeatability requires much less effort than rating of accuracy, because only one device need participate in the experiment. Logistical difficulties associated with comparison to a benchmark measurement are avoided, as is the expense of measuring a "true" profile as a basis for comparison. Further, devices that fail to provide adequate repeatability will also fail to demonstrate adequate agreement to the established benchmark for accuracy. (At least, this is the case when accuracy is defined with the proper statistical rigor, such that precision is an aspect of the criteria.)

Repeatability tests may also be carried out by the developers of candidate reference devices well in advance of the formal qualification process. Profiler designers and manufacturers who test repeatability as a routine part of their development process are much more likely to meet the criteria during the official experiment. They are also more likely to discover threats to the accuracy of their device.

Repeatability shall be tested on all six sections described above. Candidate reference devices shall be required to measure a minimum of 10 repeat runs on each section. Devices that do not make continuous contact with the pavement are required to "stagger" the placement of their supports. For example, a DipStick typically makes contact with the pavement using supports that are about 304.8 mm (12 in) apart.[4,5,118,119] In this case, five runs would be required with the same starting point. Another five runs would be required with an alternate starting point, shifted in the direction opposite the movement of the device by 152.4 mm (6 in).

As described in chapter 5, cross correlation will provide ratings of repeatability in multiple wavebands.

ACCURACY

Accuracy shall be tested on all six sections described above. The same set of runs that are made for rating repeatability will also serve as measurements of accuracy by comparing them to benchmark profile measurements. Ratings of accuracy will be provided by the gain method (chapter 4) as well as cross correlation (chapter 5).

Two methods are suggested here of measuring profile as a benchmark for the accuracy of candidate reference devices. One method seeks to measure a high level of detail about the road surface in the longitudinal direction and over a width of 70 mm (2.76 in). Bridging and enveloping qualities are provided using digital post-processing filters. The other method senses the pavement surface with a large footprint that is 70 mm (2.76 in) long and 70 mm (2.76 in) wide. In this method, the largest recording interval permitted for a reference device, 70 mm (2.76 in), is used. Both methods have potential pitfalls, and neither is proven. As a minimum, they should demonstrate the same level of repeatability required of candidate reference devices before they are considered for the experiment.

Neither of these measurement methods would necessarily succeed as a reference device for routine use, because they are labor intensive. Further, the quality of the data they would provide is extremely sensitive to operator proficiency (and care).

Detailed Measurements

One option for obtaining benchmark profile measurements is an enhanced version of the Transport and Road Research Laboratory (TRRL) Beam. The Beam is shown at the International Road Roughness Experiment (IRRE) in Brazil in figure 40. In this device, a horizontal datum is provided by the 3-m (9.84-ft) long beam.(67) The distance from the datum to the ground is measured using a pneumatic tire. The tire is connected to the beam by an instrumented assembly that slides along on rollers. Each time the Beam is placed it is leveled by adjusting the height at one end. When the measurement is complete, the Beam is moved to the next 3-m (9.84-ft) segment of pavement by lifting it and placing the upstream end in the previous position of the downstream end. At the IRRE, measurements at a sampling interval (and recording interval) of 100 mm (3.94 in) required two operators about a quarter of a day to cover a single wheel path over 160 m (524.9 ft).

For the purposes of obtaining a benchmark profile measurement, the old design would not succeed. First, contacting the road with a pneumatic tire introduces temperature sensitivity into the process, and diminishes the precision of each elevation measurement. Second, the placement of the beam each time it is moved needs to be more precise. However, the measurement concept has the potential to provide a useful benchmark profile.

A “beam” device must conform to the sampling and footprint requirements defined in chapter 6 of this report. This requires replacement of the pneumatic tire by a sweeping, non-contacting height sensor. The height sensor should collect data over a swatch of pavement that is 70 mm (2.76 in) wide, and provide rapid enough sampling to avoid gaps over the 70 mm (2.76 in) of interest. For example, the laser may have a footprint for individual readings with a lateral dimension of 1 mm (0.04 in). In this instance, the sensor must be able to record 70 side-by-side elevation readings, covering 70 mm (2.76 in), for each longitudinal distance step. Similarly, the sensor must perform a lateral sweep frequently enough to avoid gaps in the longitudinal direction. For example, if the sensor footprint for individual readings is 1 mm (0.04 in) long, a sweep is needed each time the sensor is advanced 1 mm (0.04 in) along the beam.

An alternative to the sweeping laser would be a contacting wheel with the thin rubber tire that is meant to simulate the way vehicle tire tread envelops texture and narrow surface features. However, this appears to be too problematic. Using actual tire tread rubber provides the proper envelopment, but it requires the wheel to be loaded the same way as a tire. The only way to accomplish this is with a prohibitively heavy device. Using a softer material than common tread rubber to reduce the needed loading may introduce a critical level of temperature sensitivity.



Figure 40. The TRRL Beam at the IRRE.(67)

For this application, the beam method requires several other modifications:

- The beam must be stiff enough and short enough to avoid sag.[5]
- The beam must not expand or contract in length more than 0.05 percent over a reasonable range of operating temperatures.[6]
- The beam should be low to the ground, to reduce errors caused by thermal expansion of the supports at each end. This will also permit the use of a laser with a shorter stand-off height.
- The supports at each end should be many times heavier than the assembly that moves along the beam.
- The leading end of the beam should stay in place when the beam is repositioned, so that the leading support from one sweep becomes that trailing support from another sweep.
- During the measurements, the end supports should be loaded with a standard amount of weight, to ensure consistent contact of the supports with the pavement. Further, when the trailing support is pivoted around the leading support between measurements, the weight should remain on the fixed support (i.e., the original leading support).
- The practice of pivoting the device requires that the beam is supported from above, and from only one side. This means that the beam must hang from its supports on a vertically aligned pin joint.

A critical addition to the TRRL Beam method is the static measurement of elevation at both supports each time they are placed. It is proposed that each support include a

---

[5] This is an important consideration, and may dictate the use of a shorter beam. For example, a 3-m (9.84-ft) long aluminum tube with a rectangular cross section that is 50.8 mm (2 in) high, 25.4 mm (1 in) wide, and 3.2 mm (0.126 in) thick will sag 1.25-1.35 mm (0.049-0.053 in) under its own weight.(120)

[6] For structural aluminum, expansion of 0.05 percent requires a temperature change of about 20ºC (36ºF). For structural steel, a temperature change of more than twice that much is needed.(120)

fixture for placement of a surveyor's rod directly above each end of the beam. (The fixture must be above the location where the sensor terminates its measurement range along on the beam, not at the actual beam end. This fixture should be flat, and have the proper shape to allow for consistent placement of the rod. For each beam placement, a measurement is required of the absolute vertical position of both supports. This rod and level measurement of support height must conform to ASTM requirements for road roughness measurements by the static level method.[58])

The rod and level measurement is suggested in place of beam leveling because it is expected that the needed precision can not be achieved using an inclinometer on the beam. Further, the measurement of beam support height each time the beam is placed provides two measurements of the support at each position (once when the support is at the leading edge and once when it is at the trailing edge). This way, when the process of pivoting the beam disturbs the fixed end, a correction can be made.

This method has never been tested, and is not guaranteed to provide the needed benchmark profile. However, it is worth investigation. Note that the static measurement of support elevation makes the method very slow and labor intensive. The specific dimensions recommended above represent a trade-off between possible error sources. A longer beam would speed up the measurement process, and help avoid errors associated with rod and level elevation measurements. However, a longer beam increases the possibility of beam sag, and the space needed to make the pivot. A shorter beam reduces the space needed to make the pivot, and the potential for sag, but increases the measurement effort and the potential errors associated with pivoting the beam.

The greatest threat to the accuracy of profile under this method is the systematic error in support height. If any bias exists in the vertical distance from the base of the rod to a reference point on the beam, it will appear in the profile as a bias in slope. This bias would reverse in direction each time the beam is pivoted. At a beam length of 3 m, only a very small error is needed to cause a major upward bias in roughness. Three procedures are suggested to mitigate this error source. First, verify and fine-tune the consistency of the two base assemblies on a flat, level surface in the laboratory before each day's measurements. Second, provide a pad for placement of the rod that is rigid, and fits the shape of the rod's base very closely. The rod should be fitted with a rigid, flat pad on a ball joint. Third, follow as many of the practices in ASTM 1364-95 as possible. In particular, position the level to be as low to the ground as possible, and maintain vertical alignment of the rod to the extent possible for each reading.

The profile provided by this method will consist of a very short longitudinal recording interval. A value of 1 to 2 mm (0.04 to 0.08 in) is expected. The profile will also include several elevation points in a 70-mm (2.76-in) wide lateral sweep at each longitudinal recording location. In post-processing, these data will be reduced in two steps. First, average the data within each lateral sweep (potentially 70 points) using the moving average bridging filter described in chapter 6. This will reduce each lateral sweep to a single elevation value, and hence, the gross data set is reduced to a single-track longitudinal profile. Smooth the resulting profile using a moving average bridging filter with a baselength of 70 mm (2.76 in). Decimation after the filtering is not required.

Rod and Level Measurements

The "beam" measurement method described above seeks to capture a high level of detail about the pavement surface over a pre-defined wheel path. After the measurement, the data are reduced using a smoothing and bridging filter to a profile that represents the likely path of a tire contact patch in the pitch plane (i.e., the side view). An alternative to the detailed measurements is to perform bridging and averaging that approximates the behavior of a tire using a contacting device with a large footprint. For this purpose, an enhanced rod and level measurement may provide a proper benchmark profile.

In a response-type road roughness measuring system correlation experiment, Queiroz modified a rod and level to include a large, pivoting foot pad.[121] This was needed to measure unusually rough, unpaved roads with significant loose material and lateral variation. Later, Sayers adopted the same method for the Ann Arbor Road Profilometer Meeting.[63] In the Meeting, a surveyor's rod was modified to include a rigid circular pad, 76.2 mm (3 in) in diameter, at the base. This offered a "reduction in randomness when taking readings from highly textures surfaces." The reduction occurred because the pad was able to contact the road in three (high) points within its area. A diagram of this type of rod from the Little Book of Profiling is shown in figure 41.

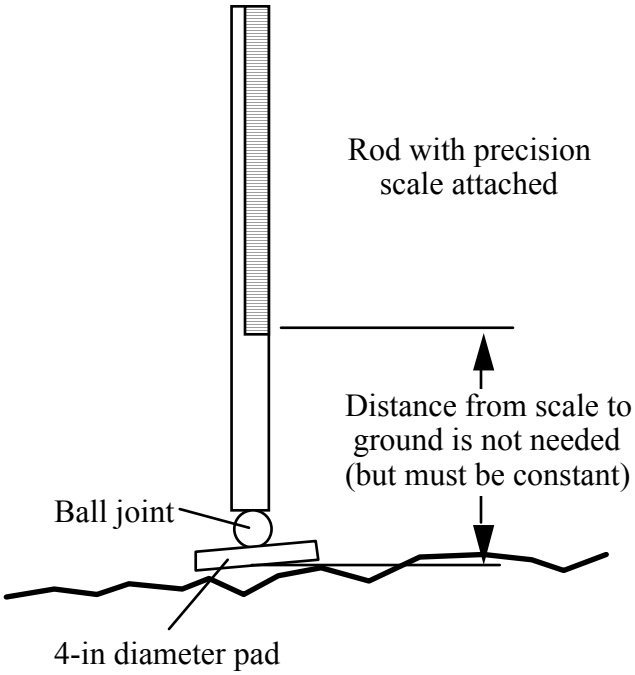


Figure 41. Rod and level with a large foot pad.[71]

A similar enhancement to the static rod and level method is recommended for benchmark profile measurements. In this case, the rod shall also include a large circular pad with a diameter of 70 mm (2.76 in), but it will not be rigid. Instead, a rubber pad is recommended that envelops texture in a manner similar to a tire tread block. Rather than averaging the three highest points under the pad, this method of contacting the pavement is expected to settle into the texture underneath it to a level that is more representative of a vehicle tire.

The pad need not use the same material as a common tire tread, but it should rest on the pavement the same way as a tire. Using genuine tread rubber is problematic. It requires the rod to be loaded so that the average pressure under the pad is similar to the pressure on a common automobile tire tread. For example, the total area of the recommended foot pad is about 38.5 cm^2 (5.97 in^2). To obtain the same behavior as a tire with a net contact area of 260 cm^2 (40.3 in^2) supporting 3900 N (877 lbs), the foot pad would need to be loaded to 577 N (130 lbs). With this in mind, an alternate to tire tread rubber may be needed. On the other hand, the use of a flexible foot pad on the rod creates the potential for problems when the rod is not held with the same downward force in every run. Thus, the device must be designed so that it weighs a significant amount.

For this application, several design and operation considerations must be observed:

- Obtain a reading every 70 mm (2.76 in).
- Guide the placement of the rod using a well marked tape along the desired wheel path. Ideally, marks may be placed on both sides of the wheel path, as well as on both sides of the top of the foot pad.
- Use a rod with the resolution specified by ASTM E 1364-95.(60) Follow as many of the procedures in ASTM E 1364-95 as possible.
- Use a rod with a bubble level attached to aid in keeping the rod vertical.
- Set up the level to be no more than 1 m (3.3 ft) above the surface.
- Design the device so that it uniformly exerts a vertical force of at least 100 N (22.5 lbs) on the foot pad during every reading. This may require the design of a special apparatus to help the rod operator move it between readings.
- Choose a foot pad material that is penetrated by texture in a manner that is as similar to a tire tread block as possible. This will involve the expert consideration of the supported weight, the foot pad thickness, the foot pad elastic modulus, and the foot pad durometer. (Note that the elastic modulus and durometer are each important. The durometer determines the depth of penetration of a sharp textural feature, and the elastic modulus determines the shape of the deflection around the feature.)
- Choose a foot pad material that is as insensitive to temperature as possible. Test the durometer of the foot pad at regular intervals throughout the profiling period.

LONGITUDINAL DISTANCE

Longitudinal distance measurement will be verified on the same test sections where profiler accuracy tests are performed. This is important, because the accuracy of a candidate reference device's longitudinal distance measurement may be sensitive to texture or roughness. A candidate reference device is expected to measure longitudinal distance between section endpoints to within 0.1 percent in all runs. Further, the reporting of longitudinal distance measurement error will take note of the average error level (i.e., the bias) over the 10 (or more) runs.

Endpoints of each section shall be clearly marked, and the overall distance shall be measured with a steel tape. The accuracy of the tape shall be verified by a standardization organization before the experiment. The following practices are also recommended:

- Attempt to lay out the section endpoints when the pavement surface temperature is 15-25 ºC (27-45 ºF).
- Make sure the tape is flat on the road surface.
- Lay out the distance in sub-sections. Do not use more than 40.25 m (132.1 ft) of tape length per sub-section.
- Carefully mark the longitudinal and lateral position of each tape landmark along the section.
- Verify the lateral position of the leading end of the tape for each subsection.
- Apply the recommended level of axial tension to the tape during each measurement. The recommended force is often inscribed on the tape. If applying tension to the tape creates a gap between the tape and the pavement of more than 5 mm (0.2 in), reduce the length of the sub-section.
- Measure the section twice, with a different set of intermediate landmarks in each trail.

For slow-speed and walking-speed devices, verification of the actual start and end of the run requires supervision of the measurements. For non-contacting and higher-speed devices, automated triggering or the placement of artificial features just outside of the section boundaries may be needed.

Note that detailed cross correlation analysis is able to provide an estimate of longitudinal distance measurement disagreement, but the physical observation of profilers of the measured distance between landmarks provides a more precise rating.

ALTERNATIVE METHODS FOR ACCURACY TESTING

This chapter recommends a method of testing candidate reference device accuracy that requires tests on natural roads (i.e., in-service pavement or test pavement without artificial roughness). This format for benchmark testing was selected so that testing could commence relatively soon. This way, the requirements set in chapters 3 through 6 could go into practice as soon as possible. However, the testing methodology recommended above has the following pitfalls:

- There is no guarantee that either of the benchmark measurement options described above will offer accuracy better than, or even equal to the performance expected of a reference device. This will require further investigation.
- Pavement profiles change with time, sometimes over only a few hours.[28] These changes in profile with time may unfairly penalize an accurate device.

- The mix of pavements that are available for the initial set of tests may not be available for future testing activities, or subsequent testing that may be needed to resolve disputes.

As a minimum, pavements should be screened for aggressive diurnal changes before they are included in the experiment, and tested with an inertial profiler at regular intervals throughout the duration of the test program. Further, if covered of indoor sites can be found, they should be favored in the selection of sites.

An alternative approach to conducting benchmark testing on natural pavement would be the development of a testing program using manufactured events and laboratory evaluation. This offers the following potential benefits:

- The testing program may be easier to defend, because changes in road profile with time could be avoided.
- The testing program would be more easily reproduced, since the nature of each evaluation activity would be more closely defined. For example, the geometry of manufactured road events would be directly specified, in contrast to natural roads, which are simply selected by type, texture, and roughness range.
- Some portion of the testing program could be performed by equipment developers under the precise set of conditions expected for the official testing.
- The testing program could include distinct tests for each portion of the waveband of interest. This may reduce the cost associated with making detailed benchmark measurements on long pavement sections.
- The testing program could more readily include a range of simulated grade and cross slope.

However, some of the potential drawbacks are:

- Defining a relevant set of manufactured events would require significant new research. This is because a direct link would have to be made between accurate measurements of these events and the expectation of good performance in the field. That research would require a project of scope at least as big as the project that produced this report.
- The manufacture of these events is likely to be expensive.
- Benchmark measurements would be required to verify that the manufactured events were indeed built to the proper tolerances. They would also be needed to resolve disputes with the offerers of devices that do not meet the specified accuracy requirements.
- Artificial events would be difficult to design with no prior knowledge of the kind of devices that must traverse them. For example, impulses in elevation, slope, or curvature are commonly used as broad-banded transient inputs to dynamic systems. However, a slow-speed device that may be very useful on natural roads may fail to pass over the transient events properly.

CHAPTER 8. REVIEW OF EXISTING DEVICES

This chapter reviews the reference devices that are used in common practice in light of the requirements defined in this report. The chapter reviews inclinometer-based devices, and typical uses of the rod and level for profile measurement. In their existing application, neither type of device appears to meet the requirements defined in this report.

INCLINOMETER-BASED DEVICES

Several inclinometer-based devices have been marketed for measurement of profile: (1) the ARRB Walking Profiler, (2) SurPro 1000, (3) DipStick, (4) Rolling DipStick, (5) IRIS, (6) YSI RoadPro, (7) ROMDAS Z250, (8) SSI CS8800, and (9) CSC Profilite Model 300. Most of these devices contact the road with a foot spacing of 200 to 305 mm (7.9 to 12 in).

Inclinometer-based devices are often used to collect reference profiles in profiler verification studies. Since the 1990s the DipStick was used often for this purpose.[4,5,28,122,123,124] The Rolling DipStick was also used in an international experiment.[124] Later, the ARRB Walking Profiler and SurPro 1000 have been used as reference devices. They are also used by many State DOTs as reference devices in profiler certification programs.[61,75,125,126]

Many of the inclinometer-based devices take and store readings while they are stationary. The supporting feet of the device are then shifted forward along the intended path so that the trailing foot pad in the new reading moves to the position of the leading foot pad from the previous reading. These devices record data at an interval that is equal to the foot pad spacing. Other inclinometer-based devices roll along the pavement and collect data at a high sampling rate, but digitize and record readings at an interval that is equal to or less than the spacing of the supports. Foot pads on all of these devices are usually plastic or hard rubber. The DipStick is sometimes operated with metal supports.

Three aspects of the operation of inclinometer-based devices are covered here: (1) foot pad (support) spacing, (2) recording interval, and (3) support footprint.

Support Spacing

In most cases, the foot pad spacing of an inclinometer-based device is the recording interval. For example, the DipStick is often operated with a spacing of 304.8 mm (12 in), the ARRB Walking Profiler has a spacing of 241.3 mm (9.5 in), and the SurPro 1000 has a spacing of 250 mm (9.84 in). The foot pad spacing is a very important property of an inclinometer-based device. It determines, in part, the response of the device to features with wavelengths up to 10 times its length.

Consider the response of the DipStick to a sinusoidal road feature with a wavelength equal to the wheelbase, as shown on the right side of figure 42. No matter where the DipStick is placed along this feature it will remain level, because the two foot pads will

have the same elevation. Thus, the device will always measure zero slope on this sinusoid, and is therefore blind to it.

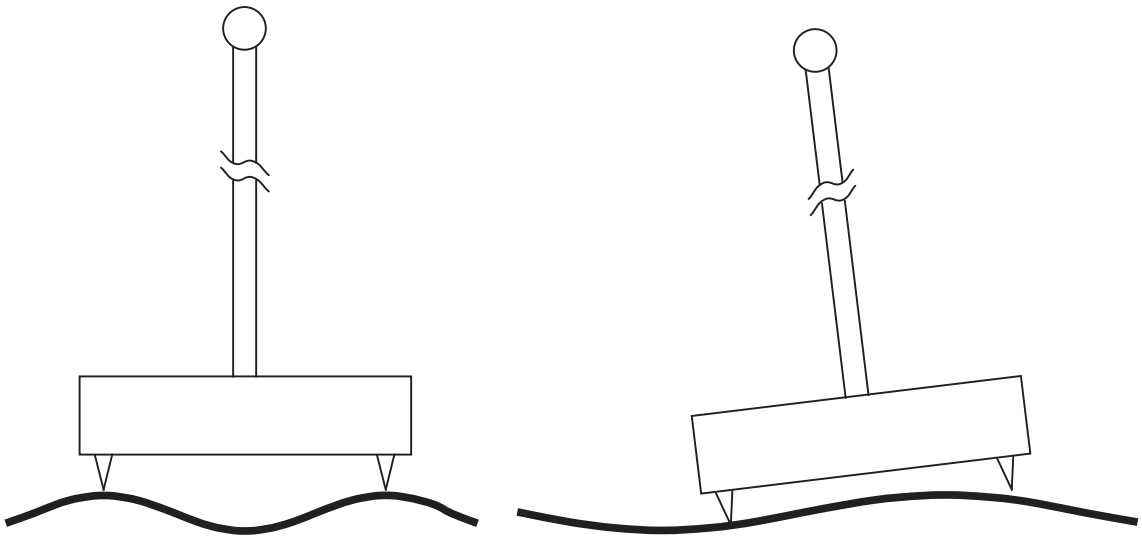


Figure 42. DipStick response to sinusoids.

The response of the DipStick to sinusoidal input increases slowly as the wavelength increases above the value of wheelbase. Consider the response to a sinusoid with a wavelength that is twice the wheelbase, and an amplitude of A. This is shown on the right side of figure 42. In this case, the DipStick is able to detect its presence, but it will register a maximum slope that is equal to 4•A/L, where L is the wavelength of the sinusoid. This sinusoid actually has a maximum slope of 2•π•A/L, which is more than 57 percent higher than the expected reading.

Figure 43 shows the gain characteristic of the DipStick, where the wavelength is normalized by the foot pad spacing (i.e., wheelbase). "Gain" for a given wavelength is defined as the ratio of the output amplitude to the input amplitude. Thus, the gain is zero when the wavelength equals the foot pad spacing, as discussed above. For a wavelength of twice the foot pad spacing, the gain is [4•A/L]/[2•π•A/L], or 2/π, as shown in figure 43. Note that a feature's wavelength must grow to over five times the foot pad spacing before the DipStick registers more than 95 percent of its amplitude.

The "wheelbase filtering" property of inclinometer-based devices causes them to underestimate or miss some short profile features. However, this aspect of its behavior does not impact the measurement of IRI very much. This is because the calculation of the IRI includes a moving average with a baselength of 250 mm (9.84 in). The gain characteristic of the moving average is identical in shape to that of figure 43, and differs only in that it is shifted somewhat when the foot pad spacing in not equal to 250 mm (9.84 in). (In some respect, these devices would be mechanical versions of the moving average.) The wheelbase filtering effect mimics the moving average quite closely when the foot pad spacing is 250 mm (9.84 in).

Recording Interval

The discussion above describes the effect of wheelbase filtering on profile measured by common inclinometer-based devices. However, the gain characteristic shown in figure 43 is only valid when the profile is sampled and stored at a small interval. In other words, the gain characteristic shown in figure 43 describes the behavior of the rolling devices, if they were able to collect and record readings at a very small interval. Many of these devices are fitted with sensors that need time to stabilize, so they do not offer a short recording interval. Many of the rolling devices advertise a high sampling rate, but do not provide a commensurably short recording interval. A likely explanation is that the recorded inclination is the average of several very noisy readings that are taken after some time for stabilization. With this in mind, most of these devices probably ignore some length of pavement between the foot pads in every recorded sample.

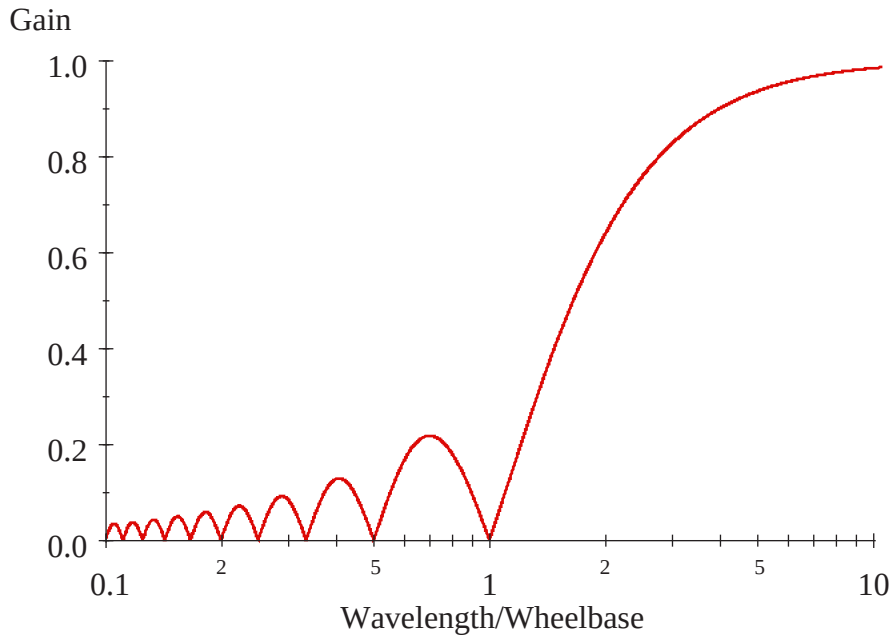


Figure 43. DipStick gain, small recording interval.

Recording data at large intervals limits the range of wavelengths that may be recognized. In the case of devices that make contact using two longitudinally spaced supporting feet, the short wavelength content is contaminated because of two mechanisms. First, the device may simply miss very short duration rough features.[119] This occurs when the feature never makes contact with the device's fixed supports, or the supporting wheels are on the feature when no reading is collected. Second, the large recording interval leads to aliasing errors, in which content shorter than twice the recording interval contaminates the measurement at wavelength longer than twice the recording interval. (See chapter 6.) The first mechanism causes roughness to be underestimated, and the second mechanism causes roughness to be overestimated. The effect that dominates depends on the properties of the road surface.

The probable effect of aliasing on IRI for a recording interval of 300 mm (11.8 in) was estimated in a recent study of profile sampling procedures.[28] This study showed

that the upward bias in IRI is likely to be on the order of 7 to 9 percent. The probable error level was estimated by decimating profiles collected with the FHWA ProRut at a sample interval of 25 mm (0.98 in). Note that the treatment of very short road features by the foot pads may be different than that of the sensor footprint and low-pass filter of the ProRut. As such, the 7 to 9 percent error level is only a rough estimate.

The way to avoid aliasing errors is to sample and record profile much more often than the shortest wavelength of interest, then apply a low-pass filter to remove the content within the signal that is not of interest. These devices inherently apply low-pass filtering that mimics the tire envelopment filter used by the IRI. This may be permitted, but the recording interval must observe the requirement of 70 mm (2.76 in) or less described in chapter 6.

Support Footprint

The bridging and envelopment of texture performed by the supports of inclinometer-based devices helps mitigate the upward bias caused by aliasing. The supports also may help improve the relevance to vehicle response when they mimic tire envelopment and bridging. In its most common configuration, the DipStick contacts the pavement with rigid circular "feet" that are 32 mm (1.26 in) in diameter. The feet are attached to the base with a ball joint, such that they are most likely to rest upon the three highest points within their footprint. This provides some bridging, but it also may lead to undue sensitivity to coarse upward textures. (A fresh chip seal, for example.) An improved version of the DipStick uses "moon feet," which are padded circular supports with a diameter of 63.5 mm (2.5 in).

The ARRB Walking Profiler contacts the pavement with three small rubber pads at both supports. The pads are 19.1 mm (0.75 in) in diameter, and cover a gross area that is 63.5 mm (2.5 in) wide and 63.5 mm (2.5 in) long. Rolling devices contact the pavement with wheels of various diameter and hardness. Each type of contact interacts with the pavement differently. A larger contact area is generally better, and a width of at least 70 mm (2.76 in) is recommended. What is not clear is the optimal contact "hardness" for establishing a datum plane of road contact that is most relevant to vehicle response.

ROD AND LEVEL

The rod and level is another common source of reference profile measurements.[61] However, measuring a profile using a rod and level requires special procedures that make the process extremely time consuming and expensive.[58] Further, special equipment is required, since conventional survey equipment lacks the precision needed for reference profile measurements.[58] For these reasons, many studies that require reference profile measurements only use the rod and level on a small subset of the test pavements.[63,75,123,126]

The rod and level is often lauded as a method to measure the true profile, inasmuch as it provides a very accurate measurement of elevation at each point of interest. However, when these points are collected to form a profile signal, they do not necessarily establish a relevant benchmark. This is the case for two reasons. First, the measurement effort is so

time consuming that profile is rarely sampled at an interval shorter than 300 mm (11.8 in). For estimates or prediction of road qualities that relate to vehicle ride response, this is much too long. (See chapters 3 and 6.) Second, the rod typically makes hard contact with the pavement at a narrow point, or over a small area. The result is a high level of aliasing error caused by coarse macrotexture.

OTHER DEVICES

Three dimensional laser scanning technology has been proposed as a way to measure road roughness.[127] However, it does not appear to be accurate enough for use as a reference device. A device in Sweden called PRIMAL is currently in use for profile reference measurements. Details were not available about this device, but it should be considered as a potential reference device.

CHAPTER 9. RECOMMENDATIONS

This report established critical accuracy requirements for a reference profiling device. The requirements pertain to devices that will be used to verify other profilers for construction quality control and network pavement monitoring. Two very important themes guided the technical work. First, a reference device must provide an accurate measurement of profile, as well as common roughness indices. Second, the sampling practices, low-pass filtering, and footprint of the device should guarantee a standard for comparison that is relevant to vehicle response.

This chapter summarizes the critical requirements from the rest of the report. As such, it is expected to provide a template for the specification and procurement of a reference device. The chapter concludes by describing future research that is needed to improve on engineering judgments that were made this report.

CRITICAL REQUIREMENTS

A general purpose reference device for road roughness measurement must capture wavelengths from 0.15 m (6 in) to 67 m (220 ft). The waveband includes the content needed for commonly used roughness indices, such as the IRI, RN, and simulated PI. This waveband also provides the needed range to cover current and anticipated future uses of road profile that are relevant to major vertical dynamics of cars and trucks. If only the IRI is of interest, the waveband may be modified to 0.9 m (2.95 ft) to 35 m (115 ft).

Within the waveband of interest, the profile must reproduce the true profile with a "gain" than will ensure accurate roughness measurement. A reference profiler must have a gain error no greater than 1.00 percent for wavelengths from 0.15 to 0.35 m (6 in to 1.16 ft), no greater than 0.25 percent for wavelengths from 0.35 to 35.9 m (1.16 to 118 ft), and no greater than 1.00 percent for wavelengths from 35.9 to 67 m (118 to 220 ft). The gain error will be calculated though comparison to extremely accurate benchmark profile measurements. At the short wavelength end of the range, the response of a candidate reference device may roll off, so long as it does so in a manner that is consistent with the sampling and filtering recommendations described below. A reference profiler must also exhibit no systematic phase distortion over the wavelength range from 0.15 to 67 m (6 in to 220 ft). A reference profiler must also measure longitudinal distance correctly to within 0.1 percent.

Profile measurements from a reference device must also cross correlate to benchmark profiles over a range of pavement surface types as follows:

- Correlation in IRI filter output to at least 0.98.
- Correlation to elevation profile in the long waveband to at least 0.98.
- Correlation to elevation profile in the medium waveband to at least 0.98.
- Correlation to elevation profile in the short waveband to at least 0.94.

- A reference device must also exhibit composite cross correlation over a set of repeat measurements at the same level.

A major recommendation of this report is that a reference profiler should sense the pavement as much like a common automobile tire as possible. Specific footprint dimensions, a maximum sample interval, and filtering methods are recommended here, but not mandated. Instead, these practices will be observed when making the benchmark profile measurements as a standard for accuracy of candidate reference devices. The device itself need not use the same sampling practices. However, candidate reference devices will be expected to reproduce benchmark profile measurements made using these sampling practices.

Profile should be recorded at an interval no larger than 70 mm (2.76 in). When data are collected at a high sampling rate, proper anti-alias filters must be applied before decimation to the recording interval. The low-pass filter should have a cutoff wavelength equal to twice the recording interval. The low-pass filter should also bridge over downward features that are too narrow to affect tire vertical forces. A "bridging filter" is recommended in which the filtered elevation only depends on the portions of the surface within the baselength that penetrate into a half-plane by an average of 1 mm (0.04 in). (See chapter 6.)

Alternatively, the profiler may sense the pavement with a very large footprint within each reading, often by contact with the surface. In this case, the length of contact should be equal to the recording interval, and no more than 70 mm (2.76 in) long. Whether the measurement is made through contact with the surface or not, a footprint width of at least 70 mm (2.76 in) is recommended.

The profile sampling interval may not be larger than the profile recording interval. In other words, measurement of profile with lesser detail, and interpolation to the required recording interval is not permitted. Further, the footprint within each recorded sample must include the anti-aliasing measures described here.

None of the reference devices in common practice adheres to all of these requirements.

BENCHMARK TESTING

Benchmark tests should be performed to determine the: (1) profile measurement accuracy, (2) profile repeatability, and (3) longitudinal distance measurement accuracy. The recommended testing program will take place on six pavement sections of diverse texture, pavement type, and roughness. On each section testing will cover one well-marked wheel path. At least one section will be 321.8 m (1056 ft) long, and the rest will be roughly 160.9 m (528 ft) long.

A candidate reference device must demonstrate adequate repeatability on all 6 test sections over a minimum of 10 runs each. Adequate repeatability is defined by a minimum level of composite cross correlation in four wavebands. "Composite" cross correlation for the 10 runs is defined as the average correlation level for the 45 possible pairs of profiles.

Devices that have gaps in contact with the pavement, or a recording interval greater than 70 mm (2.76 in) will be asked to stagger the starting point of their runs. In this instance, 10 runs will be required: 5 with the original starting point, and 5 others with the device offset upstream by half the spacing of the supports.

A candidate reference device must demonstrate adequate agreement to a benchmark profile measurement on all 6 test sections over a minimum of 10 runs each. Adequate agreement is defined by the gain criteria and cross correlation criteria described above.

Benchmark profile measurements shall be made to provide a standard for evaluation of candidate reference profiler accuracy. Two methods are suggested, both of which adhere to the sampling requirements defined in this report. One method seeks to measure the pavement surface with a very short longitudinal distance interval, and a high level of detail over a width of 70 mm (2.76 in). The profile data are then reduced using a bridging filter in the lateral direction with a baselength of 70 mm (2.76 in) and a "depth" of 1 mm (0.04 in), then the same bridging filter in the longitudinal direction. The other method measures the pavement with a specialized rod and level. This device should contact the pavement with a pivoting circular pad, 70 mm (2.76 in) in diameter. The underside of the pad must be fitted with rubber that envelops texture in a manner that is similar to common tire tread, but is as insensitive to temperature as possible.

The measured length of all six test sections must agree with a steel tape to within 0.1 percent on all runs. No explicit requirement is needed for lateral tracking accuracy. However, candidate reference devices are unlikely to meet the repeatability and accuracy requirements on profiler measurement if they fail to follow a designated path accurately.

When the testing program is complete, compilation of a "report card" for each device is recommended that includes: summary roughness index values, cross correlation results for repeatability, cross correlation results for accuracy, and gain error plots for each test section. The test report for each device should also cover aspects of its operation and performance that may be of interest to an agency that is establishing a profiler verification site. If a candidate reference device is found to qualify in all aspects of performance on some test sections, but not on others, it may be granted conditional status as a reference device. The qualification would cover only the type of texture for which it succeeded, and only pavements of equal or greater roughness.

Both benchmark measurement methods proposed in this report present potential problems. Further, either one will be very expensive. With this in mind, a "pre-qualifying" experiment may be useful, in which only tests of repeatability and longitudinal distance measurement accuracy are performed. This also provides an opportunity for an assessment of operational aspects of each device, and shakedown of key aspects of the device, such as recording interval, footprint, and the precision and accuracy of individual readings.

COMPARISON TO THE REFERENCE DEVICE

Once a reference device is qualified as valid, it may be used to verify profilers for construction quality control. Cross correlation should replace precision and bias in

elevation measurement as a standard for profile accuracy and repeatability. Profile certification for construction quality control should require:

- Correlation in IRI filter output to at least 0.94.
- Correlation to elevation profile in the long waveband to at least 0.94.
- Correlation to elevation profile in the medium waveband to at least 0.94.
- Correlation to elevation profile in the short waveband to at least 0.88.

FUTURE RESEARCH

The sampling and footprint requirements proposed in this report are based on the best available information. However, it is anticipated that the state of knowledge in this area will improve in the near future. When the most relevant sampling practices are known, they may alter the benchmark. As such, perfect correlation to the current benchmark may prompt unproductive effort.

The theoretical study of longitudinal sampling interval presented in this report should be augmented with a numerical study using very detailed short-interval profiles. This is needed to capture influences of macrotexture and megatexture that are not represented accurately in the spectral models studied here. In addition, a direct connection to vehicle response is needed. Two types of study are recommended.

First, make direct observations of the manner in which texture and short-duration surface features protrude into the tread of standing or slowly rolling tires. This will provide the basis for designing a non-linear filter, which attempts to assign weighting to textural features in proportion to their influence on vertical forces at the tire contact patch.

Second, perform a statistical study of the link between measured vehicle response and key aspects of very detailed, simultaneously measured profiles. To support the study, measure the profile at a very small interval in the longitudinal direction, and measure several densely spaced side-by-side profiles within the zone of tire contact. With coherence to spindle response as a correlation standard, parse the profiles to find the optimal trade-off between the level of detail needed in the measurement, and prediction of spindle response.

Finally, the Pooled Fund Study participants should discuss the next steps within this initiative in detail. In particular, whether to proceed immediately with the recommended benchmark measurements, or to conduct the research needed to define a testing program an manufactured artificial events. While using manufactured events may offer a more systematic and defensible alternative to testing on natural roads, the development of a relevant testing program will delay the progress of the initiative. The group should also discuss ways to get the recommendations for waveband of interest, footprint and sampling practices, longitudinal distance measurement accuracy, and profile repeatability into practice as soon as possible, even if benchmark testing is delayed.

CHAPTER 10. REFERENCES

1. Carey, W. N. and P. E. Irick, "The Pavement Serviceability-Performance Concept." *Highway Research Board Bulletin 250* (1960) pp. 40-58.
2. Balmer, G. G., "Road Roughness Measurement and Its Application." *Public Roads*, Vol. 39, No. 4, March 1976, pp. 148-153.
3. Spangler, E. B. and W. J. Kelley, "GMR Road Profilometer–A Method for Measuring Road Profile." General Motor Research Laboratory, Warren Michigan, *Research Publication GMR-452* (1964) 44 p.
4. Perera, R. W. and S. D. Kohn, *Road Profiler User Group Fifth Annual Meeting. Road Profiler Data Analysis and Correlation.* Soil and Materials Engineers, Inc. Research Report No. 92-30 (1994) 87 p.
5. Perera, R. W. and S. D. Kohn, *Road Profiler User Group Sixth Annual Meeting. Road Profiler Data Analysis.* Soil and Materials Engineers, Inc. (1995) 87 p.
6. Karamihas, S. M., "The 2004 FHWA Profiler Round-Up." Draft Report (2005).
7. American Association of State Highway and Transportation Officials, "Standard Equipment Specification for Inertial Profiler." AASHTO MP 11-03 (2003) 11 p.
8. Hrovat, D. and M. Hubbard, "Optimum Vehicle Suspensions Minimizing RMS Rattle Space, Sprung Mass Acceleration and Jerk." *ASME Transactions*, Vol. 103 (1981) pp. 228-236.
9. Cole, D., "Elementary Vehicle Dynamics," course notes in Mechanical Engineering, University of Michigan, Ann Arbor, MI (1972).
10. Mousseau, C. W., et. al., "On the Modeling of Tires for the Prediction of Automotive Durability Loads." *International Association for Vehicle System Dynamics*, Vol. 25 Supplement (1996) pp. 466-488.
11. Gillespie, T. D., "Heavy Vehicle Ride." *Society of Automotive Engineers SP-607* (1985) 68 p.
12. Prem, H., et. al., "Characterisation of Heavy Vehicle Response to Road Surface Profile: Options for a Truck Ride Index." *ARRB Transport Research Contract Report RC7008* (1998) 34 p.
13. Fu, T.-T. and D. Cebon, "Analysis of a Truck Suspension Database." *International Journal of Vehicle Design, Heavy Vehicle Systems*, Vol. 9, No. 4 (2002) pp. 281-298.
14. Sayers, M. W. and T. D. Gillespie, "The Effect of Suspension System Nonlinearities on Heavy Truck Vibration." *Proceedings*, 7th IAVSD Symposium on the Dynamics of Vehicles on Roads and on Tracks, Cambridge, U. K., A. H. Wickens, Ed., Swets and Zeitlinger, Lisse (1981) pp. 154-166.

15. Sayers, M. W., "Characteristic Power Spectral Density Functions for Vertical and Roll Components of Road Roughness." American Society of Mechanical Engineers, *AMD-Vol. 80* (1986) pp. 113-129.

16. Karamihas, S. M., et. al., "Axle Tramp Contribution to the Dynamic Wheel Loads of a Heavy Truck." *4th International Symposium on Heavy Vehicle Weights and Dimensions,* Ann Arbor, Michigan. Ed. C. B. Winkler (1995).

17. Cebon, D., "Vehicle-Generated Road Damage: A Review." *Vehicle System Dynamics*, Vol. 18, Nos. 1-3 (1989) pp. 107-150.

18. Cebon, D., "Interaction Between Heavy Vehicles and Roads." *Society of Automotive Engineers SP-951* (1993) 81 p.

19. Griffin, M.J., *Handbook of Human Vibration*, Academic Press, London (1990).

20. British Standards Institution. *Measurement and Evaluation of Human Exposure to Whole-Body Mechanical Vibration and Repeated Shock BS6841*. London (1987).

21. ISO, "Guide for the Evaluation of Human Exposure to Whole-Body Vibration." *Second Edition, International Standard ISO 2631-1:1997(E)*, International Organization for Standards (1997) 17 p.

22. *Highway Performance Monitoring System, Field Manual, Appendix J.* U.S. Department of Transportation, Washington, D.C. FHWA Publication 5600.1A (1990).

23. Gramling, W. L., "Current Practices in Determining Pavement Condition." *National Cooperative Highway Research Program Synthesis of Highway Practice 203* (1994) 57 p.

24. TRDF, *A Summary of Pavement Performance Data Collection and Processing Methods Used by State DOTs.* Federal Highway Administration Report FHWA-RD-95-060, (1994) 62 p.

25. Sayers, M. W., et. al., "Guidelines for Conducting and Calibrating Road Roughness Measurements." *World Bank Technical Paper Number 46* (1986) 87 p.

26. Sayers, M. W. and S. M. Karamihas, "Interpretation of Road Roughness Profile Data*." Federal Highway Administration Report FHWA/RD-96/101* (1996) 177 p.

27. Sayers, M. W., "On the Calculation of International Roughness Index from Longitudinal Road Profile." *Transportation Research Record 1501* (1995) pp. 1-12.

28. Karamihas, S. M., et. al., "Guidelines for Longitudinal Pavement Profile Measurement." *National Cooperative Highway Research Program Report 434* (1999) 75 p.

29. Wedner, R. J. Jr., "Road Profiler Calibration Results." Presented at the 4th Annual Road Profiler Users' Group Meeting (1992) 51 p.

30. Janoff, M. S., et al., "Pavement Roughness and Rideability." *National Cooperative Highway Research Program Report 275* (1985) 69 p.

31. Janoff, M. S., "Pavement Roughness and Rideability Field Evaluation." *National Cooperative Highway Research Program Report 308* (1988) 54 p.

32. Sayers, M. W. and S. M. Karamihas, "Estimation of Rideability by Analyzing Longitudinal Road Profile." *Transportation Research Record 1536* (1996) pp. 110-116.

33. Holbrook, L. F., "Prediction of Subjective Response to Road Roughness Using the General Motors-Michigan Department of State Highways Rapid Travel Profilometer." *Michigan Department of State Highways Report R-719* (1970) 65 p.

34. Darlington, J. R., "Evaluation and Application Study of the General Motors Corporation Rapid Travel Profilometer." *Michigan Department of Sate Highways Research Report No. R-731* (1970) 92 p.

35. de Pont, J., "Road Profile Characterisation." *Transit New Zealand Research Report No. 29* (1994) 45 p.

36. Sweatman, P. F., "A Study of Dynamic Wheel Forces in Axle Group Suspensions of Heavy Vehicles." *Australian Road Research Board Special Report 27* (1983) 65 p.

37. Hassan, R. and K. McManus, "Heavy Vehicle Ride and Driver Comfort." *Society of Automotive Engineers SP-1591* (2001) pp. 145-149.

38. Papagiannakis, A. T., "The Need for a New Pavement Roughness Index; RIDE." *Society of Automotive Engineers SP-1308* (1997) pp. 133-140.

39. Papagiannakis, A. T. and M. Gujarathi, "A Roughness Model Describing Heavy Vehicle-Pavement Interaction." *Washington State Department of Transportation Report WA-RD 372.1* (1995) 55 p.

40. Winkler, C.B. and Hagan, M., "A Test Facility for the Measurement of Heavy Vehicle Suspension Parameters." *Society of Automotive Engineers Paper No.800906* (1980) 29 p.

41. Winkler, C. B., et. al., "Roll Stability Performance of Heavy Vehicle Suspensions." *Society of Automotive Engineers Paper 922426* (1992) 9 p.

42. Prem H., et. al., "A Road Profile Based Truck Ride Index (TRI)." *Proceedings*, 6th International Symposium on Heavy Vehicle Weights and Dimensions. Saskatoon, Saskatchewan, Canada (2000) pp. 483-505.

43. Devore, J. J. and M. Hossain, "An Automated System for Determination of Pavement Profile Index and Location of Bumps from the Profilograph Traces." *Kansas State University Report K-TRAN: KSU-93-2* (1994).

44. Parcells, W. H. Jr. and M. Hossain, "Kansas Experience with Smoothness Specifications for Concrete Pavements." *Transportation Research Record 1435* (1994) pp. 115-123.

45. Scofield, L., "Profilograph Limitations, Correlations and Calibration Criteria for Effective Performance Based Specifications." National Cooperative Highway Research Program Project 20-57, Task 53 (1992) 161 p.

46. Karamihas, S. M., "Assessment of Profiler Performance for Construction Quality Control. with Simulated Profilograph Index." *Transportation Research Record 1900* (2004) pp. 12-18.

47. Bendat, J. S. and A. G. Piersol, *Random Data: Analysis and Measurement Procedures*, Wiley-Interscience, John Wiley and Sons, Inc., New York (1971).

48. Gillespie, T. D., et. al., "Calibration of Response-Type Road Roughness Measuring Systems." *National Cooperative Highway Research Program Report 228* (1980) 81 p.

49. Sayers, M. W., "Dynamic Terrain Inputs to Predict Structural Integrity of Ground Vehicles." *University of Michigan Transportation Research Institute Report UMTRI-88-16* (1988) 114 p.

50. Curtis, A. J. and T. R. Broykin, Jr., "Response of Two-Degree-of-Freedom Systems to White Noise Base Excitation." *Journal of the Acoustical Society of America*, Vol. 33 (1961) pp. 655-663.

51. Crandal, S. H. and W. D. Mark, *Random Vibration in Mechanical Systems*. Acedemic Press, Inc., Orlando, Florida (1963).

52. Houbolt, J. C., "Runway Roughness Studies in the Aeronautical Field." *ASCE Transactions Paper N3364*, V127, Pr. IV (1962) pp. 427-448

53. Van Deusen, B. D. and G. E. McCarron, "A New Technique for Classifying Random Surface Roughness." *SAE Transactions* 670032 (1967).

54. La Barre, R. P., et. al., "The Measurement and Analysis of Road Surface Roughness." *Motor Industry Research Association, Report 1970/5* (1970) 31 p.

55. Dodds, C. J., and J. D. Robson, "The Description of Road Surface Roughness." *Journal of Sound and Vibration*, Vol. 31, No. 2 (1973) pp. 175-183.

56. Robson, J. D., "Road Surface Description and Vehicle Response." *International Journal of Vehicle Design*, Vol. 1, No. 1 (1979) pp. 25-35.

57. Cebon, D., *Handbook of Vehicle Road Interaction*. Swets and Zeitlinger. Lisse, Nethrlands. (1999) pp. 22-23.

58. American Society for Testing and Materials, "Standard Test Method for Measuring Road Roughness by Static Level Method." ASTM E 1364-95, *Annual Book of ASTM Standards*, Vol. 04.03 (1996) pp. 750-755.

59. American Society for Testing and Materials, "Standard Test Method for Measuring the Longitudinal Profile of Traveled Surfaces with an Accelerometer Established Inertial Profiling Reference." ASTM Standard E 950-98, *Annual Book of ASTM Standards*, Vol. 04.03 (1998).

60. American Society for Testing and Materials, "Standard Test Method for Measuring Pavement Roughness Using a Profilograph." ASTM Standard E 1274-88, *Annual Book of ASTM Standards*, Vol. 04.03 (1996) pp. 730-733.

61. Fernando, E. G. and S. I. C. Leong, "Profile Equipment Evaluation." *Texas Transportation Institute Research Report 1378-2* (1998) 186 p.

62. Still, P. B. and P. G. Jordan, "Evaluation of the TRRL High-Speed Profilometer." *Transport and Road Research Laboratory, Laboratory Report 922* (1980) 45 p.

63. Sayers, M. W. and T. D. Gillespie, "The Ann Arbor Road Profilometer Meeting." *Federal Highway Administration Report FHWA/RD-86/100* (1986) 237 p.

64. American Association of State Highway and Transportation Officials, "Standard Practice for Certification of Inertial Profiling Systems." AASHTO MP 49-03 (2003) 8 p.

65. Texas Department of Transportation, "Operating Inertial Profilers and Evaluating Pavement Profiles." Specification Tex-1001-S.

66. Gillespie, T. D., et. al., "Effects of Heavy Vehicle Characteristics on Pavement Response and Performance." *National Cooperative Highway Research Program Report 353* (1993) 126 p.

67. Sayers, M. W., et. al., "The International Road Roughness Experiment." *World Bank Technical Paper Number 45* (1986) 453 p.

68. Holbrook, L. F. and J. R. Darlington, "Analytical Problems Encountered in the Correlation of Subjective Response and Pavement Power Spectral Density Functions." *Highway Research Record 471* (1973) pp. 83-90.

69. Karamihas, S. M. and T. D. Gillespie, "Development of Cross Correlation for Objective Comparison of Profiles." *University of Michigan Transportation Research Institute Report UMTRI-2002-36* (2002) 146 p.

70. Li, Y. and J. Delton, "Approaches to Profiler Accuracy." *Transportation Research Record 1860* (2003) pp. 129-136.

71. Sayers, M. W. and S. M. Karamihas, *The Little Book of Profiling.* University of Michigan Transportation Research Institute (1998) 100 p.

72. Prem, H., "Development and Evaluation of a Method for Validation of Pavement Roughness Measurements." *ARRB Transport Research Ltd. Contract Report RE7135* (1998) 30 p.

73. American Association of State Highway and Transportation Officials, "Operating Inertial Profilers and Evaluating Pavement Profiles." AASHTO MP 50-03 (2003) 8 p.

74. Karamihas, S. M., "Development of Cross Correlation for Objective Comparison of Profiles." *International Journal of Vehicle Design*, Vol. 36, Nos. 2/3 (2004) pp. 173-193.

75. Karamihas, S. M. and T. D. Gillespie, "Assessment of Profiler Performance for Construction Quality Control. Phase I." *University of Michigan Transportation Research Institute Report UMTRI-2003-1* (2003) 57 p.

76. CALTRANS, “Operation of California Profilographs and Evaluation of Profiles.” California Department of Transportation, *California Test 526* (1978) 6 p.

77. Huft, D. L., “Analysis and Recommendations Concerning Profilograph Measurements on F0081(50)107 Kingsbury County.” *Transportation Research Record 1348* (1992) pp. 29-34.

78. Smith, K. L., et. al., “Smoothness Specifications for Pavements.” *National Cooperative Highway Research Program Web Document 1* (1997) 540 p.

79. Bertrand, C. B., “Automated Versus Manual Profilograph Correlation.” *Transportation Research Record 1410* (1993) pp. 67-79.

80. Zegelaar, P. W. A.,“The Dynamic Response of Tyres to Brake Torque Variations and Road Unevenness.” Ph.D. Dissertation, Delft University of Technology (1998) 315 p.

81. Schuring, D. and M. R. Belsdorf, “Analysis and Simulation of Dynamical Vehicle–Terrain Interaction.” *Technical Memorandum CAL No. VJ-2330-G-56*, Cornell Aeronautical Laboratory, Inc., Buffalo, New York (1969) 206 p.

82. Van Deusen, B. D., “A Statistical Technique for the Dynamic Analysis of Vehicles Traversing Rough Yielding and Non-yielding Surfaces.” *NASA Contractor Report No. 659*, Washington, D. C. (1966).

83. Rasmussen, R. E. and A. D. Cortese, “Dynamic Spring Rate Performance of Rolling Tires.” *Society of Automotive Engineers Paper 680408* (1968) 8 p.

84. Lins, W. F., et. al., “Comparison of Time Domain and Frequency Domain Analysis of Off-Road Vehicles.” *Society of Automotive Engineers Paper 690353* (1969) 16 p.

85. Jurkat, M. P., “Mathematical Formulation of Wheeled Vehicle Dynamics for Hybrid Computer Simulation.” *Report No. SIT-DL-70-1452*, Stevens Institute of Technology, Hoboken, New Jersey (1970) 69 p.

86. Lippmann, S. A., et. al., “Enveloping Characteristics of Truck Tires–A Laboratory Evaluation.” *Society of Automotive Engineers Transactions*, Vol. 74 (1966) pp. 831-836.

87. Guo, K., “Tire Roller Contact Model for Simulations of Vehicle Vibration Input.” *Society of Automotive Engineers SP-991* (1993) pp. 45-52.

88. Mizun, V., “Road Loads when a Vehicle Moves over an Unevenness in a Road.” *International Journal of Vehicle Design, Heavy Vehicle Systems*, Vol. 1, No. 4 (1994) pp. 417-432.

89. Metcalf, W. H., “The Ride Behavior of a Multi-Element Vehicle Traversing Cross-Country Terrain.” *Report No. CAL YM-1424-V-16*, Cornell Aeronautical Laboratory, Inc., Buffalo, N.Y. (1961) 123 p.

90. Bogdanoff, J. L. and F. Kozin, “Additional Results on the Statistical Analysis of a Linear Vehicle Model Using Measured Ground Power Spectral Density.” *Report*

No. 8392LL96, Land Locomotion Laboratory, U.S. Army TACOM, Warren Michigan (1963) 27 p.

91. Captain, K. M., et. al., "Analytical Tire Models for Dynamic Vehicle Simulation." *Vehicle System Dynamics*, Vol. 8 (1979) pp 1-12.
92. Mousseau, C. W., et. al., "Computer Synthesis of Light Truck Ride Using a PC-Based Simulation Program." *Society of Automotive Engineers Paper 1999-01-1796* (1999) 11 p.
93. Albert, C. J., "A Method of Simulating Tire Enveloping Power in Calculations of Vehicle Ride Performance." *Report No. YM-1424-V-300*, Cornell Aeronautical Laboratory, Inc., Buffalo, New York (1961) 34 p.
94. Lessem, A. S., "Dynamics of Wheeled Vehicles. Report 1. A Mathematical Model for the Traversal of Rigid Obstacles by a Pneumatic Tire." *Technical Report M-68-1*, U.S. Army Engineer Waterways Experiment Station, CE, Vicksburg, Mississippi (1968).
95. Bernard, J., et. al., "Tire Models for the Determination of Vehicle Structural Loads." *Proceedings*, 7th IAVSD Symposium on the Dynamics of Vehicles on Roads and on Tracks, Cambridge, U. K., A. H. Wickens, Ed., Swets and Zeitlinger, Lisse (1981) pp. 141-153.
96. Davis, D. C., "A Radial-Spring Terrain-Enveloping Tire Model." *Vehicle System Dynamics*, Vol. 4, No. 1 (1975) pp. 55-69.
97. Gong, S., "A Study of In-Plane Dynamics of Tires." Ph.D. Dissertation, Delft University of Technology (1993) 163 p.
98. Zegelaar, P. W. A., et. al., "Tyre Models for the Study of In-plane Dynamics." *Vehicle System Dynamics Supplement 23* (1994) pp. 578-590.
99. Bruni, S., et. al., "On the Identification in Time Domain of the Parameters of a Tyre Model for Study of In-plane Dynamics." *Supplement to Vehicle System Dynamics Volume 27* (1997) pp. 136-150.
100. Sharp, R. S. and D. J. Allison, "In-plane Vibrations of Tyres and their Dependence on Wheel Mounting Conditions." *Supplement to Vehicle System Dynamics Volume 29* (1998) pp. 192-204.
101. Clark, S. K., "The Rolling Tire Under Load." *Society of Automotive Engineers Paper 650493* (1965) 12 p.
102. Soedel, W., "On the Dynamic Response of Rolling Tires According to Thin Shell Approximations." *Journal of Sound and Vibration*, Vol. 41, No. 2 (1975) pp. 233.
103. Kilner, J. R., "Pnuematic Tire Model for Aircraft Simulation." *AIAA Journal of Aircraft*, Vol. 19, No. 10 (1982) pp. 851-857.
104. Padovan, J. and O. Paramadilok, "Transient and Steady State Viscoelastic Rolling Contact." *Computers and Structures*, Vol. 20 (1985) pp. 545-553.

105. Zegelaar, P. W. A. and H. B. Pacejka, "The In-Plane Dynamics of Tyres on Uneven Roads." *Vehicle System Dynamics Supplement 25* (1996) pp. 714-730.

106. Lippmann, S. A. and J. D. Nanny, "A Quantitative Analysis of the Enveloping Forces of Passenger Tires." *Society of Automotive Engineers Paper 670174* (1967) 12 p.

107. Ayton, G. J., et. al., "Concrete Pavement Manual, Roads and Traffic Authority," Pavements Branch, New South Wales, Australia (1991).

108. Kummer, H. W. and E. Meyer, "Skid or Slip Resistance?" *Journal of Materials*, Vol. 1, No. 3 (1966) pp. 667-688.

109. Clapp, T. G. and A. C. Eberhardt, "Computation and analysis of Texture-Induced Contact Information in Tire-Pavement Interaction." *Transportation Research Record 1084* (1986) pp. 23-29.

110. Flintcsh, G. W., et. al., "Pavement Surface Macrotexture Measurement and Applications." *Transportation Research Record 1860* (2003) pp. 168-177.

111. McDaniel, R. S. and W. D. Thornton, "Field Evaluation of a Porous Friction Course for Noise Control." *Transportation Research Board Paper Number 05-0508* (2005).

112. Hoerner, T. E., et. al., "Current Practice of Portland Cement Concrete Pavement Texturing." *Transportation Research Record 1860* (2003) pp. 178-186.

113. Kuemmel, D. A., et. al., "Noise and Texture on PCC Pavements - Results of a Multi-State Study." *Wisconsin Department of Transportation Report Number WI/SPR-08-99* (2000) 87 p.

114. Wayson, R. L., "Relationship Between Pavement Surface Texture and Highway Traffic Noise." *NCHRP Synthesis 268* (1998) 85 p.

115. Crocker, M. J., et. al., "Measurement of Acoustical and Mechanical Properties of Porous Road Surfaces and Tire and Road Noise." *Transportation Research Record 1891* (2004) pp. 16-22.

116. Watson, D. E., et. al., "Verification of Voids in Coarse Aggregate Testing: Determining Stone-on-Stone Contact of Hot-Mix Asphalt Mixtures." *Transportation Research Record 1891* (2004) pp. 182-190.

117. Ahlin, K., et. al., "Comparing Road Profiles with Vehicle Perceived Roughness." *International Journal of Vehicle Design*, Vol. 36, Nos. 2/3 (2004) pp. 270-286.

118. Bertrand, C., et. al., "Evaluation of the Performance of the Auto-Read Version of the Face Dipstick." Center for Transportation Research, University of Texas at Austin, *Research Report 969-1* (1997).

119. Perera, R. W. and S. D. Kohn, "Quantification of Smoothness Index Differences Related to LTPP Equipment Type." Report Submitted to Federal Highway Administration, December 2004.

120. Beer, F. P. and E. R. Johnson, Jr., *Mechanics of Materials.* McGraw-Hill Book Company, New York (1981).

121. Queiroz, C. V., "A Procedure for Obtaining a Stable Roughness Scale from Rod and Level Profiles." Working Document #22, Research on the Interrelationships between Costs of Highway Construction, Maintenance, and Utilization, Empressa Brasileria de Planejamente de Transportes (GEIPOT), Brasilia (1979).

122. Perera, R. and S. Kohn, "Comparison of the SHRP Profilometers." *Strategic highway Research Program Report No. SHRP-P-639* (1993) 153 p.

123. Perera, R. W., et al., "Comparative Testing of Profilers" *Transportation Research Record 1435* (1994) pp. 137-144.

124. Schmidt, B., et. al., "International Experiment to Harmonise Longitudinal and Transverse Profile Measurement and Reporting Procedures. Draft Report." *Danish Road Institute Report 93* (1999) 35 p.

125. Larsen, D. A., "Evaluation of Lightweight non-Contact Profilers for Use in Quality Assurance Specifications on Pavement Smoothness." Connecticut Department of Transportation (1999).

126. El-Korchi, T., "Correlation Study of Ride Quality Assessment Using Pavement Profiling Devices." Worcester Polytechnic Institute Research Report CEE 00-0122 (2000).

127. Chang, J. R., et. al., "Application of 3D Laser Scanning on Measuring Pavement Roughness." *Transportation Research Board Paper 05-1630* (2005) 23 p.